PhD THESIS

DECEMBER 2010

Development of a brine treatment protocol using Eutectic Freeze Crystallization

DYLLON GARTH RANDALL

Department of Chemical Engineering
University of Cape Town
Rondebosch, 7700
South Africa

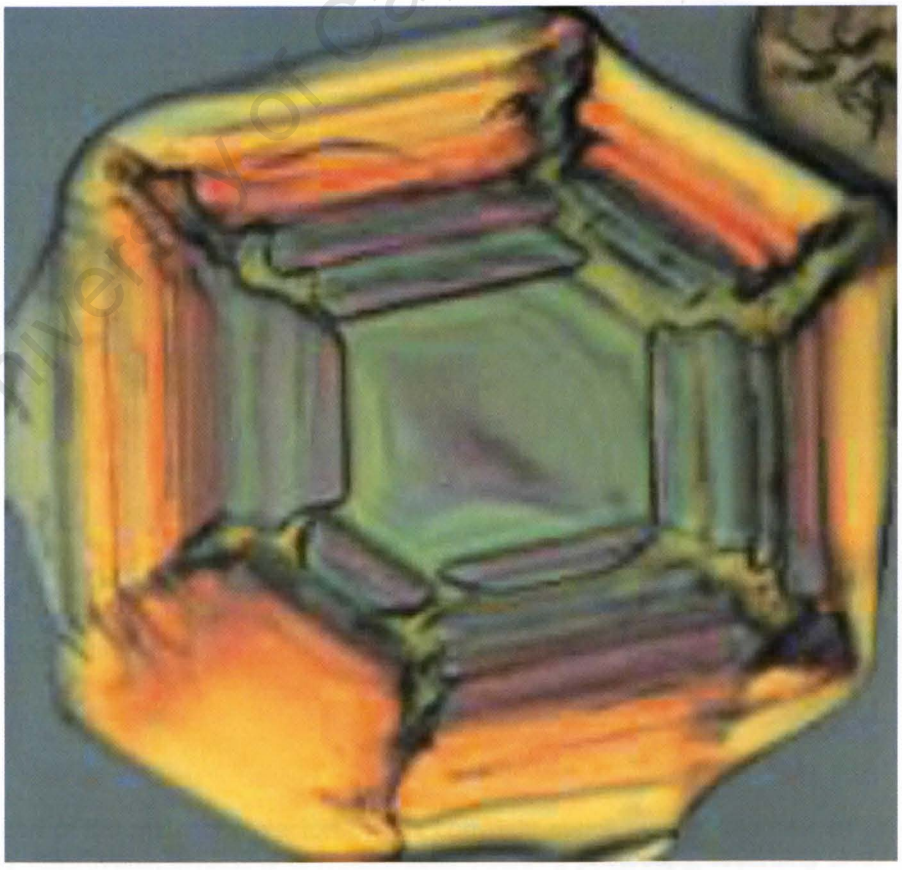

A thesis submitted for the degree of Doctor of Philosophy in Chemical Engineering

DEPARTMENT OF CHEMICAL ENGINEERING
UNIVERSITY OF CAPE TOWN

Crystallization &
Precipitation Unit

This research was financially supported by the Water Research Commission of South Africa, Coaltech and Anglo Coal. The financial support from the University of Cape Town, the Crystallization and Precipitation Unit and the Max and Lillie Sonnenburg Scholarship are also gratefully acknowledged.

Cover design & layout by D.G. Randall
Cover picture ($Na_2SO_4.10H_2O$ crystal) by D.G. Randall

This research was financially supported by the Water Research Commission of South Africa, Coaltech and Anglo Coal. The financial support from the University of Cape Town, the Crystallization and Precipitation Unit and the Max and Lillie Sonnenburg Scholarship are also gratefully acknowledged.

Cover design & layout by D.G. Randall
Cover picture ($Na_2SO_4.10H_2O$ crystal) by D.G. Randall

"Be the change you want to see in the world"

Mahatma Gandhi

ACKNOWLEDMENTS

I owe my deepest gratitude to my supervisor, Prof. Alison Lewis, whose inspiration, encouragement and support from the initial to the final stages of this project enabled me to develop an understanding of crystallization and a love for research. It is your passion and dedication to research that has made this journey so enjoyable. It has been a great pleasure to work with you. You ultimately steered my career path towards research and for this I will always be grateful. Dear "Prof", thank you sincerely for all you have done.

To Jeeten Nathoo, thank you so much for all your advice, encouragement and support. The many brain-storming sessions we had with regards to the experimental work is gratefully acknowledged. Your help and guidance made this project a reality. For this, I thank you.

This research would not have been successful without the support of the Eutectic Freeze Crystallization team. A heartfelt thanks to Traci, Rinesh and Sinethemba for everything.

To Gerda, Prof Witkamp, Prof Kramer and Elif from the Technical University of Deflt, thank you for hosting me and for the many scientific discussions and attention you gave to my research.

Thank you Prof Thomsen for all the help with regards to phase diagrams. Your knowledge about the subject is outstanding.

Thank you Prof Haines for explaining and helping me with the statistical analysis of my results.

To all the other members of the Crystallisation and Precipitation Unit in the Department of Chemical Engineering, thank you all for your friendship and support.

I would also like to thank the staff of the analytical lab in the Chemical Engineering building for their willingness, patience and dedication in conducting the analysis on my many samples. Thank you Helen, Suzana, Lloyd and Salwa.

Most importantly, a special thank-you to my parents, my brother, Warren, and to Anja, Craig and Ureshnie for your encouragement and loving support throughout the course of this project. It is much appreciated.

PUBLICATIONS LIST

Journal articles

- Lewis, A.E., Nathoo, J., Thomsen, K., Kramer, H.J., Witkamp, G.J., Reddy, S.T. and Randall, D.G., Design of a Eutectic Freeze Crystallization process for multicomponent waste water stream, Chemical Engineering Research and Design 88 (2010) 1290-1296.

- Randall, D.G., Nathoo, J., Lewis, A.E., A case study for treating a reverse osmosis brine using Eutectic Freeze Crystallization – approaching a zero waste process, Desalination 266 (2011) 256-262.

List of publications in prep

- Randall, D.G., Nathoo, J., Lewis, A.E., Separation of $Na_2SO_4 \cdot 10H_2O$ and $MgSO_4 \cdot 7H_2O$ by selective nucleation – an application for Eutectic Freeze Crystallization, (submitted to *Separation and Purification Technology*).
- Randall, D.G., Genceli-Guner, F.E., Kramer, H.J.M., Witkamp, G.J., Lewis, A.E., Determining the metastable zone of the ice region for a binary sodium sulphate system from cumulative probability curves, (in prep).
- Randall, D.G., Nathoo, J., Lewis, A.E., The sequential removal of calcium sulphate, ice and sodium sulphate from a hypersaline brine using Eutectic Freeze Crystallization, (in prep).

International peer-reviewed published conferences and presentations

- Randall, D.G., Nathoo, J., and Lewis, A.E., 2009. Seeding for selective salt recovery during Eutectic Freeze Crystallization, *in* C Taylor, ed., International Mine Water Conference, Pretoria, 639-646.
- Lewis, A.E., Randall, D.G., Reddy, T., Jivanji, R., Nathoo, J., 2009. Worth its salt - How Eutectic Freeze Crystallisation can be used to recover water and salt from hypersaline mine waters., Water in Mining, Perth, AusIMM.

Local peer-reviewed published conferences and presentations

- Randall, D.G., Nathoo, J., Lewis, A.E., 2010. Pass the salt – recovery of water and salts from multi-component hypersaline brines using Eutectic Freeze Crystallization, SAIMM Conference, Cape Town, 6-7 August 2010.
- Randall, D.G., Lewis, A.E., Nathoo, J., 2008. Kinetic aspects of multi-component systems operated under eutectic freeze crystallisation conditions, SAIMM Conference, Cape Town, 6-8 August 2008.
- Randall, D.G., and Lewis, A.E., 2007. Investigating characteristics of ice crystals formed in eutectic freeze crystallization, SAIMM Conference, Cape Town, 2-3 August 2007.

Research/Technical Reports to Industry

- Lewis, A.E., Nathoo, J., Randall, D.G., 2010. Part 2 - Development of Eutectic Freeze Crystallization Technology for Water and Salt Recovery from Hypersaline Brine, Anglo Coal, Research Report – Part 2.
- Lewis, A.E., Nathoo, J., Randall, D.G., 2009. Part 1 - Development of Eutectic Freeze Crystallization Technology for Water and Salt Recovery from Hypersaline Brine, Anglo Coal, Research Report – Part 1.
- Lewis, A.E., Nathoo, J., Reddy, S.T., Jivanji, R. and Randall, D.G., 2010. Novel technology for recovery of water and solid salts from hypersaline brines: Eutectic Freeze Crystallization, *Water Research Commission*, Private Bag, X03, Gezina, 0031, South Africa., Research Report, May 2010.
- Lewis, A.E., Nathoo, J., Randall, D.G., 2009. Part 1 - Development of Eutectic Freeze Crystallization Technology for Water and Salt Recovery from Hypersaline Brine, Anglo Coal, Research Report – Part 1.
- Petrik, L.F., Lewis, A.E., Hendry B.A., Randall, D.G., Balfour, G., Yalala, Z.G.B., Musyoka, N., and Barnard, B., 2008. Brine treatment and disposal Progress Report for *Coaltech 2020*, October 2008.

AWARDS AND SCHOLARSHIPS

The following is a list of awards and scholarships received for the research presented in this thesis:

- 2010 Institution of Chemical Engineers Sustainable Technology Award (highly commended, 2nd place),
- 2010 University of Cape Town Research Associateship (1 of 18 postgraduate students across the university),
- 2010 Water Institute of South Africa SAIWA Award for "outstanding contribution in industrial water technology",
- 2009 International Mine Water Conference, Pretoria, South Africa – Best Paper Award,
- 2009 Max & Lillie Sonnenberg Scholarship.

ABSTRACT

Hypersaline inorganic brines are generated from many global mining operations and the volume of these brines is increasing at an exponential rate. The environment and water resources in the vicinity of these mining operations are at a risk of being polluted as a result of this increase in brine volume. These are the key reasons why these brines need treatment.

Eutectic Freeze Crystallization (EFC) has been identified as a possible novel brine treatment method, but to date it has not been applied to multi-component streams such as brines. Therefore, the aim of this thesis was to develop a brine treatment protocol and to demonstrate the "proof of concept" of EFC as a brine treatment method. Three key aspects essential to the brine treatment protocol were identified as being crucial to the treatment process. These key aspects were brine analysis, thermodynamic modelling and kinetic aspects.

A combination of standard water analysis techniques and wet chemistry were used to characterize the brine, while OLI Stream Analyser was used to perform the thermodynamic modelling of the brine. It was found that the difference between the total cations and total anions (ion imbalance) from the analysis of two brine samples, **Brine 1** and **Brine 2**, were 5.8% and 6.3% respectively. The brines were also very dilute with a total dissolved solid content of 29.77g/L for **Brine 1** and 31.26g/L for **Brine 2**.

OLI Stream Analyser was able to predict and simulate the phase equilibria of an aqueous system over a wide temperature range by estimating the standard state terms and the excess terms with the use of various thermodynamic frameworks. This was an important step because the identities of the potential salts, the temperatures at which they would crystallize and the potential yields of the various products could be predicted before any experiments were conducted. The thermodynamic modelling predicted that the brine samples were saturated with respect to $CaSO_4 \cdot 2H_2O$. The modelling also predicted that ice, $Na_2SO_4 \cdot 10H_2O$ as well as $K_2SO_4 \cdot CaSO_4 \cdot 1H_2O$ would crystallize in a narrow temperature range from -0.8°C to -2.2°C. The thermodynamic results also showed that a high overall ion recovery (85% for **Brine 1** and 71% for **Brine 2**) would be obtained at an operating temperature of -5°C.

However, the thermodynamics merely offered a prediction. It was only by investigating the kinetic aspects of the system that the identity, crystallization temperatures and yield of products could be confirmed. The kinetic aspects incorporated three phases. The first phase

focused on determining the metastable zone (MSZ) of ice in a binary sodium sulphate solution, as well as the MSZ of ice for the brine. This essentially defined the operating region in which heterogeneous ice nucleation could occur. The results confirmed the inherently stochastic nature of nucleation and showed that a number of experiments were needed in order to define the MSZ. The MSZ for a 1wt% sodium sulphate solution (1.8ml volume) was 2.56 Δ°C for a cooling rate of 2°C/hour, 2.76 Δ°C for a cooling rate of 4°C/hour and 4.76 Δ°C for a cooling rate of 8°C/hour.

The effect of solution volume on the nucleation process and hence the MSZ was determined. The MSZ for a 250ml, 1wt% solution and a 1000ml, 1wt% solution were similar (2.3 Δ°C and 2.2 Δ°C respectively).

The second kinetic phase investigated the problem associated with the crystallization of two salts and ice. The EFC process is based on the principle that ice can be separated from a salt because of their density differences, thus producing pure products. However, if two salts crystallize at the same conditions, then salt contamination would occur (similar densities for the salts). This problem was avoided by utilizing knowledge obtained from phase diagrams and by seeding with a specific salt. It was found that seeding as a separation technique was feasible in a ternary Na_2SO_4-$MgSO_4$-H_2O system. The addition of $Na_2SO_4 \cdot 10H_2O$ seeds to a supersaturated solution at 12°C resulted in pure $Na_2SO_4.10H_2O$ (96% purity) being formed.

The third kinetic phase focused primarily on the sequential removal of pure salts from a single brine during EFC conditions. The experimental work showed that pure calcium sulphate (98.0% purity), pure sodium sulphate (96.4% purity) and potable water (ice) could be formed with a brine mass reduction of ~97%. The problem with the brines initially being saturated with respect to calcium sulphate was also solved by successfully removing calcium sulphate and ice under EFC conditions. This meant that pure sodium sulphate and ice could be removed in the subsequent stage.

This thesis ultimately showed that EFC could be used to treat multi-component streams and that pure salts could be sequentially produced along with potable water.

TABLE OF CONTENTS

LIST OF FIGURES

LIST OF TABLES

CHAPTER 1 : INTRODUCTION

Children of a culture born in a water-rich environment, we have never really learned how important water is to us. We understand it, but we do not respect it.

William Ashworth, 1982

Graphic from : http://www.jobwerx.com/images/ciba_949526_neat_coatings_water-drop_hr.jpg

The majority of the Earth's water is salty (97.5%) and over 70% of the remaining water is frozen in the polar ice caps and glaciers [1]. This leaves only 1% of the world's total fresh water available for human use. However, this fresh water is under extreme stress as the world's urban population is set to nearly double in the next 40 years, from its current 3.4 billion to over six billion people [2]. To sustain this population increase, agricultural, industrial and mining activities will need to increase substantially which will ultimately add to the water demand and the amount of waste water needing treatment [3].

Water pollution causes more than 1.7 million deaths annually [3] and, while the industrialized world generates 5 times more wastewater per person than the developing world, it treats over 90% of the wastewater compared to only a few percent in the developing world. Almost 20% of the useable water is used in industrial process with mining being a major source of unregulated wastewater discharge in the developing world [1].

The mining industry indirectly pollutes large volumes of fresh water through Acid Mine Drainage (AMD) and it is said that this is the biggest environmental concern facing this industry [4]. Figure 1.1 shows how mining initiates the AMD problem. Rain water and atmospheric oxygen mixes with sulphide rocks to form sulphuric acid, which has the potential to alter the ecology of local ecosystems.

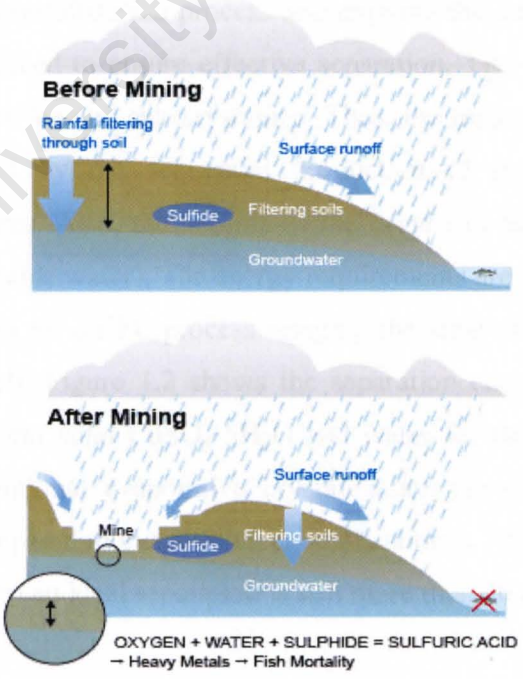

Figure 1.1: How Acid Mine Drainage is initiated [1].

It can also seep into ground water reserves, creating an even bigger environmental problem. Treatment of these waters is therefore crucial so that these problems are overcome. There are currently a number of remediation options (aeration and limestone addition; sulfidogenic bioreactors; aerobic wetlands [5]) that are available to neutralize the acidic nature of the waters. However, the product streams from these remediation techniques usually need further treatment. Reverse Osmosis (RO) is perhaps the best treatment option that can be utilized to treat this water if potable water or process water is desired [6] since it is the most efficient treatment method for producing very high quality water [7]. Even so, RO still produces a concentrated brine that needs to be treated or disposed of. Major brine treatment methods (evaporation ponds and evaporative crystallizers) are able to reduce the volume of these brines significantly but they, in most cases, also produce a mixed salt product.

The ideal brine treatment method needs to consider the waste stream as raw materials and produce reusable products. This approach would be beneficial economically as well as environmentally. A technology that aims to utilise the minimum amount of energy for treatment purposes would be the most beneficial treatment technique. A recent report from the Green Economy Initiative [1] states that the payback (health, societal and environmental benefits) for every dollar invested in water treatment is between US$3 to US$34.

Eutectic Freeze Crystallization (EFC) is a novel technology that is able to treat brines. It is an extension of the freeze crystallization process and exploits the density differences between the ice and the salt produced to ensure effective separation. The process is operated at the eutectic point, where both ice and salt crystallize. Thus, the major problems of a mixed salt product can be avoided by the sequential production of pure salts at their unique crystallization temperatures. Also, the volume of the brine can be considerably reduced by the production of ice (potable water). The energy requirements are also significantly less than evaporative crystallization for a EFC process bringing the ideal minimum theoretical energy requirements within reach. Figure 1.2 shows the separation energy required to separate a 10wt% $CuSO_4$ solution into solid $CuSO_4 \cdot 5H_2O$ and water for the thermodynamic minimal (W_{min}), EFC and conventional evaporative crystallization (Evaporation) [8]. The energy requirement for EFC compared to evaporative crystallization is 70% lower but the amount of energy required to perform an ideal separation is still more than 20 times higher for EFC.

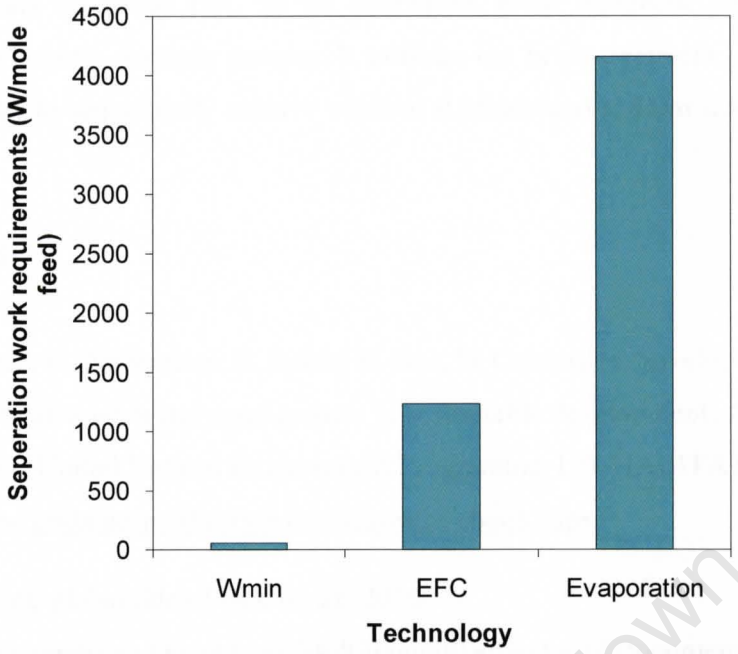

Figure 1.2: Separation work requirements in W/mole feed for three separation processes [8].

Eutectic Freeze Crystallization works best with concentrated streams because the streams are usually closer to the eutectic point. Although Reverse Osmosis works well with dilute streams, an enhanced process utilising the benefits of each technology would be achieved if both technologies were used together to treat brines. Figure 1.3 shows the water treatment performance as a function of different technologies. The next big step is envisioned as a combination of EFC and reverse osmosis [7].

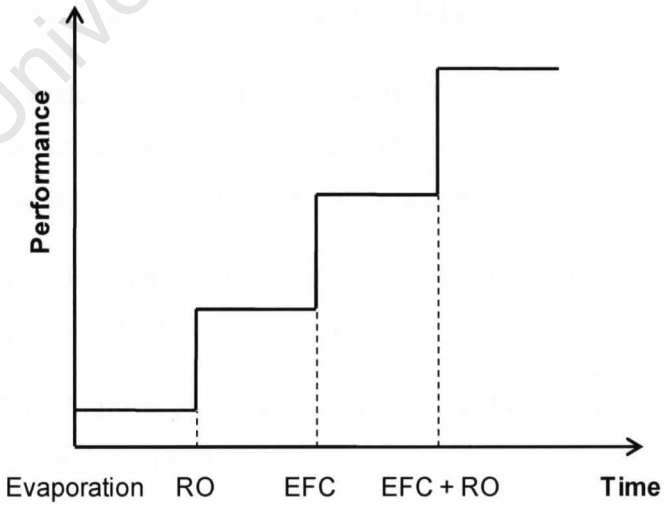

Figure 1.3: Intermediate innovation along the transition path increasing the performance of water treatment [7].

This thesis focuses on using EFC as an alternative brine treatment method for brines generated from a reverse osmosis process. It outlines the brine treatment protocol that was developed in order to sequentially remove calcium sulphate and sodium sulphate along with potable water.

References

[1] E. Corcoran, C. Nellemann, E. Baker, R. Bos, D. Osborn, H. Savelli, Sick Water? The central role of wastewater management in sustainable development. A rapid response assessment, United Nations Environment Programme, UN-HABITAT, 2010 http://www.grida.no/publications/rr/sickwater/ebook.aspx.

[2] Time to cure global tide of sick water, 2010 http://www.unep.org/Documents.Multilingual/Default.asp?DocumentID=617&ArticleID=6504&l=en&t=long.

[3] M. Palaniappan, P.H. Gleick, L. Allen, M.J. Cohen, J. Christian-Smith, C. Smith, Clearing the waters. United Nations Environent Programme, UN-HABITAT, 2010 http://www.unep.org/PDF/Clearing_the_Waters.pdf.

[4] A. Akcil, S. Koldas, Acid Mine Drainage (AMD): causes, treatment and case studies, Journal of Cleaner Production 14 (2006) 1139-1145.

[5] D.B. Johnson, K.B. Hallberg, Acid mine drainage remediation options: a review, Science of the total environment 338 (2005) 3-14.

[6] P. Gunter, T. Naidu, Mine water reclamation – towards zero disposal, WISA Biennial Conference, Johannesburg, South Africa, 2008 http://www.ewisa.co.za/misc/WISAConf/default2008.htm.

[7] F.E. Genceli, Scaling-up eutectic freeze crystallization. PhD Thesis. Technical University of Delft, The Netherlands, 2008.

[8] F. Van der Ham, Eutectic Freeze Crystallization. PhD Thesis. Technical University of Delft, The Netherlands, 1999.

CHAPTER 2 : LITERATURE & THEORY

Freedom alone is not enough without light to read at night, without time or access to water to irrigate your farm, without the ability to catch fish to feed your family.

Nelson Mandela

Graphic from : http://www.jobwerx.com/images/ciba_949526_neat_coatings_water-drop_hr.jpg

2.1 Background and brine treatment methods

In the past 20 years mine water management in South Africa has evolved from simply dealing with a pollution issue to recognizing mine water as a valuable resource [1]. The common perception that protecting the environment is a luxury and costs money is changing.

Substantial water resources are currently stored in old and active mines. Consider the following information to place this in perspective [1]:

- Mine water stored in the Highveld Coalfields, South Africa = 522 million m^3;
- Combined storage capacity of Witbank Dam, Middleburg Dam and Loskop Dam (dams situated near these mining operations) = 514million m^3.

These mine waters can be ultimately reclaimed for any of the following users [1]:

- municipal and potable,
- industrial operations,
- new mining ventures,
- support of aquatic ecosystems and wetlands,
- agriculture.

Reverse osmosis is often selected as the preferred treatment option of mine water from coal mines [2] because it works well for dilute streams. However, this treatment technique produces a brine concentrate as a result of the high levels of water removal and this ultimately needs to be disposed of because of the serious environmental harm it can impose [3]. The brine generated from reverse osmosis can range from 3 to 25 percent of the mine water feed and a significant cost is associated with its disposal (5-33% of the reverse osmosis treatment cost [4]), especially for non-coastal operations. Coastal operations usually utilize the much cheaper disposal option of discharging the brine into the ocean [5] but this disposal option can impact the nearby benthic environment [4].

The four primary brine treatment options available for non-coastal reverse osmosis operations are evaporation ponds, deep-well-injection, mechanical evaporation methods [6] and biological methods. However, no single treatment method can completely treat a brine.

Evaporation ponds rely on solar energy to evaporate water from the brine. The ponds are easy to construct and require low maintenance and little operator attention [4]. The brine is pumped into a specially lined pond and, while this may seem an effective treatment method in the short run, this is certainly not sustainable in the long run. There is no water recovery (other than to the natural water cycle) from evaporation ponds and the mixed salt product that is produced at the end of the life of the pond has to be disposed of at an additional cost [7]. Evaporation ponds are also limited to regions where the evaporation rate exceeds the annual precipitation rate [6]. Large surface areas of land are also required for the construction of the evaporation pond and this cost of land is often overlooked [7]. Evaporation ponds also have the potential of contaminating the ground water table by the percolation of reject water through the earth [8].

Deep Well Injection is a brine treatment option that stores brines in subsurface geologic formations [8]. The use of this as a brine disposal option is limited because of the underlying geology near the treatment operation. The deep well discharge also has to be protected against contaminating drinking water aquifers [6].

Mechanical evaporation is driven by the heat transfer between steam and the brine with the absorbed heat of the brine causing vaporization of water and an increase in the salt concentration [8]. Mechanical evaporation requires a significant amount of energy to form the steam and often a mixed salt product is formed that ultimately needs to be disposed of at additional cost.

Biological treatment methods usually use sulphate reducing bacteria [9] and micro-organisms to remove contaminants. Wetlands, for example, are a biological treatment method that are able to achieve this in a cost-effective, low-energy and natural manner compared to alternative and often more energy intensive treatment methods [8]. However, these processes are sensitive to feed concentration fluctuations and are usually only able to reduce the concentration of specific ions; for example the sulphate ion.

Most of these treatment options are usually able to reduce the volume of brines extensively but the concentration of various components increase considerably and since many disposal regulations are based on concentrations and not volume, a significant cost can be associated with their disposal [4]. These methods of treatment do not recover potable water and can produce mixed salt products that also need to be disposed of.

Alternative brine treatment technologies are needed that are able to significantly reduce the volumes of the generated brines while also being able to deal with high ion concentrations. The technology should be able to produce potable or process water along with pure salts in a sustainable, environmentally friendly and economical manner. Eutectic Freeze Crystallization is a novel technology that aims to achieve this.

Eutectic Freeze Crystallization is an extension of the freeze crystallization process and exploits the density differences between the ice and the salt produced to ensure effective separation. The process is operated at the eutectic point, where both ice and salt crystallize. Thus, the major problems of a mixed salt product can be avoided by the production of many pure salts at their unique crystallization temperatures.

2.2 Theory of crystallization

Crystallization can be defined as a phase change where a crystalline solid is obtained from the solution [10]. This can only be achieved in a supersaturated solution; that is a solution that has a concentration of the solute exceeding the equilibrium solute concentration. The thermodynamic driving force for crystallization is called supersaturation. Hence, the nucleation of particles and their subsequent growth are driven by the existing supersaturation in the solution [11].

Supersaturation can be expressed as a ratio as follows [12]:

$$S = \frac{C}{C_{eq}} \qquad \textbf{(2.1)}$$

where

S - supersaturation ratio, -

μ - solute concentration, mol/L^3

μ^* - equilibrium concentration, mol/L^3

For cooling crystallization, the supersaturation can be expressed as a temperature difference:

$$S = T - T^* \qquad \textbf{(2.2)}$$

Where

T - actual temperature, K

T^* - equilibrium temperature, K

2.2.1 Nucleation

A crystalline material can only develop if there is a critical number of nuclei in a solution. The nucleation process can be divided into three categories namely primary homogenous, primary heterogeneous and secondary nucleation [12]. The process of nucleation in systems containing no previous crystalline matter is termed homogeneous nucleation while heterogeneous nucleation occurs in the presence of a solid interface of a foreign seed [12].the process of artificially inducing nucleation with a solute particle is known as secondary nucleation [13]. In the primary homogeneous nucleation system, many nuclei are formed at high supersaturation resulting in small crystals. Secondary nucleation dominates at low supersaturation where the supersaturation is consumed gradually. Thus, the control of supersaturation in the solution is possible for secondary nucleation systems. As a result, large crystals can be prepared [14].

2.2.1.1 Heterogeneous nucleation and critical free energy

Nucleation almost always occurs as heterogeneous nucleation because homogeneous nucleation is difficult to achieve in practice since impurities are usually present regardless of the care taken to remove them [15].

However, a critical size of nucleus needs to form before nucleation will occur. It is easier to form this critical nucleus on a flat surface (impurity) than on a three-dimensional surface-free volume of water because less energy is required [15]. This phenomenon can be explained by considering the critical free energy, ΔG_{cr}, required to create a critical nucleus that will lead to nucleation [10]:

$$\Delta G_{cr} = \frac{4\sigma r_c^{\,2}}{3} \qquad (2.3)$$

Where:

ΔG_{cr} - critical free energy, J

σ - surface tension, J/m^2

r_c - critical cluster radius, m

For heterogeneous nucleation, however, the critical free energy equation (equation 2.3) is multiplied by a catalytic potency factor which is defined as follows [15]:

$$f(\theta) = \frac{(1+\cos\theta)^2(2-\cos\theta)}{4} \qquad \textbf{(2.4)}$$

Where theta, θ, is a function ranging between 0 and 1.

The energy required to form a critical nucleus during heterogeneous nucleation is therefore lower and hence heterogeneous nucleation is more likely to occur at a particular supersaturation. Repeat experiments will therefore show some variability in nucleation temperatures because a critical nucleus will form at different conditions. It is for this reason that heterogeneous nucleation is said to be stochastic in nature.

2.2.1.2 The influence of volume on nucleation

The number of detectable nuclei, N_{det}, in a given volume, V, and time, t, is given by the following equation [16]:

$$\frac{N_{det}}{V} = \int_0^t J(t).dt \qquad \textbf{(2.5)}$$

Where:

J - nucleation rate, #./m^3.s

V - solution volume, m^3

t - time, s

N_{det} - detectable nuclei, -

Equation 2.5 shows that the nucleation rate is inversely proportional to the volume of solution. A smaller solution volume will result in a slower nucleation rate and thus more time will be required for nucleation to occur. Thus, smaller volumes of solution will need to be cooled substantially further from the solubility line before nucleation will occur. This trend was observed by Chen and co-workers [17] where they noticed that a larger volume of water resulted in higher nucleation temperatures, thus indicating that the system required less time to nucleate. Similar observations were reported by Zachariassen and co-workers [18]. They concluded that the nucleation temperature of ice should increase as the sample volume is increased.

2.2.2 The Metastable Zone and seeding

The metastable zone width (MSZW) is usually defined in terms of the maximum obtainable undercooling temperature during unseeded operations. Figure 2.1 explains the definition of the MSZ using a phase diagram. A solution is initially at point **A′** with a solute concentration of $\mathbf{C_1}$. Point **A**, the thermodynamic solubility limit, is reached as the solution is cooled to $\mathbf{T^*}$. Further cooling to **T** causes the solution to move along line **AB** into the metastable region until the metastable limit is reached at point **B**. In the metastable zone, between points **A** and **B**, crystallization will only occur in the presence of seeds. Spontaneous nucleation commences when the metastable limit is reached.

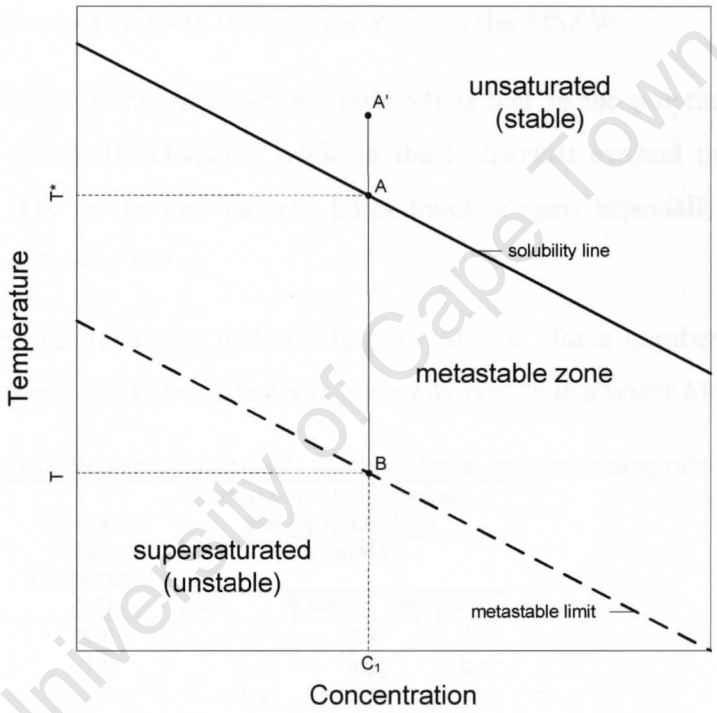

Figure 2.1: Phase diagram of a binary solid-liquid system showing the metastable region.

The MSZW has been discussed by many authors [16, 19-20] and, while many agree that the nucleation event is a stochastic process [21], the MSZW is usually characterized using one experiment. The fact that nucleation is stochastic in nature implies that the MSZW would be different for repeat experiments at exactly the same conditions. It is only by analyzing a number of experiments that an estimate can be made as to the actual width of the metastable zone. Significant differences in nucleation temperatures during the spontaneous nucleation of ice have been reported by Chen and co-workers [17]. In their investigation into the

crystallization of supercooled water, the researchers reported large variations (-3°C to -10°C) in the nucleation temperatures of ice.

The MSZW can be determined in one of two ways, namely the polythermal and the isothermal methods [16]. In the polythermal method, the solution is cooled from the saturation temperature at a fixed cooling rate.

The isothermal method involves rapidly cooling the solution to a predetermined temperature which is below the saturation (equilibrium) temperature of the component of interest. The solution is left at this temperature until spontaneous nucleation occurs [16]. The time taken for spontaneous nucleation to occur at each temperature for a specific concentration of the component provides one data point towards determining the MSZW.

The principle difference between these two methods is that in the polythermal method the supersaturation is constantly changing while in the isothermal method the supersaturation remains constant. The isothermal method takes much longer, especially if the specified supersaturation level is very low.

Table 2.1 tabulates the maximum undercooling, or MSZW, for a number of substances at cooling rates of 2, 5 and 20°/hour. A faster cooling rate results in a wider MSZW.

Table 2.1: Maximum undercooling for different components at various cooling rates [10].

Substance	Saturated Solution Temperature (°C)	Maximum Undercooling Before Nucleation Cooling Rate 2°C/h	5°C/h	20°C/h
$Ba(NO_3)_2$	30.8	1.65	2.17	3.27
$CuSO_4.5H_2O$	33.6	5.37	6.82	9.77
	60.4	0.93	1.30	2.16
$FeSO_4.7H_2O$	30.0	0.89	1.21	1.93
	40.6	0.57	0.83	1.46
KBr	30.3	1.62	2.33	4.03
	61.0	1.69	2.41	4.11
KCl	29.8	1.62	1.86	2.3
	59.8	1.02	1.18	1.48
$MgSO_4.7H_2O$	32.0	1.95	2.63	4.15
$NH_4Al(SO_4)_2.12H_2O$	30.2	0.81	1.34	2.88
	63.0	1.19	1.95	4.13
$NaBr.2H_2O$	30.6	4.60	6.97	13.08

Seeds usually consist of crystalline material of the solute and the addition of these seed particles to a supersaturated solution is called seeding. There are two seeding approaches that can be used to promote crystallization. The first involves the addition of seed material at a

temperature just below the solubility temperature [14]. Subsequent cooling will result in crystallization occurring at some temperature below the solubility temperature.

The second approach involves cooling the solution to a lower temperature (and thus a higher supersaturation) at which stage the seed material is added. This approach usually leads to crystallization occurring at the moment the seed material is added.

2.2.3 Selective nucleation

Selective nucleation involves the production of nuclei of a desired component from a supersaturated solution that has the potential of nucleating more than one substance [22]. This can be achieved by adding seed crystals to a supersaturated solution. These seed crystals cause secondary nucleation to occur because the secondary nucleation process requires less energy than that needed for primary nucleation [10]. However, the seed crystals will generally only catalyse the nucleation process if there is an impact between the seed crystals and another object in their immediate vicinity (other crystals, stirrer, crystallizer wall etc) [23]. Rousseau and co-workers [22] showed experimentally that selective nucleation was a potential technique for the separation of potassium chloride from potassium dichromate as well as for the separation of potassium dichromate from potassium sulphate. They also concluded that the order of seeding was important since an addition of $K_2Cr_2O_7$ crystals enhanced the nucleation of KCl in the KCl-$K_2Cr_2O_7$-H_2O system rather than the nucleation of $K_2Cr_2O_7$.

Van der Ham and co-workers [24] also showed that with the addition of ice seed crystals, ice could be formed without any salt formation in a region where both are favoured. Similarly, salt was formed by seeding with salt crystals. Seeding with both salt and ice crystals resulted in two distinct solid phases.

2.3 Thermodynamic phase diagrams

A phase diagram indicates the equilibrium phases of a crystallization system present at a given temperature and concentration. The phase diagram is for conditions of thermodynamic equilibrium and therefore do not describe the kinetics of a system.

2.3.1 Binary phase diagrams

A binary system is defined as a single salt dissolved in a solvent, typically water. Figure 2.2 is a theoretical binary phase diagram showing the different phases present and their corresponding conditions. The diagram is divided into different areas as follows:

Area I – solution of salt in water

Area II – saturated solution and solid salt

Area III – saturated solution and ice

Area IV – mixture of solid salt and ice

Point E – saturated solution with solid salt and ice

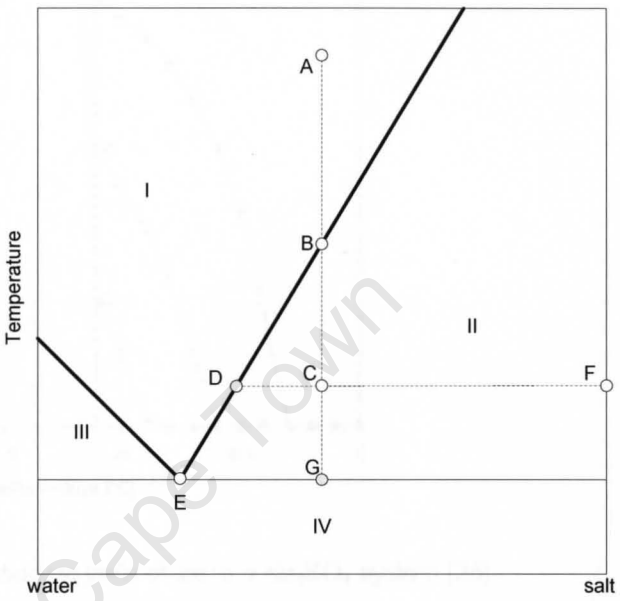

Figure 2.2: Theoretical binary phase diagram [21].

Cooling the solution from A to B results in the formation of salt crystals at B. Further cooling to point C leads to a situation where the pure solid phase is in equilibrium with a solution of composition D [21].

The theoretical yields for each species are also given by the phase diagram. The relative weight ratios are given by lever rule:

$$\text{Weight of salt/weight complete system} = CD/DF \qquad (2.6)$$

If the system is cooled further to G, then the salt will be in equilibrium with a saturated solution of composition E. At this point ice will also begin to form. The second solid phase, ice, at concentration H, will be in equilibrium with the system.

Figure 2.3 shows the effect of a temperature reduction on the yield of ice for different concentrations of sodium sulphate. The solution concentrations (1wt%, 2wt% and 3wt%) are to the left of the eutectic concentration of sodium sulphate (4.2wt%) and therefore ice is expected to crystallize first. The eutectic temperature is indicated by the dotted line in

Figure 2.3 and describes the temperature at which $Na_2SO_4 \cdot 10H_2O$ begins to crystallize simultaneously with ice.

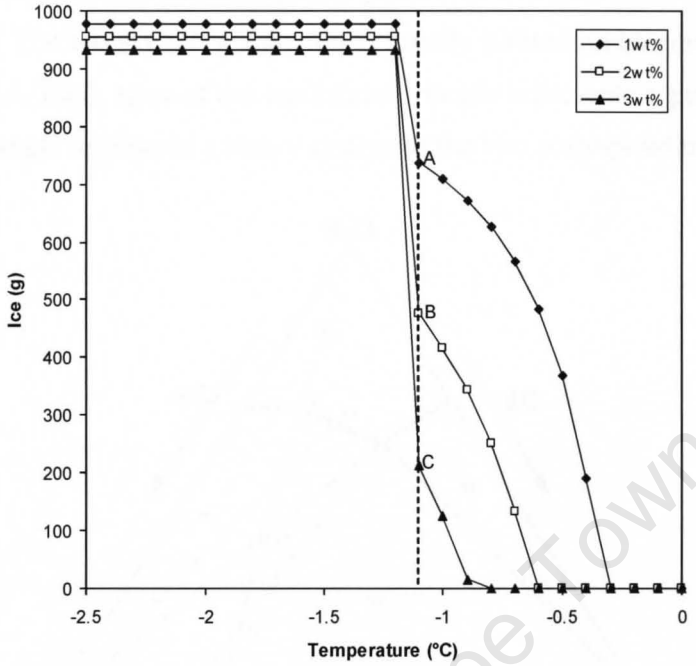

Figure 2.3: Effect of temperature reduction on yield of ice in a Na_2SO_4 system [25].

The highest yield of ice is obtained from the lowest concentration of sodium sulphate (1wt%). The temperature at which ice begins to crystallize (-0.4°C) is also the highest for a 1wt% solution. Also, more than 70% of the water needs to be removed in the form of ice (point **A**) before any salt will begin to crystallize while 48% (equivalent of point **B**) and 21% (equivalent of point **C**) of the water needs to be removed for concentrations of 2wt% and 3wt% sodium sulphate respectively. Each concentration profile also does not reach a 100% yield of ice. The reason for this is as a result of some of the water molecules being used to form the hydrates in the $Na_2SO_4 \cdot 10H_2O$ salt. Highly concentrated streams will therefore have a reduced yield of ice since more solvent would be needed to form the salt hydrates. The results shown in Figure 2.3 do not take into account the kinetics of the system. For example, a 1wt% solution would require more time to reach eutectic conditions compared to the more concentrated profiles in Figure 2.3. The 1wt% solution is also likely to result in excessive ice scaling as well as salt-ice separation issues as a result of the high solid content in the crystallizer compared to the other concentration levels.

2.3.2 Ternary phase diagrams

In the context of this thesis, a ternary system is defined as two salts, with a common ion, dissolved in water. The ternary phase diagram is usually plotted on an equilateral triangle as shown in Figure 2.4. Each apex of the equilateral triangle represents a pure component and each side of the triangle represents a binary system of the two corresponding components.

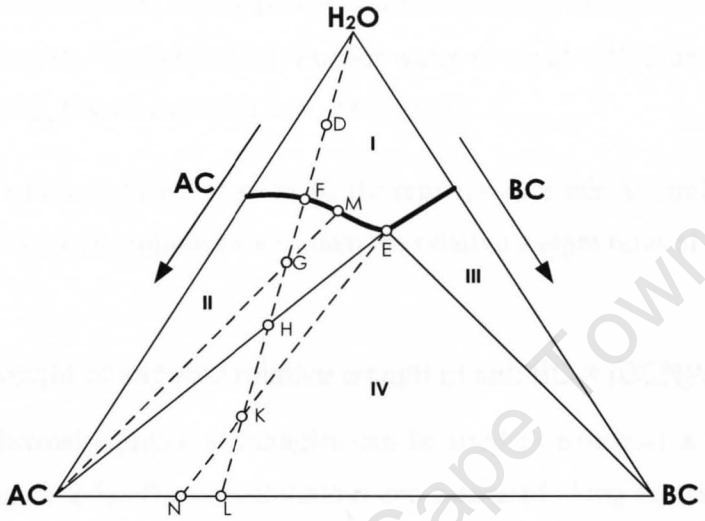

Figure 2.4: Theoretical ternary phase diagram [21].

The equilateral triangle in Figure 2.4 shows the isothermal phase diagram of two salts, AC and BC, dissolved in water. The different areas of the ternary phase diagram are:

Area I – unsaturated aqueous solution of the salts

Area II – solid salt AC in solution

Area III – salt BC in solution

Area IV – both salts in a saturated solution of composition represented by E

Point E – ice, solid AC and solid BC

The interior of the triangle shows the thermodynamic equilibrium conditions for all three components at a specific temperature, called an isotherm. The lever rule can again be used to determine the weight ratios of each species [21].

The lines separating regions **I** from **II** and **I** from **III** indicate the saturated solutions of salts AC and BC. Starting at point **D**, if water is removed, the composition change would occur along the line through **D** and the apex representing pure water. Once point **F** is reached, solid

AC begins to crystallize. As more water is removed, point **G** is reached which has a saturated solution composition of **M** and is in equilibrium with pure salt AC.

The relative weight of salt AC at point **G** is given by:

$$\text{Relative weight of salt AC} = GM/ACM \quad (2.7)$$

With further removal of water, the system reaches point **H**. From point **H** onwards the composition of the equilibrium saturated solution moves along the curve FME until point **E**, the ternary eutectic point, is reached [21]. Further water removal will result in no composition change of the solution, but a mixture of salts AC and BC.

If the composition of the system is at point **K**, the region where salt AC and salt BC coexist with a saturated solution of composition E, then the relative weight ratio of the salt is given by:

$$\text{Relative weight of salt AC/ relative weight of salt BC} = (BCN)/(ACN) \quad (2.8)$$

A number of isothermal equilateral triangles can be used to construct a three dimensional phase diagram (Figure 2.5). The concentrations are measured along the sides of the base of the triangle while the temperature is measured vertically. The surface of Figure 2.5 shows contours representing constant temperatures (isotherms).

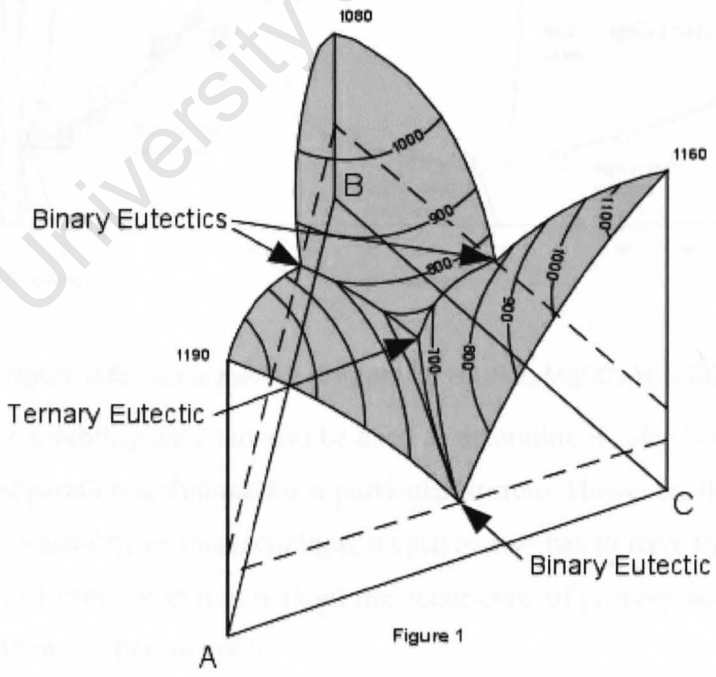

Figure 2.5: 3D Ternary phase diagram [26].

Another method of depicting a ternary phase diagram is shown in Figure 2.6. The diagram, however, does not show the water content. The salt fraction, sf, is defined as follows:

$$sf = \frac{[Na_2SO_4]}{[Na_2SO_4]+[MgSO_4]} \qquad (2.9)$$

Where

$[Na_2SO_4]$ - molal concentration of anhydrous sodium sulphate (mol/kg H_2O)

$[MgSO_4]$ - molal concentration of anhydrous magnesium sulphate (mol/kg H_2O)

Thus a salt fraction of one refers to a pure binary Na_2SO_4-H_2O system while a salt fraction of zero refers to a binary $MgSO_4$-H_2O system.

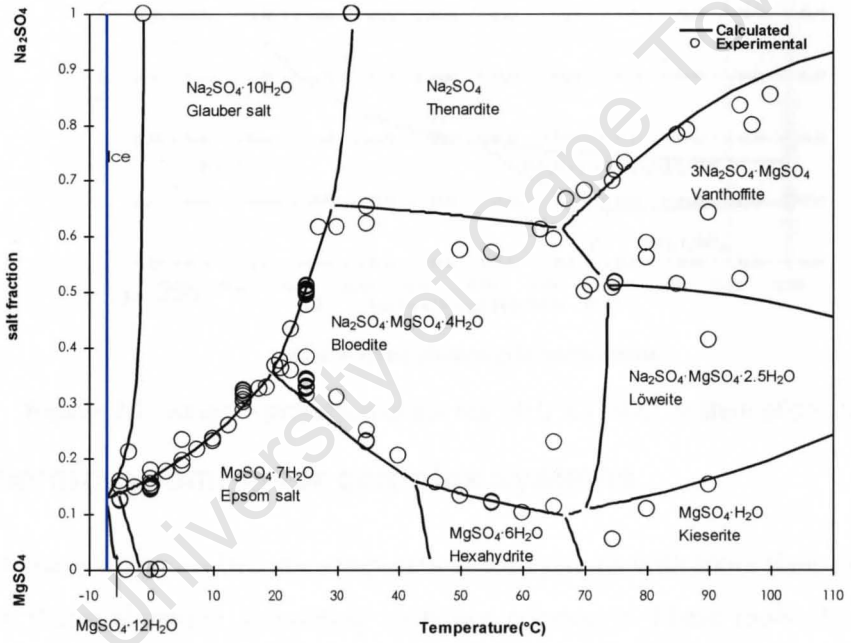

Figure 2.6: Ternary phase diagram for Na_2SO_4-$MgSO_4$-H_2O [27].

Phase diagrams or solubility data can also be used to determine if selective nucleation can be used as a solute separation technique for a particular system. However, this data alone does not guarantee the feasibility of this technique; a system also has to have the ability to sustain a significant level of supersaturation without the occurrence of primary nucleation [21]. This can only be determined experimentally.

2.3.3 Quaternary phase diagrams

Quaternary systems (four different ions) can be depicted on a Jänecke projection. Figure 2.7 shows such a projection for a system with the following ions Na^+, NH_4^+, SO_4^{2-} and Cl^-. The water content is given as a weight percent on the grid line intersections.

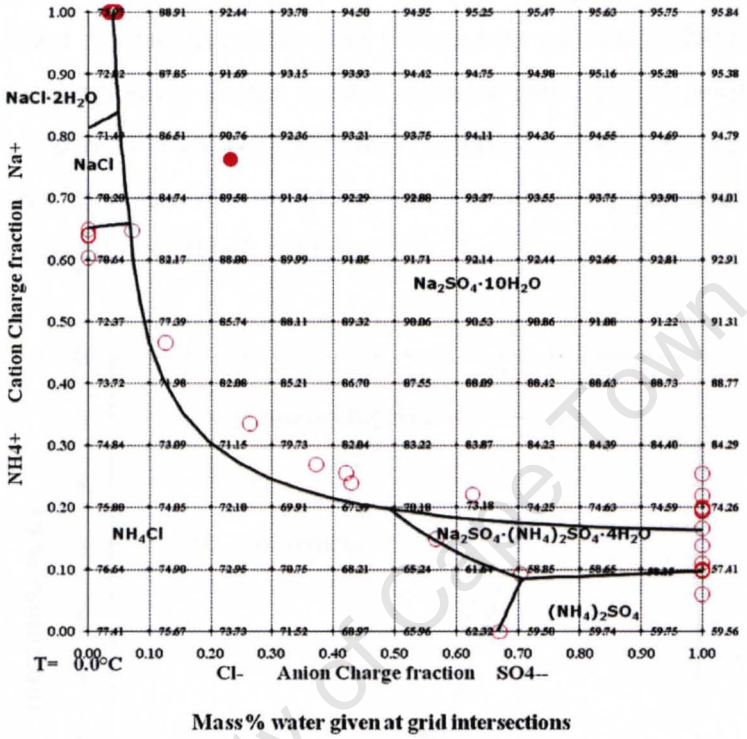

Figure 2.7: Jänecke projection of the Na^+:NH_4^+:Cl^-:SO_4^{2-} system at 0°C [27].

2.3.4 Thermodynamics for complex systems

The use of phase diagrams becomes impractical for systems with more than four ions and for this reason thermodynamic simulating tools are necessary. These tools should be able to accurately predict and simulate the phase equilibria of an aqueous system over a wide temperature range.

A simulating tool developed by OLI [25] is able to achieve this. It uses the framework of Helgeson and co-workers [28] for the standard state terms and the frameworks of Bromley, Zemaitis, Pitzer, Debye-Huckel and others for the excess terms [29]. The temperature at which the salts and ice crystallize, as well as the recoveries and yields of all solids, can be predicted using this simulation tool.

The phase equilibria of a system can also be simulated using the Extended UNIQUAC model [27]. This activity coefficient model is used to calculate the different salt saturation points directly and from this the phase equilibria can be described.

It is important to take into account the accuracy of the thermodynamic simulating tool during modelling since this can significantly affect the results obtained. Figure 2.8 shows a binary sodium sulphate phase diagram as predicted by OLI and the extended UNIQUAC model. The trends for the phase equilibria predicted by each model are similar. The results obtained from each model also compare well with experimental solubility data for a binary sodium sulphate system [27]. The results obtained from OLI are also at higher temperatures than the results predicted by the extended UNIQUAC model.

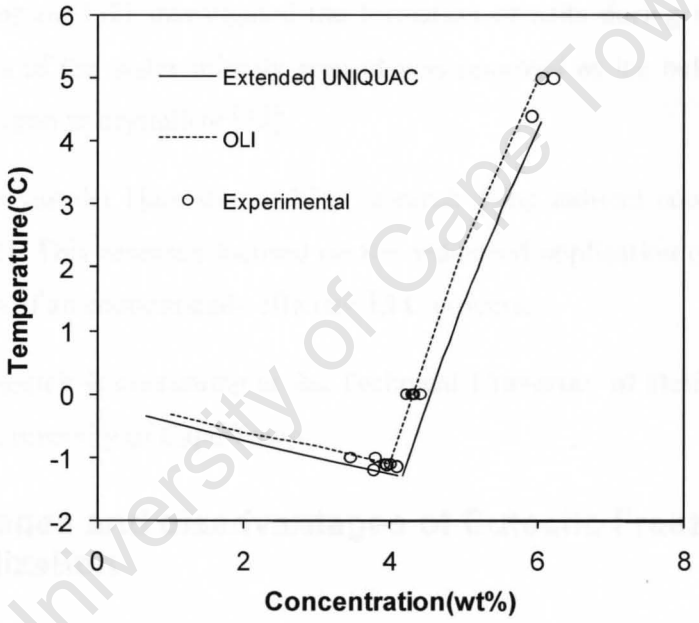

Figure 2.8: Thermodynamic modelling comparison [27;29].

2.4 The Eutectic Freeze Crystallization Process

2.4.1 The history of Eutectic Freeze Crystallization

In 1952, the Organisation for European Economic Cooperation convened a meeting to discuss options for sea water desalting. This team, with delegates from Belgium, Denmark, England, France, Germany, The Netherlands and Sweden, and observers from Australia, South Africa, United States of America and the Rockefeller Foundation, concluded that a freezing method for sea water desalting was difficult and economically impractical [30]. It

was this conclusion that lead to a delay into the research of using freezing as a water treatment method. In fact, it was only in the 1970's that this research was conducted. To this day people remain sceptical of freeze concentration as a water treatment option.

Stepakoff and co-workers first introduced EFC in the early 1970's as a separation technique [24] while Barduhn and co-workers devised the first process [31]. A decade later Swenne and co-workers investigated using this technique for the production of sodium chloride. Direct cooling, as opposed to indirect cooling, was used by these three researchers [24].

Barduhn and Manudhane investigated the use of EFC with natural waters in 1979. They concluded that EFC would operate well at temperatures no lower than -25°C for natural waters containing the following ions: Na^+,$K^+$$Ca^{2+}$,$Mg^{2+}$,$Cl^-$,$SO_4^{2-}$,$HCO_3^-$ [31].

Nelson and Thompson [32] investigated the formation of salts during the freezing of sea water. About 80% of the water initially present was removed as ice before $Na_2SO_4 \cdot 10H_20$ and $NaCl \cdot 2H_2O$ began to crystallize [33].

In the late 1990's van der Ham started EFC research using indirect cooling as opposed to direct cooling [32]. This research focused on the industrial application of the EFC concept and the realization of an economically efficient EFC process.

Presently EFC research is continuing at the Technical University of Delft and is also being conducted at the University of Cape Town.

2.4.2 Advantages and disadvantages of Eutectic Freeze Crystallization

The concept of freezing a solution in order to separate water and solutes is not a new one. Many authors have described such a method as a means of separation [30, 32, 34-35]. Eutectic Freeze Crystallization uses these concepts and focuses on a specific area of freeze crystallization, namely operating at the eutectic point of two components (ice and salt). By so doing a number of advantages can be achieved over conventional brine treatment methods, some of which are listed below:

- The process is not complicated by the addition of chemical compounds [35];

- From a thermodynamic perspective, as the heat of vaporisation is six times higher than the heat of fusion [24], freezing the brine as a means of treating it is theoretically less energy intensive than an evaporative process;
- Impurities are excluded from the ice structure during the crystallization of ice [36];
- The ice crystals that are produced can be used for cold heat storage [37];
- Gravitational separation of ice and salt is an added advantage during Eutectic Freeze Crystallization since, at eutectic conditions, both products separate as a result of their density differences. Salt sinks to the bottom of the crystallizer while ice floats to the top [38]. This phenomenon occurs in reality even though the thermodynamics predicts that two solids would exist at the eutectic point. This is because the system requires time (kinetics) to reach the equilibrium conditions predicted by the thermodynamics;
- Theoretically, a 100% yield can be obtained when operating at eutectic conditions [24];
- As the potential for corrosion is minimised due to the low operating temperatures [34], cheaper materials of construction can be used;
- Freeze crystallization is already used extensively in the concentrating of fruit juices as well as for the purifying of organic chemicals [3].

The most significant disadvantages of EFC are the capital costs (two or three times those of distillation or evaporation systems [3]) and scale limitations, but these can be overcome as the technology develops [24]. Industries are reluctant to accept a fundamentally new technique, especially when acceptable results are being obtained from old and proven techniques (Muller, 1976; as cited by [3]). Wiegandt and Von Berg [30] suggested that someday people and universities would realise that a freeze crystallization process for the treatment of waste water would be achievable with sound concepts and engineering. Only when brine disposal has to be considered, the economic focus changes, since the cost of disposal may be as much as the cost of fresh water produced, thus making a technology such as EFC more attractive as a separation method [31].

2.4.3 The operating principle

The operating principle of EFC can be described using a typical phase diagram for a binary aqueous solution as shown in Figure 2.9. The concentration of dissolved solids in waste waters is usually very low [39] (<35g/L), thus ice will generally crystallize first.

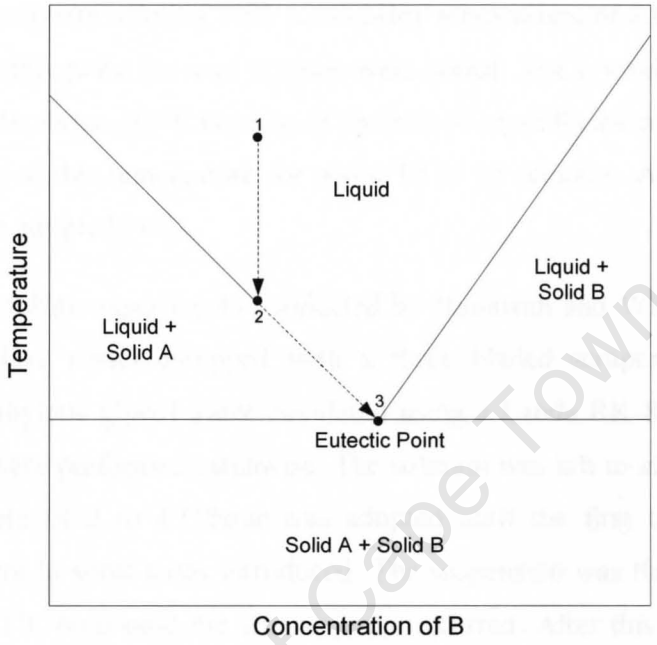

Figure 2.9: Typical phase diagram for an inorganic aqueous system.

The phase diagram used to describe the EFC process therefore has the starting position on the left side of the eutectic point because this is the region where ice crystallizes first. In EFC, the unsaturated solution (1) is cooled until the first crystal of A forms (2). The eutectic point is reached if the solution is cooled more (3). At this point both solid A and solid B are formed (3). Similarly, for a solution with a higher starting concentration than the eutectic concentration, the crystallization of salt will occur first, followed by ice at the eutectic point [38].

2.5 Review of previous experimental work for EFC

2.5.1 Case study: $MgSO_4$ solution

Himawan and Witkamp [40] investigated the use of EFC for the treatment of a magnesium sulphate stream. They determined that there was a narrow window of operation for batch crystallization during the crystallization of $MgSO_4 \cdot 12H_2O$ (between 0°C and -4°C and 17.4wt% to 20wt%). The $MgSO_4 \cdot 12H_2O$ crystals were unstable above 0°C since they

spontaneously transformed to $MgSO_4 \cdot 7H_2O$. This made the measurement of the crystal product difficult. The metastable zone of $MgSO_4 \cdot 12H_2O$ was also wide since ice crystallized above the thermodynamic eutectic composition.

The experimental procedure for treating a $MgSO_4$-H_2O system using EFC was as follows:

A 20wt% magnesium sulphate solution, with a solubility temperature of 3.09°C, was cooled down to -1.5°C and at this point ice seed crystals were added. The crystallizer temperature increased immediately to about -0.9°C because of the heat of crystallization. The temperature was then kept constant at this temperature for about 10 to 15 minutes. A linear or natural cooling policy was then adopted [40].

In other magnesium sulphate experiments conducted by Himawan and Witkamp [40], a 2L cylindrical jacketed glass vessel equipped with a three bladed scraper was used. The refrigerant used was ethylene glycol-water circulated using a Lauda RK 8 KP thermostatic unit. All experiments were performed batchwise. The solution was left to stabilize at 0°C for 2 hours. A cooling rate of 2 to 4°C/hour was adopted until the first temperature jump occurred. Ice seeds were in some cases introduced. The suspension was then cooled further with a cooling rate of 1°C/hour until the second jump occurred. After this second jump the cooling rate was kept constant. The experiments were stopped once an overload indication was signalled by the motor as a result of excessive scaling of the reactor contents which made stirring more difficult. This usually occurred 2 hours after the first temperature jump. Ultra pure water and a saturated magnesium sulphate solution were used to wash ice and salt crystals when measuring the purity of the products. The actual purity was obtained by chemical analysis [40].

Himawan and Witkamp [40] reported that the most stable hydrate at subzero temperatures was magnesium sulphate dodecahyrate ($MgSO_4.12H_2O$) when in actual fact it was $MgSO_4.11H_2O$ [38]. This salt (mineral) has since been accepted by the Industrial Minerals Association (IMA) and named meridianiite.

2.5.2 Case study: $CuSO_4$ solution

Van der Ham and co-workers [32] ran EFC experiments using a copper sulphate solution. Experiments were performed in a 250ml jacketed glass vessel. Indirect cooling, with ethylene glycol as the coolant, was used in the experiments. A Lauda RK 8 KP thermostatic unit was

used to cool the ethylene glycol. Agitation was provided by a magnetic stirrer. The crystallizer temperature was measured using a PT-100 sensor connected to the RK 8 KP.

In batch experiments the solution was supercooled to 1.0°C below the eutectic temperature of the system. The temperature was kept constant and ice seeds were added. After one hour a solid ice phase formed. The reactor was then heated until all the solids vanished. The liquid was again supercooled and the experiment was repeated, but this time with salt seeds. The eutectic temperature of the copper sulphate system from the experiments was found to be -1.55°C [32].

2.5.3 Case study: K_2SO_4 solution

Drummond and co-workers [41] used EFC technology on an industrial solution containing potassium sulphate and organic impurities and successfully demonstrated EFC as a separation technique for this stream [41].

The experimental equipment of Drummond and co-workers [41] consisted of a 2L batch suspension crystallizer with a 3 legged scraper set at a speed of 80rpm. A thermostatic unit provided the cooling. Experiments were conducted in a climate chamber kept at 10°C. All experiments were unseeded. A linear cooling rate of 0.1°C/min was applied before the eutectic condition was reached. After the eutectic temperature was reached, the cooling rate was set at 0.03°C/min. During the experiments, samples were taken using a 5ml pipette. Ice crystals were washed with sub-cooled demineralised water. Both solid and liquid samples were analysed by inductive coupled spectrometry. The purity of the ice increased from about 85 to 99wt%.

2.5.4 Case study: KNO_3 solution

Vaessen and co-workers [32] investigated the application of EFC to a KNO_3 solution. The experimental equipment consisted of a crystallizer with a conical shape at the top and bottom for collection of solids. The conical sections of the crystallizer were not cooled. Scrapers were used to prevent scaling on the walls of the crystallizer. The rotation rate of the scraper was between 7rpm to 43rpm. Ice samples were taken directly from the crystallizer and filtered on a glass filter. Washing was performed with sub-cooled demineralised water on a glass filter. All samples were quickly transported to a climate chamber kept at -2°C. Samples

of both ice and salt were analysed for cationic impurities by ICP-AES spectrometry. Anionic impurities in the KNO_3 samples were determined by ion chromatography [32].

These case studies showed that an aqueous inorganic stream could be separated into pure salt as well as pure ice. However, no research has been conducted on the sequential removal of more than one salt from a complex stream.

2.6 The economics of an EFC process

Eutectic Freeze Crystallization has been successfully utilized for the separation of a single salt and water. However, a complete economic and technical feasibility have not been determined for the sequential removal of salt(s) from complex hypersaline brines that are typical of reverse osmosis retentates in South Africa. Although the focus of this thesis is primarily on the technical feasibility of an EFC system as applied to hypersaline brine treatment, a brief summary of the economics of the process, as applied to other systems, is also given.

Vaessen [32] investigated the use of EFC for the separation of $CuSO_4 \cdot 5H_2O$ and ice from a copper sulphate solution. The researcher determined that energy reductions of up to 70%, when compared to conventional 3-stage evaporative crystallization, were achievable for copper sulphate solutions.

A separate study involving an industrial KNO_3-HNO_3 solution was conducted by van der Ham [24]. The researcher concluded that the energy costs (total costs for steam, electricity and cooling water) were significantly lower for an industrial KNO_3-HNO_3 solution, with a 69% reduction when compared to evaporative crystallization.

Himawan [42] conducted an economic evaluation of an EFC system for recovering magnesium sulphate and ice from an industrial waste stream. It was found that EFC could save up to 60% of the energy costs when compared to evaporative crystallization. In addition, the investment cost only increased by 7%.

Two synthetic brines, based on actual brines from the South African mining industry, were evaluated in terms of economic feasibility by Nathoo and co-workers [43]. The researchers showed that the operating cost savings of using EFC over evaporative crystallization was

80% and 85% for two Na_2SO_4 and NaCl brines of varying concentrations. Furthermore, these calculated cost savings excluded the potential income that could be generated from the sale of the pure salts produced during the EFC process thus further strengthening the case for EFC. The capital cost for an EFC process, as compared to evaporative crystallization, was 179% to 208% higher for EFC. However, the researchers highlighted that EFC is a new process with significant room for technology improvements and thus capital cost reductions. Conversely, evaporative crystallization, as well as many other existing technologies, is already well established, with only incremental future equipment cost savings expected as a result of any further technology improvements.

In summary, the economics of an EFC process depends very much on the composition of waste water used. Substantial operating cost savings are likely be achieved with EFC, whilst the capital cost for EFC, when compared to evaporative crystallization processes, are expected to be higher for EFC. As with all new technologies, the EFC capital cost is expected to decrease as the technology develops. Despite this, it is expected that for moderate operating temperatures (+10°C to -10°C), the substantially lower EFC operating cost is likely to, within a short period, offset the initial higher capital cost for EFC with continued savings over evaporative crystallization and many other technologies.

2.7 Problem statement

Eutectic Freeze Crystallization is an attractive water treatment technology but to date it has not been utilized for complex systems such as brines. A protocol for the treatment of hypersaline brines using EFC is therefore necessary in order to show the feasibility of this technology.

2.8 Objectives of the present study

The major objectives of the project are as follows:

1. To establish a brine treatment protocol using Eutectic Freeze Crystallization,
2. Determine the operating region or metastable zone of a brine for Eutectic Freeze Crystallization,
3. Investigate methods to sequentially remove pure salts from a brine.

The brine treatment protocol consists of three important aspects, namely brine analysis (1), thermodynamics (2) and kinetic aspects (3). These aspects are interlinked like a gear and are shown in Figure 2.10.

Figure 2.10: Important steps of the brine treatment protocol.

The corresponding colour coding for each aspect of the protocol is used to describe chapters of this thesis that correspond to the appropriate step of the protocol. For example, chapters 5, 6 and 7 are described by a red gear because the main focus of these chapters all relate to kinetic aspects of the brine treatment protocol.

2.9 Scope and novel aspects of study

This study is confined to a single industrial brine (of varying concentration) that is typical of a complex hypersaline brine produced in the mining industry of South Africa. It focuses on the extreme case of a dilute brine since, if EFC is shown to be feasible for a dilute brine, it would certainly be feasible for a concentrated one. The project only focuses on the sequential removal of sodium sulphate, calcium sulphate and water from the brine. All the experimental work will be conducted at atmospheric pressure and will only utilise indirect cooling.

One of the original contributions of this project lies in the fact that the metastable zone has not been determined using the stochastic nature of nucleation. Also, the concept of seeding

within the metastable zone to prevent salt contamination has not been conducted under EFC conditions. Finally, the sequential removal of salts during EFC operation has not been achieved before (proof of concept).

References

[1] A.M. van Niekerk, Mine water reclamation and re-use – South African experience, International Mine Water Conference, Pretoria, South Africa, 2009 http://www.ewisa.co.za/misc/WISAConf/default2008.htm.

[2] P. Dama-Fakir, A. Toerien, A. Wurster, Field testing to determine the evaporation rate of brine solutions formed during membrane treatment of mine water, Water Research Commission, South Africa, 2010, report no.: K5/1895-1.

[3] M.S. Rahman, M. Ahmed, X.D. Chen, Freezing-melting process and desalination: review of present status and future prospects, International Journal of Nuclear Desalination 2 (2007) 253 –264.

[4] M. Ahmed, W.H. Shayya, D. Hoey, A. Mahendran, R. Morris, J. Al-Handaly, Use of evaporation ponds for brine disposal in desalination plants, Desalination 130 (2000) 155-168.

[5] S. Adham, J. Oppenheimer, M. Kumar, Innovative approaches to RO concentrate management: beneficial reuse and concentration minimization, WEFTEC, Dallas, USA, 2006.

[6] G. Johnson, L. Stowell, M. Monroe, VSEP Treatment of RO Reject from brackish well water- A comparison of conventional treatment methods and VSEP, a Vibrating Membrane Filtration System, El Paso Desalination Conference, El Paso Texas, United States of America, 2006.

[7] Proxa, An investigation of innovative approaches to brine handling, Water Research Commission, South Africa, 2007, report no.: K5/1669-3.

[8] L. Foster, J. Kepke, R. Sommer, D. McCann, Hold the salt: innovative treatment of RO concentrate,WEFTEC, Chicago, USA, 2008.

[9] A. Neba, P.D. Rose, The Rhodes Biosure process in Acid Mine Drainage wastewater treatment: process development at pilot-scale, WISA Biennial Conference, Durban, South Africa, 2006.

[10] A. Myserson, Handbook of Industrial Crystallization. 2nd edn, Butterworth-Heinemann, USA, 2002.

[11] M. Loffelmann, A. Mersmann, How to measure supersaturation, Chemical Engineering Science 57 (2002) 4301-4310.

[12] J.A. Dirksen, T.A. Ring, Fundamentals of crystallization: kinetic effects on particle size distributions and morphology, Chemical Engineering Science 46 (1991) 2389–2427.

[13] C.Y. Tai, C. Tai, M. Chang, Effect of interfacial supersaturation on secondary nucleation, Journal of the Taiwan Institute of Chemical Engineers 40 (2009) 439-442.

[14] J.W. Mullin, Crystallization. 4th Edition, Butterworth Heinemann, London, 2001.

[15] P.W. Wilson, A.F. Heneghan, A.D.J. Haymet, Ice nucleation in nature: supercooling point (SCP) measurements and the role of heterogeneous nucleation, Cryobiology 46 (2003) 88-98.

[16] K. Sangwal, Novel approach to analyze Metastable Zone Width determined by the polythermal method: physical interpretation of various parameters, Crystal Growth and Design 9 (2009) 942-950.

[17] S. Chen, P. Wang, T. Lee, An experimental investigation of nucleation probability of supercooled water inside cylindrical capsules, Experimental Thermal and Fluid Sciences 188 (1998) 299-306.

[18] K.E. Zachariassen, E. Kristiansen, S.A. Pedersen, H.T. Hammel, Ice nucleation in solutions and freeze-avoiding insects- homogeneous or heterogeneous?, Cryobiology 48 (2004) 309-321.

[19] J. Nyvlt, R. Rychly, J. Gottfried, J. Wurzerlova, Metastable zone-width of some aqueous solutions, Journal of Crystal Growth 6 (1970) 151-162.

[20] N. Kubota, A new interpretation of metastable zone widths measured for unseeded solutions, Journal of Crystal Growth, 310 (2008) 629-634.

[21] J. Nyvlt, Industrial Crystallization from solutions, 1st edn, Butterworth, London, 1971.

[22] R.W. Rousseau, F.P. O'Dell, Separation of multiple solutes by selective nucleation, Industrial and Engineering Chemistry Process Design and Development 19 (1980) 603-608.

[23] C.Y. Tai, W.L. McCabe, R.W. Rousseau, Contact nucleation of various crystal types, American Insitute Of Chemical Engineers Journal 21 (1975) 351-358.

[24] F. Van der Ham, Eutectic Freeze Crystallization. PhD Thesis. Technical University of Delft, The Netherlands, 1999.

[25] OLI Systems Inc., OLI Stream Analyser, Version 3.0, Morris Plains, New Jersey, USA, 2010.

[26] Ternary phase diagrams, 2008 http://www.tulane.edu/~sanelson/geol212/ternaryphdiag.htm

[27] K. Thomsen, Aqueous electrolytes: model parameters and process simulation, PhD Thesis, Technical University of Denmark, Denmark, 1997.

[28] H.C. Helgeson, D.H. Kirkham, G.C. Flowers, Theoretical prediction of the thermodynamic behavior of aqueous electrolytes at high pressures and temperatures, American Journal of Science 274 (1974) 1089-1198.

[29] OLI Systems Inc., Getting started with Hysis OLI, Morris Plains, New Jersey, USA, 2006.

[30] H.F. Wiegandt, R.L. von Berg, Myths about freeze desalting, Desalination 33 (1980) 287-297.

[31] A. Barduhn, A. Manudhane, Temperature required for eutectic freezing of natural waters, Desalination 28 (1979) 233-241.

[32] R. Vaessen, Development of scraped eutectic crystallizers. PhD Thesis. Technical University of Delft, The Netherlands, 2003.

[33] G.L. Stepakoff, D. Siegelman, R. Johnson, W. Gibson, Development of eutectic freezing process for brine disposal, Desalination 14 (1974) 25-38.

[34] W.E. Johnson, State of the art freezing processes, their potential and future, Desalination 19 (1976) 349-358.

[35] O. Lorain, P. Thiebaud, E. Badorc, Y. Aurelle, Potential of freezing in wastewater treatment: soluble pollutant applications, Water Research 35 (2001) 541-547.

[36] R. Halde, Concentration of impurities by progressive freezing, Water Research 14 (1980) 575-580.

[37] Y. Shirai, M. Wakisaka, O. Miyawaki, S. Sakashita, Effect of seed ice on formation of tube ice with high purity for a freeze wastewater treatment system with a bubble-flow circulator, Water Research 33 (1999) 1325-1329.

[38] F.E. Genceli, Scaling-up eutectic freeze crystallization. PhD Thesis. Technical University of Delft, The Netherlands, 2008.

[39] O. Lorain, P. Thiebaud, E. Badorc, Y. Aurelle, Potential of freezing in wastewater treatment: soluble pollutant applications, Water Research 35 (2001) 541-547.

[40] C. Himawan, G.J. Witkamp, Crystallization kinetics of $MgSO_4.12H_2O$ from different scales of batch cooling scraped crystallizers, Crystal Research Technology 41 (2006) 865-873.

[41] L.S. Drummond, R. Vaessen, C. Himawan, M.M. Seckler, G.J. Witkamp, A method for rapid development of eutectic freeze crystallization processes: application to potassium sulphate solution contaminated with organics, Chemical Engineering Transactions AIDIC 1 (2002) 921-926.

[42] C. Himawan, Characterization and Population Balance Modelling of Eutectic Freeze Crystallization. PhD Thesis. Technical University of Delft, The Netherlands, 2005.

[43] J. Nathoo, R. Jivanji, A.E. Lewis, Freezing your brines off: Eutectic Freeze Crystallization for brine treatment, International Mine Water Conference, Pretoria, South Africa, 431-437, 2009.

CHAPTER 3 : BRINE ANALYSIS

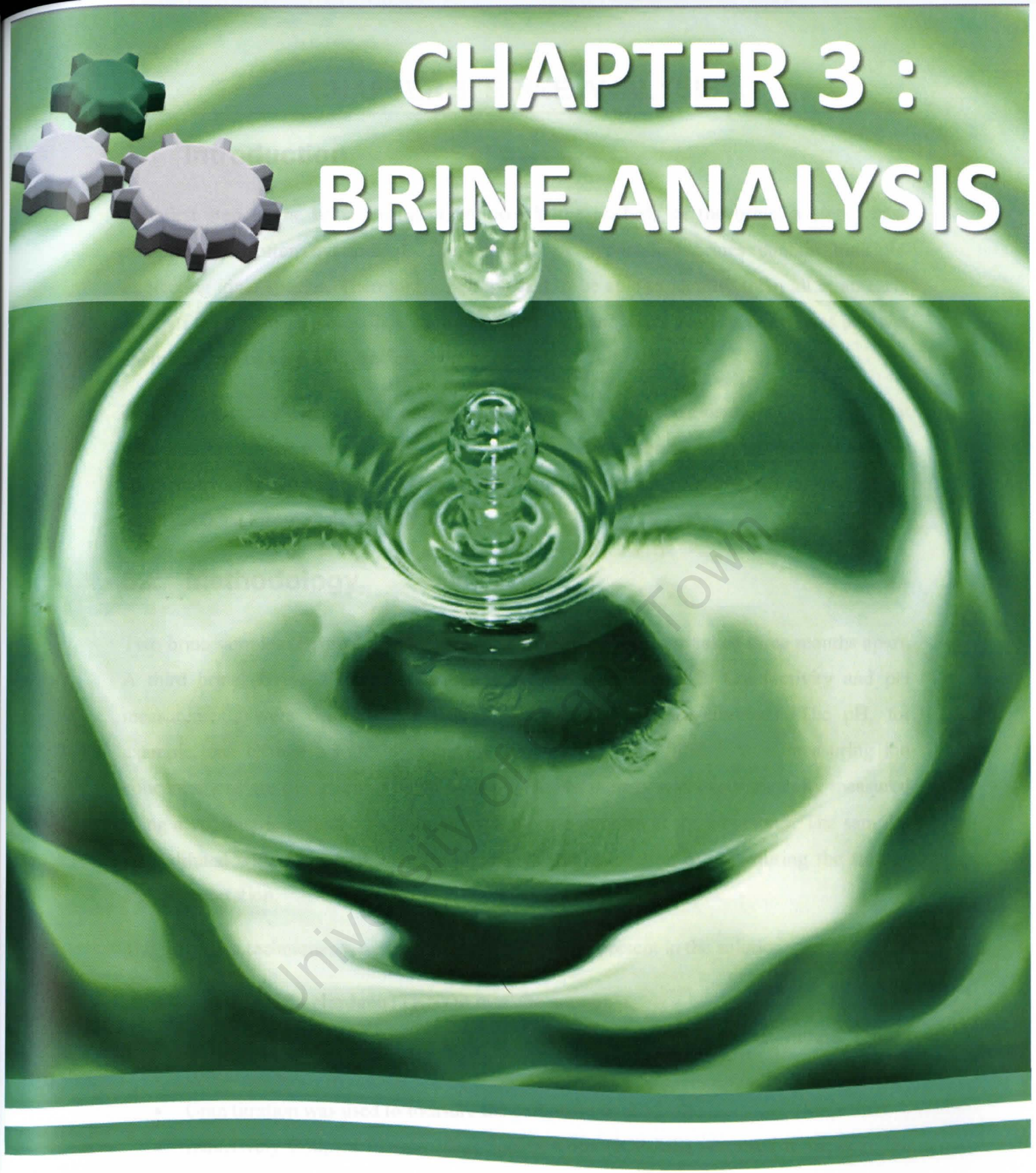

In an age when man has forgotten his origins and is blind even to his most essential needs for survival, water along with other resources has become the victim of his indifference

Rachel Carson

Graphic from: http://farm3.static.flickr.com/2494/3908668250_0778e6388d_o.jpg

3.1 Introduction

The first step in the brine treatment protocol is the analysis of the brine, a step whose complexity is often overlooked. The majority of hypersaline brines contain multiple, interacting ionic species. Therefore it is important to be able to identify them all at an early stage of the treatment protocol. A combination of standard water analysis techniques and wet chemistry can be used to characterize the brine.

The brine samples used in this study were obtained from a reverse osmosis (RO) plant that was built to recover potable water from the waste water generated during coal mining.This chapter gives the procedure necessary to perform the analysis of the brines as well as the results obtained from such an analysis.

3.2 Methodology

Two brine samples (**Brine 1** and **Brine 2**) from the RO plant were taken three months apart. A third brine (**Brine 2'**) was obtained by concentrating **Brine 2**. Conductivity and pH measurements were conducted on site to ensure accurate measurements. The pH, for example, can change within 24 hours of sampling [1]. The difficulties in measuring ion concentrations are discussed in depth by Zibi [1]. The density was experimentally measured using a volumetric cylinder upon arrival of the brine samples at the laboratory. The samples were diluted with de-ionised water to prevent the crystallization of salts during the storage and transportation.

The following techniques were used to measure the ions present in the solution:

- Total Kjeldahl Nitrogen (TKN) to measure ammonia,
- The Spectroquant® NOVA 60 A photometer to measure the nitrate (NO_3^-) concentration,
- Gran titration was used to measure the carbonate concentration,
- Inductively Coupled Plasma Mass Spectroscopy (ICP-MS) was used to measure the other cations and anions.

Figure 3.1 gives a summary of the methodology for the brine analysis.

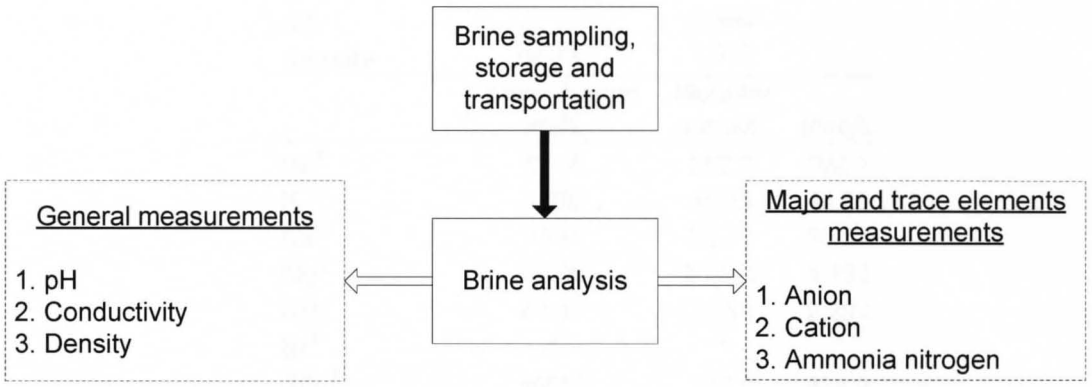

Figure 3.1: Brine analysis procedure [2].

3.3 Results and discussion

3.3.1 The RO brine samples

Table 3.1 shows the results obtained from the analysis of the two RO brine samples (**Brine 1** and **Brine 2**). The conductivity and density of the samples are similar while the pH is different (6.56 for **Brine 1** and 7.28 for **Brine 2**).

The dominant cations (Na^+, K^+, Ca^{2+}) and anions (SO^{2-}, Cl^-) give an indication of the possible identities of the salts that could crystallize under EFC conditions. The salts will likely be sodium, potassium and calcium sulphate or chloride salts. However, this does not necessarily mean these salts will form under EFC conditions. It is only by conducting a thermodynamic modelling exercise and experimental work that the identity of the salts can be predicted and confirmed.

The concentration of anhydrous sodium sulphate is less than 2wt% for both brines and this is lower than the eutectic concentration (4.2wt%; [3]) of a binary sodium sulphate system. This indicates that ice is expected to crystallize before any salt crystallization. The presence of other components can affect the eutectic temperature of either ice or salt [4]. However, the crystallization temperature of ice will be different while the sequence of the crystallizing components (ice and salts) is unlikely to be affected.

Table 3.1: Brine analysis results for two different RO samples.

Brine 1			
Temperature	**°C**	22	
Conductivity	**mS/cm**	22.2	
pH		6.560	
Density	**g/cm^3**	1.019	
	Concentration mg/L	**Molality mmol/L**	**meq/L**
Na^+	6718	292.2	292.2
K^+	1808	46.25	46.25
Ca^{2+}	1338	33.39	66.78
Mg^{2+}	74.96	3.0840	6.168
NH_4^+	41.47	2.299	2.299
Sr^{2+}	*	*	*
SO_4^{2-}	16050	167.1	334.2
Cl^-	954.6	26.92	26.92
NO_3^-	398.4	6.425	6.425
HCO_3^-	61.24	1.004	1.004
F^-	*	*	*
PO_4^{3-}	*	*	*
Total Cation	**meq/L**	413.7	
Total Anion	**meq/L**	368.5	
Imbalance	**%**	5.766	

*ions not measured

Brine 2			
Temperature	**°C**	22	
Conductivity	**mS/cm**	19.26	
pH		7.28	
Density	**g/cm^3**	1.020	
	Concentration mg/L	**Molality mmol/L**	**meq/L**
Na^+	5796	252.1	252.1
K^+	3871	99.00	99.00
Ca^{2+}	1058	26.39	52.78
Mg^{2+}	170.2	7.005	14.01
NH_4^+	66.43	4.743	4.743
Sr^{2+}	11.89	0.1357	0.2715
SO_4^{2-}	15600	162.03	324.1
Cl^-	1504	42.42	42.42
NO_3^-	167.3	2.699	2.699
HCO_3^-	151.1	2.476	2.476
F^-	13.57	0.7141	0.7141
PO_4^{3-}	4.703	0.04952	0.1486
Total Cation	**meq/L**	422.9	
Total Anion	**meq/L**	372.5	
Imbalance	**%**	6.335	

The concentration of individual ions does vary between each brine with no observable trend. This variation in the concentrations of cations and anions for the two brine samples is unlikely to affect the operation of the EFC process since the system will adjust or move to a new eutectic point where the crystallization of two components can still occur.

The concentrations of various cations and anions are only useful for the thermodynamic modelling step if the ion imbalance is within an acceptable range (<10% [5]). If the ion imbalance is too high then the accuracy of the analysis and hence the actual component concentrations can be questioned. The ion imbalance, shown in Table 3.1, was 5.8% for **Brine 1** and 6.3% for **Brine 2**. This was deemed acceptable considering the complex nature of the brines.

Table 3.2 gives an indication of how dilute the brine samples are. The salts making up the synthetic brine in Table 3.2 are calculated based on the brine analysis shown in Table 3.1. Table 3.2 gives a purely theoretical indication of the amount of salts necessary for a synthetic brine so that every possible ion is accounted for. However, because there is a charge imbalance, a dominant ion needs to be added to ensure a balance is achieved. The dominant ion in both instances was the sulphate ion.

Table 3.2: Synthetic brine makeup based on ion concentrations.

	Brine 1 g/L	Brine 2 g/L
Na_2SO_4	18.77	14.72
$CaSO_4$	4.545	3.593
K_2SO_4	3.470	7.585
NaCl	1.574	2.479
KNO_3	0.6496	1.208
$MgSO_4$	0.3713	0.8432
$(NH_4)_2SO_4$	0.3038	0.6267
$NaHCO_3$	0.08432	0.2080
Total	29.77	31.26

Note: Excess sulphate ions added to ensure there was an ion balance.

Table 3.2 also indicates that both brine samples were dilute when compared with sea water which generally has about 35g/L dissolved solids [6]. In addition, **Brine 1** was slightly more dilute than **Brine 2** (29.77g/L and 31.26g/L respectively). The reason for the low concentration of dissolved solids can be attributed to the source of the brine. The brine was obtained from an RO plant and although RO does concentrate a water stream significantly, it

can only concentrate it up to the level of the component with the lowest solubility, in this instance calcium sulphate. For example, the solubility of anhydrous $CaSO_4$ at 25°C is 2.1g/L [3] while the solubility of Na_2SO_4, also anhydrous, is more than a hundred times higher (215g/L at 25°C [3]). The remaining component concentrations in the stream will therefore remain low. The other components would have a much higher final concentration if there was no calcium present in the water stream and if the stream was then passed through an RO plant.

3.3.2 The concentrated brine

Brine 2 was concentrated by removing ~70% of the water, resulting in **Brine 2'** (see Chapter 7 for details of the concentrating procedure). The analysis of this concentrated brine is shown in Table 3.3. The brine was significantly concentrated, as indicated by the increase in the ion concentrations compared to those of the original **Brine 2** (Table 3.2). The ion imbalance for this brine was low, with a value of 2.4%.

Table 3.3: Concentrated brine analysis.

		Brine 2'
Temperature	°C	20
Conductivity	mS/cm	39.23
pH		8.3
Density	g/cm^3	1.042

	Concentration mg/L	Molality mmol/L	meq/L
Na^+	14200	617.5	617.5
K^+	4351	111.3	111.3
Ca^{2+}	2927	73.028	146.06
Mg^{2+}	347.2	14.29	28.57
NH_4^+	331.2	18.36	18.36
Sr^{2+}	41.20	0.4702	0.9403
SO_4^{2-}	41400	431.1	862.3
Cl^-	2115	59.65	59.65
NO_3^-	2105	33.95	33.95
HCO_3^-	735.0	12.046	12.046
F^-	3.200	0.1684	0.1684
PO_4^{3-}	4.200	0.04424	0.1327

Total Cation	meq/L	922.7
Total Anion	meq/L	968.2
Imbalance	%	2.406

3.4 Conclusions

The ion imbalances from the analysis of two brine samples obtained from a RO plant were found to be 5.8% and 6.3% while the concentrated brine, **Brine 2'**, had a charge imbalance of 2.4%. The dominant sulphate anion was chosen in order to ensure an ion balance. This was used to makeup the synthetic brine. The brines were also very dilute with a total dissolved content of 29.77g/L for **Brine 1** and 31.26g/L for **Brine 2**.

References

[1] W. Pulles, *Mine water reference manual*, Pulles Howard & de Lange Incorporated, 1993.

[2] L.M. Zibi, Industrial brine characterisation and modelling, MSc. Thesis. University of Cape Town, South Africa, 2010.

[3] K. Thomsen, Aqueous electrolytes: model parameters and process simulation, PhD Thesis, Technical University of Denmark, Denmark, 1997.

[4] A.E. Lewis, J. Nathoo, S.T. Reddy, D.G. Randall, Novel technology for recovery of water and solid salts from hypersaline brines: Eutectic Freeze Crystallization, Water Research Commission, South Africa, Progress Report 2, 2008.

[5] L. Carvalho, Costly mistakes in water treatment plant design for power plant projects, Conference of Electric Power Supply Company, Macau, China, 2008.

[6] Physics and chemistry of sea water, 2010 http://www.waterencyclopedia.com/Re-St/Sea-Water-Physics-and-Chemistry-of.html.

CHAPTER 4 : THERMODYNAMIC MODELLING

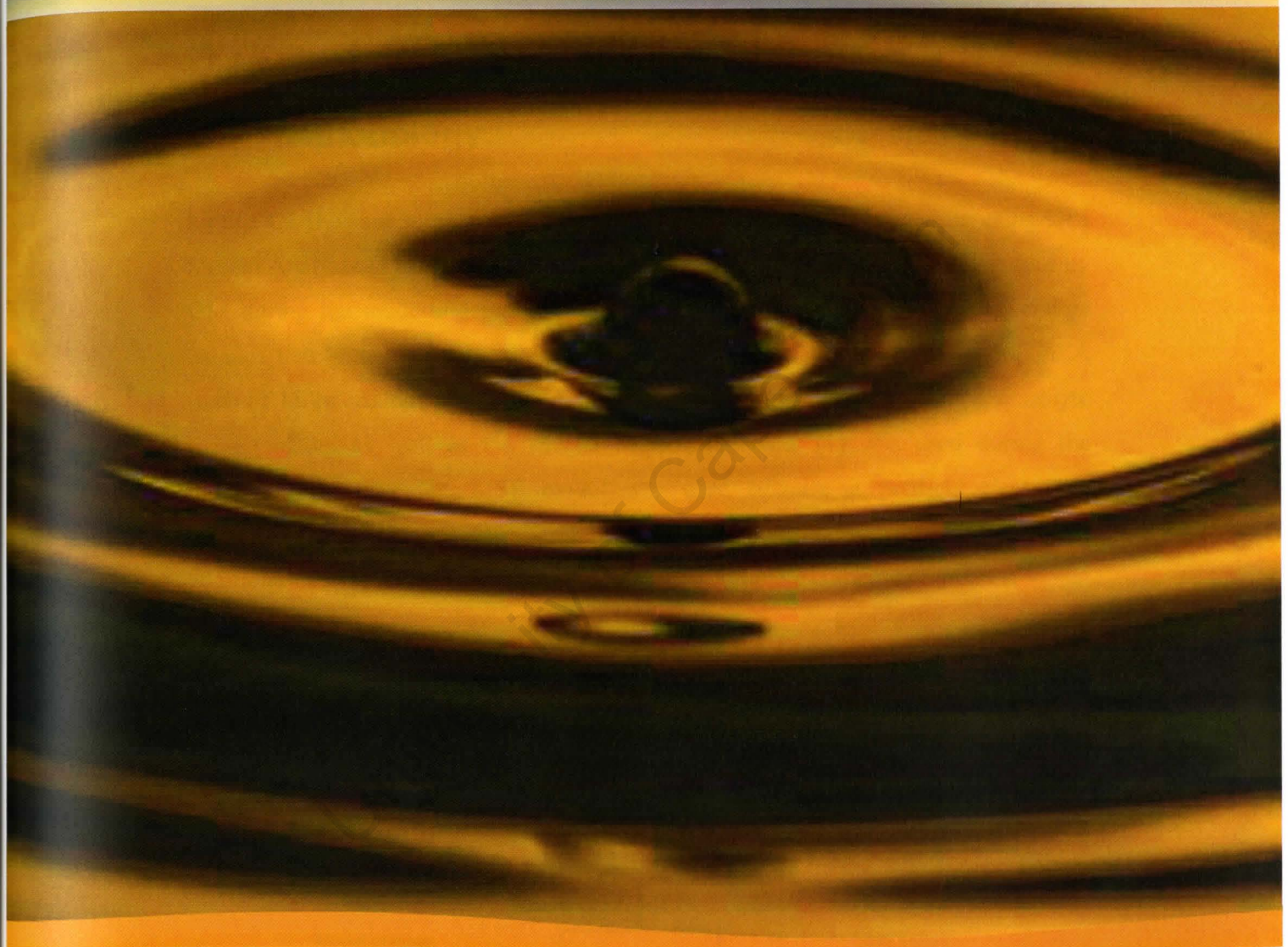

Water is a good servant, but it is a cruel master.

John Bullein, 1562

Graphic from: http://www.ephotozine.com/article/Water-drop-photography-12434

4.1 Introduction

Once the analysis of the brines has been attained, thermodynamic modelling can be used to predict the identities of the potential salts, the temperatures at which they will crystallize, as well as the potential yields of the various products.

This chapter gives the procedure necessary to perform the thermodynamic modelling for such brines as well as the results obtained.

4.2 Methodology

Figure 4.1 shows a summary of the thermodynamic modelling procedure using OLI Stream Analyser [1]. The blocks in bold are the particular names of the steps used by OLI during the modelling process. The **Water Analysis** option performs a charge balance that is then used to model the aqueous chemistry in the **Stream** option. A basis of 1L of solution was used for the simulations. The Mixed Solvent Electrolyte (MSE) model as well as the special $MgSO_4$ databank [1] was used during the modelling process. The MSE model was used because it predicts electrolyte behaviour for a wide concentration range; from infinite dilution to molten salts. The addition of the $MgSO_4$ databank provided a more complete component list.

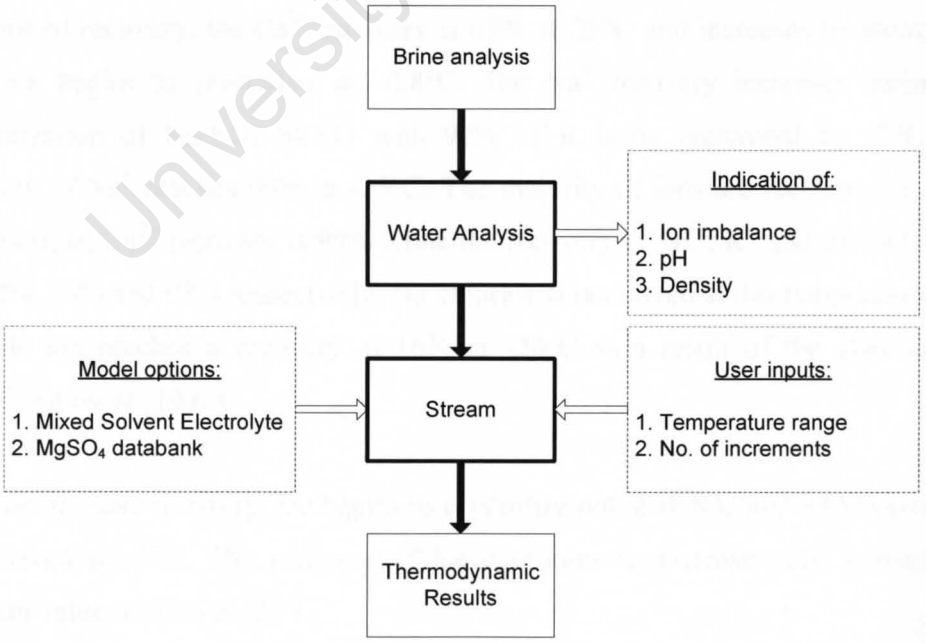

Figure 4.1: Thermodynamic modelling procedure [1].

The final result is a thermodynamic simulation of the brines, similar to Figure 4.2 and Figure 4.4 in this chapter.

4.3 Results and discussion

4.3.1 Brine 1 and Brine 2

Figure 4.2 shows the recovery of water and various salts and ions as the temperature of **Brine 1** is decreased from 25°C to -25°C. The data used to plot Figure 4.2 was obtained from OLI Stream Analyser [1]. The salt and ion recoveries are plotted on the primary y-axis, and the water recovery on the secondary y-axis. Each data point in Figure 4.2 represents an equilibrium condition. The mass of a component crystallizing from the solution is therefore as a result of the system reaching a new equilibrium condition. Table 4.1 shows the nucleation temperatures of the various components as predicted by the OLI thermodynamic modeling procedure.

The model predicts that the system is already saturated with respect to $CaSO_4 \cdot 2H_2O$ at 25°C. It also predicts that water (in the form of ice) will begin to crystallize at -0.8°C followed by $Na_2SO_4 \cdot 10H_2O$ at -1.5°C. A double salt, $K_2SO_4 \cdot CaSO_4 \cdot 1H_2O$, begins to crystallize at -2.2°C followed by KCl at a lower temperature of -19.6°C.

In terms of recovery, the Ca^{2+} recovery is 65% at 25°C and increases to above 77% once ice begins to crystallize at -0.8°C. The Na^+ recovery increases during the crystallization of $Na_2SO_4 \cdot 10H_2O$ with 92% of it being recovered by -5°C. The recovery of Na^+ reaches 99% at -25°C. The majority of ions are recovered at -5°C. For example, Ca^{2+} recovery is 99% while the recovery of Na^+, K^+ and the SO_4^{2-} ions are 92%, 74% and 97% respectively. No chloride is recovered at this temperature. The chloride ion reaches a recovery of 16% at -20°C as a result of the start of KCl crystallization at -19.6°C.

In terms of water recovery, ice begins to crystallize out at -0.8°C and a 95% recovery is achieved at -5°C. The recovery of ice continues to increase until it reaches a constant value of 97% at -21°C.

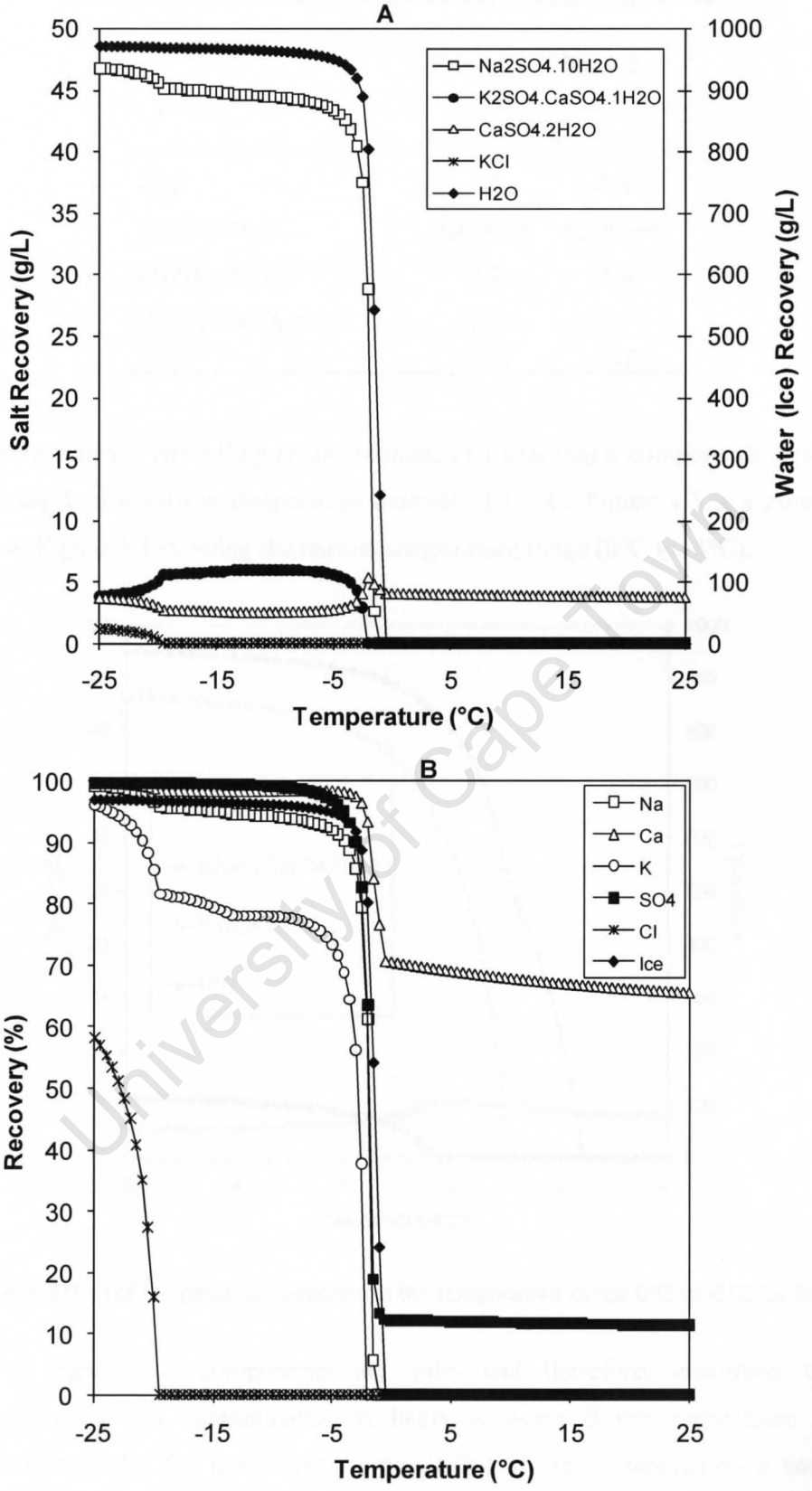

Figure 4.2: Effect of temperature reduction on salts and water recovery for **Brine 1** (salts (A) and ions (B).

Table 4.1: Solid nucleation temperatures for **Brine 1** and **Brine 2**.

	Brine 1	**Brine 2**
	Temperature °C	
H_2O	-0.8	-0.9
$CaSO_4 \cdot 2H_2O$	saturated	saturated
$Na_2SO_4 \cdot 10H_2O$	-1.5	-1.9
$K_2SO_4 \cdot CaSO_4 \cdot 1H_2O$	-2.2	-2.1
KCl	-19.6	-16.6

The thermodynamic modelling results indicate that four major components crystallize from **Brine 1** in a narrow temperature interval of 1.4°C. Figure 4.3 is a zoomed in section of Figure 4.2 showing the narrow temperature range (0°C to -5°C).

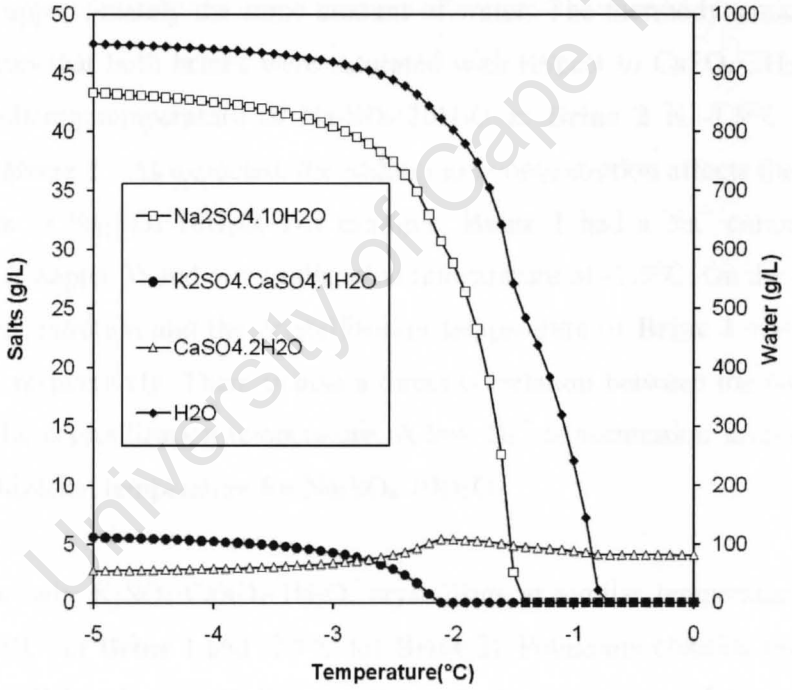

Figure 4.3: Effect of temperature reduction in the temperature range 0°C to -5°C for **Brine 1**.

Three of these four components are salts and therefore, according to the thermodynamics, salt contamination is likely to occur if the temperature is not controlled precisely. The reason for the possibility of salt contamination is based on the fact that the EFC process works on the utilization of the density difference between salt and ice. The process is not effective if two or more salts crystallize at

EFC conditions since the salts, having similar densities, would sink to the bottom of the crystallizer making separation unlikely. The purity of the salts formed would therefore ultimately be affected.

However, these results are based on thermodynamic predictions and do not consider the use of kinetics and process manipulations, such as selective seeding, that could be adopted in order to prevent salt contamination.

The thermodynamic modelling results for **Brine 2** (Figure 4.4) are similar to those obtained for **Brine 1**. The same salts crystallize out, even though there is a difference in ion concentrations between the brines. However, the crystallizing temperatures and amounts are different. Table 4.1 shows that both brines have ice crystallizing at similar temperatures (-0.8°C and -0.9°C). This is not surprising considering that both brines have similar amounts of total dissolved solids (30g/L and 31g/L, Chapter 3) and hence approximately the same amount of water. The thermodynamic modelling also indicates that both brines were saturated with respect to $CaSO_4 \cdot 2H_2O$ at 25°C. The crystallizing temperature of $Na_2SO_4 \cdot 10H_2O$ in **Brine 2** is -1.9°C while it is -1.5°C for **Brine 1**. As expected, the sodium ion concentration affects the nucleation temperature of $Na_2SO_4 \cdot 10H_2O$. For example, **Brine 1** had a Na^+ concentration of 6718mg/L (Chapter 3) and a crystallization temperature of -1.5°C. On the other hand, the Na^+ concentration and the crystallization temperature of **Brine 2** was 5796mg/L and -1.9°C respectively. There is also a direct correlation between the concentration level and the crystallization temperature. A low Na^+ concentration level results in a low crystallization temperature for $Na_2SO_4 \cdot 10H_2O$.

The double salt, $K_2SO_4 \cdot CaSO_4 \cdot 1H_2O$, crystallizes at similar temperatures for both brines (-2.2°C for **Brine 1** and -2.1°C for **Brine 2**). Potassium chloride crystallizes at -19.6°C for **Brine 1** and -16.6°C for **Brine 2**. A comparison of the chloride ion concentration (955mg/L for **Brine 1** and 1504mg/L for **Brine 2**) shows that once again the lowest concentration of a specific ion results in the lowest crystallization temperature. This indicates that, for certain ions, there is a direct correlation between the concentration of that ion and the crystallization temperature of its corresponding salt.

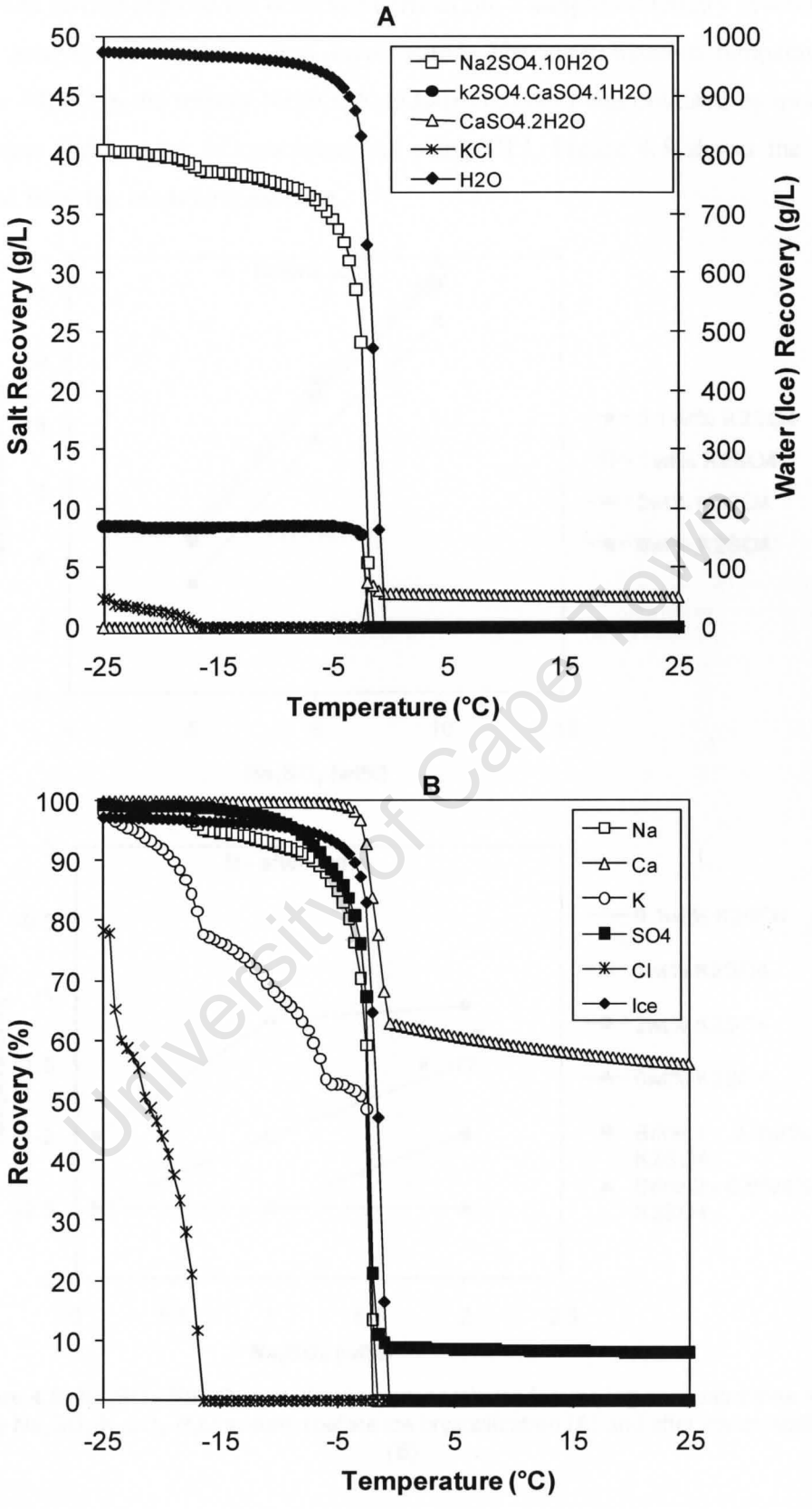

Figure 4.4: Effect of temperature reduction on salt and water recovery for **Brine 2** (salts (A) and ions (B).

In order to further explore the observed correlation, a simplified ternary system based on the analysis of the brine was investigated. The crystallization temperature of $Na_2SO_4 \cdot 10H_2O$ in the ternary Na_2SO_4-K_2SO_4-H_2O system was obtained by modelling the system for a range of concentrations using OLI. Figure 4.5 shows the results obtained from the modelling exercise.

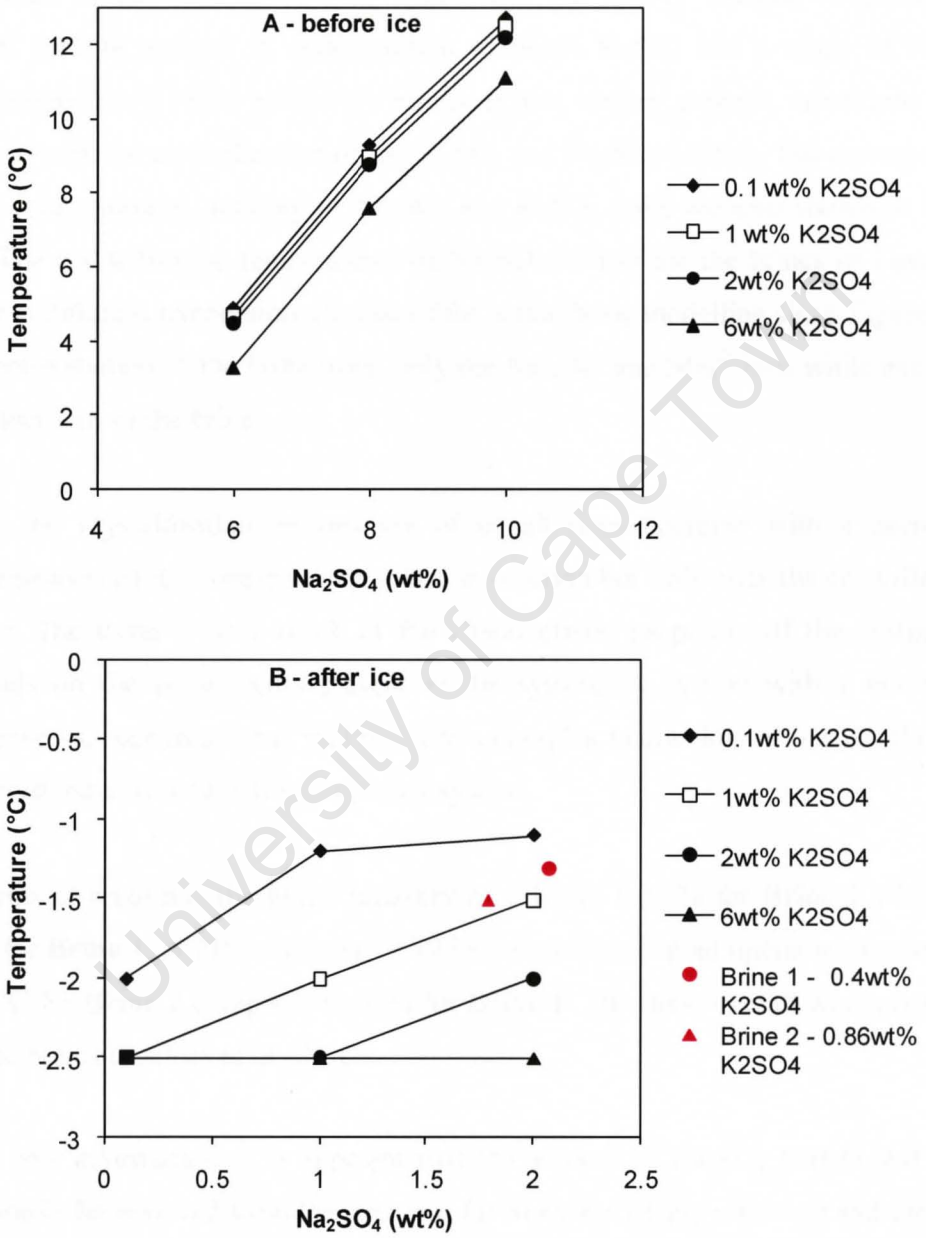

Figure 4.5: $Na_2SO_4 \cdot 10H_2O$ crystallization temperatures for varying concentrations in the ternary Na_2SO_4-K_2SO_4-H_2O system (before ice crystallization (A) and after ice crystallization (B).

The results from the thermodynamic modelling (Figure 4.5) indicate that for concentrations that result in the crystallization of $Na_2SO_4 \cdot 10H_2O$ before ice

crystallization (Figure 4.5 A), the crystallization temperature of $Na_2SO_4 \cdot 10H_2O$ increases as the concentration of the Na_2SO_4 solute increases. The opposite is true for a 6wt% K2SO4 solution (after the crystallization of ice, Figure 4.5 B). The crystallization temperature of $Na_2SO_4 \cdot 10H_2O$ decreases as the concentration of Na_2SO_4 decreases and the concentration of the non-crystallizing component (K_2SO_4) increases. In addition, the system approaches the ternary eutectic temperature at -2.5°C for this system. A concentration of 6wt% K_2SO_4 and a range of Na_2SO_4 concentrations (0.1wt% to 2wt%) results in the ternary eutectic conditions being reached with the crystallization of ice, K_2SO_4 and $Na_2SO_4 \cdot 10H_2O$. The corresponding brine concentrations, relating to Na_2SO_4 and K_2SO_4 only, are also shown in Figure 4.5. The crystallization temperatures of $Na_2SO_4 \cdot 10H_2O$ for the brines in Figure 4.5 occur at different temperatures to that of the actual brine modelling since Figure 4.5 is an approximation of the brine using only the Na^+, K^+ and SO_4^{2-} ions while excluding the other ions of the brine.

Thus, the crystallization temperature of a salt does decrease with a decreasing concentration of its corresponding solute in solution but only after the crystallization of ice. The trend is as a result of the characteristic properties of the system and depends on the components present in the system. A system with a number of components, such as a brine, will result in a complex interaction of ions but the same observed trend as seen in this simplified system.

In terms of recovery, the initial recovery of calcium is 60% for **Brine 2** while it is 65% for **Brine 1**. A 71% recovery of all ions is achieved at an operating temperature of -5°C for **Brine 2** compared to 85% for **Brine 1**. The same overall recovery (90%) for the brines is achieved at -20°C.

From this information, it is apparent that the amount of $Na_2SO_4 \cdot 10H_2O$ that could potentially be removed from the stream is far in excess of any other salt and therefore any process should ultimately aim to produce this salt. The other salts can be produced but because these salts are present in smaller quantities, it may not be economically viable to have a separate crystallizer merely to produce them.

The information also shows that a freeze crystallizer operating at -5°C could theoretically be used to recover both $Na_2SO_4 \cdot 10H_2O$ and ice, with the sodium salt being denser than water and thus being recovered at the bottom of the reactor. In addition, ice, being less dense than water, can be recovered at the top of the reactor. However, the thermodynamic modelling also shows that:

- the water recovery is far in excess of that of the salt, and it will be necessary to pre-concentrate the brine to remove the excess water since the high solid (ice) content would make the separation of ice and salt difficult and
- the presence of the solid $CaSO_4 \cdot 2H_2O$ at ambient temperatures could potentially contaminate the recovered $Na_2SO_4 \cdot 10H_2O$. The thermodynamic modelling also predicts the formation of a double salt, $K_2SO_4 \cdot CaSO_4 \cdot 2H_2O$, at -2.2°C (**Brine 1**) and -2.1°C (**Brine 2**) that could also potentially contaminate the recovered $Na_2SO_4 \cdot 10H_2O$.

The brine treatment process should include a series of three stages, the first being a pre-concentration step, the second being an ice-$CaSO_4 \cdot 2H_2O$ recovery step and the third being an ice-$Na_2SO_4 \cdot 10H_2O$ recovery step. The removal of $CaSO_4 \cdot 2H_2O$ in the second stage would serve two functions in that this stage would further concentrate the brine and hence produce more ice and the crystallizer would also remove $CaSO_4 \cdot 2H_2O$. The removal of calcium sulphate in stage 2 would prevent the salt contamination of $Na_2SO_4 \cdot 10H_2O$ in stage 3. The removal of calcium sulphate could be neglected if sodium sulphate crystallized before calcium sulphate (only 2.7g/L $CaSO_4 \cdot 2H_2O$ formed at -5°C compared to 43g $Na_2SO_4 \cdot 10H_2O$ at -5°C). Thus, the only reason for removing calcium sulphate would be to prevent $Na_2SO_4 \cdot 10H_2O$ contamination.

4.3.2 Concentrated Brine 2'

The thermodynamic modelling for **Brine 2'** is based on the results obtained from the experimental concentrating procedure and the analysis of this stream (Chapter 7). It is not based on merely removing water in the thermodynamic model. Figure 4.6 shows two options for the thermodynamic procedure for obtaining a concentrated brine. The concentrated brine in this section was obtained using option 1. Option 2 is based on a theoretical approach because there is no experimental section. Water (ice) and salts

are "removed" from the thermodynamic model resulting in a theoretical concentrated brine (**Brine 2***). This brine is then used in thermodynamic model.

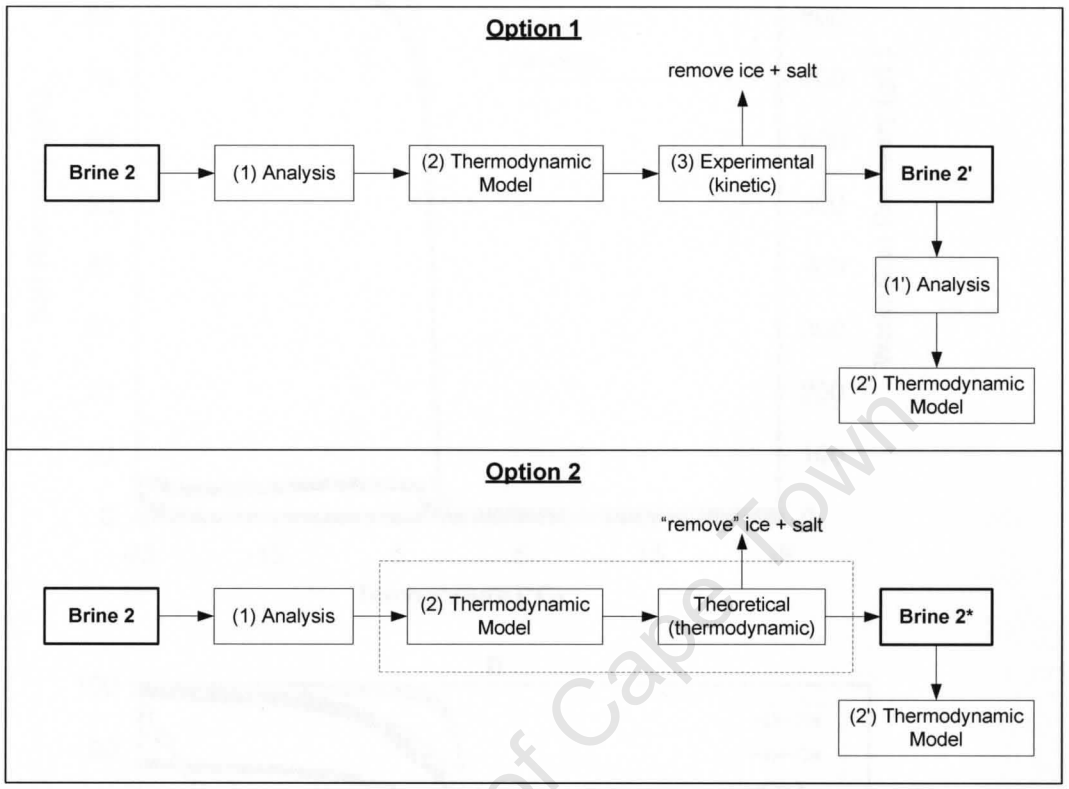

Figure 4.6: Two different options for obtaining a concentrated brine.

The thermodynamic model can therefore predict how a stream concentration will change based on the theoretical removal of specific components (option 2). However, it is the experimental work that gives a more realistic result (option 1). This is the option that was used in this work.

Figure 4.7 shows the thermodynamic modelling results for the concentrated brine (**Brine 2'**).

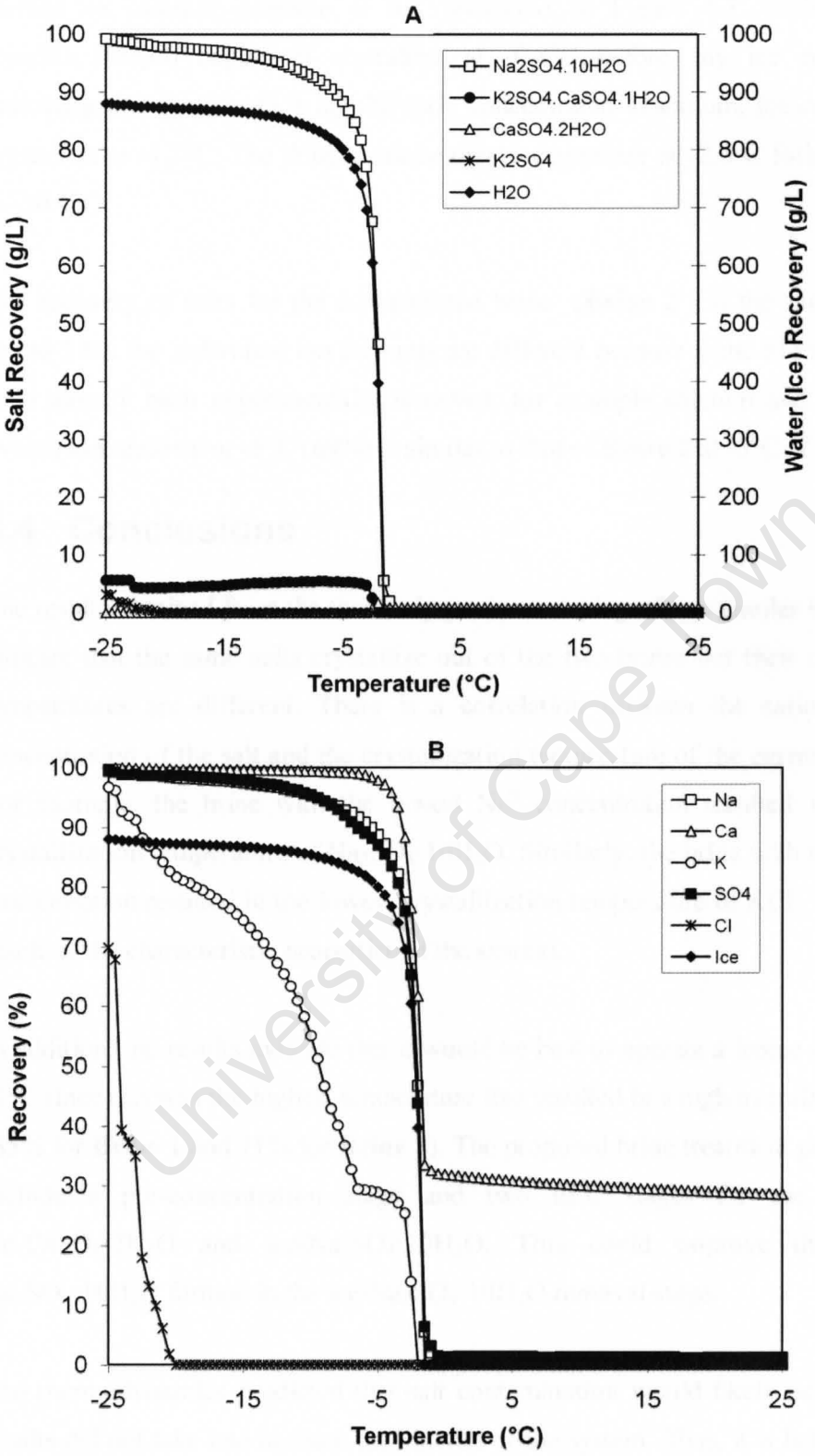

Figure 4.7: Effect of temperature reduction on salt and water recovery for **Brine 2'**.

The model predicts that the solution is saturated with respect to $CaSO_4 \cdot 2H_2O$ but the concentration is low (0.76g/L) when compared to the other concentrations of salts

formed so calcium sulphate is not presented in Figure 4.7. Sodium sulphate ($Na_2SO_4 \cdot 10H_2O$) begins to crystallize at -0.8°C before any ice crystallization, indicating that the stream is significantly concentrated in sodium. Ice only begins to crystallize at -1.7°C. The double salt begins to crystallize at -2.4°C followed by KCl at -20.4°C

The recovery of salts for the concentrated brine (**Brine 2'**) is the same as that of **Brine 2** but the individual ion amounts are different because some of the ions would have already been experimentally removed, for example calcium and sodium. The overall ion removal at -5°C (69%) is similar to that of **Brine 2** at -5°C (71%).

4.4 Conclusions

The results obtained from the thermodynamic modelling of two similar brine samples indicate that the same salts crystallize out of the two brines but their crystallization temperatures are different. There is a correlation between the cation and anion concentration of the salt and the crystallization temperature of the corresponding salt. For example, the brine with the lowest Na^+ concentration resulted in the lowest crystallization temperature of $Na_2SO_4 \cdot 10H_2O$. Similarly, the brine with the lowest Cl^- concentration resulted in the lowest crystallization temperature of KCl. This was as a result of the characteristic properties of the system.

In addition, the results indicate that it would be best to operate a freeze crystallizer at -5°C since this was the highest temperature that resulted in a high overall ion recovery (85% for **Brine 1** and 71% for **Brine 2**). The proposed brine treatment process should include a pre-concentration stage and two EFC stages for the removal of ice-$CaSO_4 \cdot 2H_2O$ and ice-$Na_2SO_4 \cdot 10H_2O$. This could improve the purity of $Na_2SO_4 \cdot 10H_2O$ formed in the ice-$Na_2SO_4 \cdot 10H_2O$ removal stage.

The thermodynamics predicted that salt contamination would likely occur but these results did not take into account the kinetics of the system. Thus, it is believed that by understanding the kinetics and through concepts such as selective seeding, the challenge of salt contamination can be overcome. This will be discussed in the next chapter.

The concentrated brine (**Brine 2'**) resulted in the crystallization of $Na_2SO_4 \cdot 10H_2O$ before ice. The overall ion recovery for this brine (69%) was similar to the value calculated for **Brine 2** (71%).

Thermodynamic modelling provides the first indication of what could be expected during an EFC process but these thermodynamic results need to be experimentally verified.

References

[1] OLI Systems Inc., OLI Stream Analyser, Version 3.0, Morris Plains, New Jersey, USA, 2010.

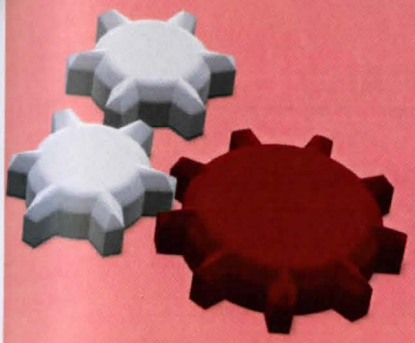

CHAPTER 5 : THE METASTABLE ZONE WIDTH

Don't empty the water jar until the rain falls.

Philippine proverb

Graphic from: http://farm4.static.flickr.com/3070/2782765652_147e199269_o.jpg

5.1 Introduction

The metastable zone (MSZ) is an important concept in crystallization since it defines the operating region of a process. It is a region where no spontaneous nucleation can occur and therefore operating within this region can allow for better process control. Figure 5.1 shows a binary phase diagram for sodium sulphate, which indicates the various phases present at equilibrium. A 1wt% sodium sulphate solution, for example, will be free of solids above -0.4°C, but below this temperature ice will begin to crystallize. When cooled below -1.2°C, salt will begin to crystallize. However, this phase diagram describes conditions of thermodynamic equilibrium. In a real world process, thermodynamic equilibrium is unlikely to be reached as the system is dominated by kinetics. This means that, for the 1wt% sodium sulphate solution example, salt is unlikely to crystallize for the duration of a process unless the solution is significantly concentrated. It is therefore important to determine the kinetics of a system in order to obtain a better understanding of a process. In the context of this chapter, the kinetic aspects are related directly to the MSZ since, by definition, the MSZW is the difference between the solubility line and the limit of non-spontaneous nucleation.

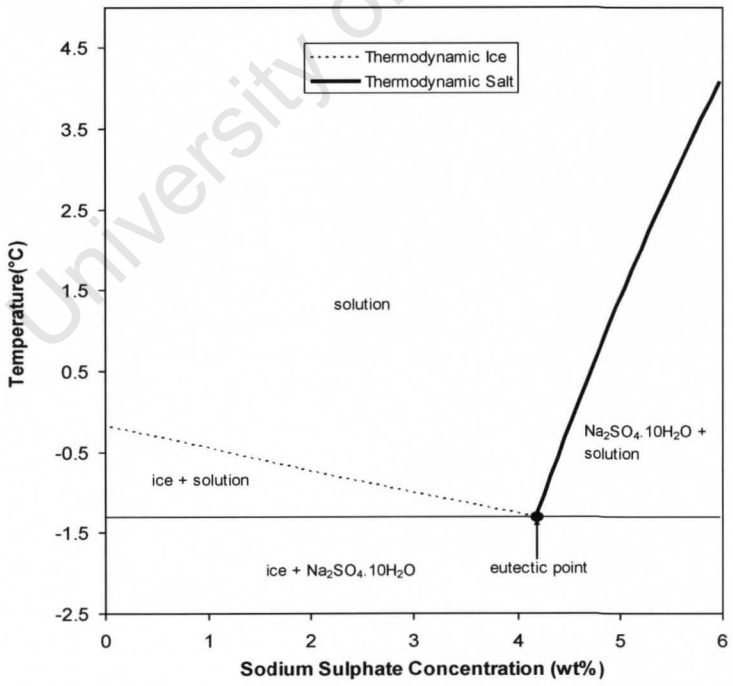

Figure 5.1: Binary sodium sulphate phase diagram [1].

CHAPTER 5: THE METASTABLE ZONE WIDTH

This chapter characterizes the MSZ for a 1wt% sodium sulphate solution as well as the MSZ near the eutectic composition. It also looks at the effect of solution volume and the presence of other ions on the MSZ of ice.

5.2 Methodology

The aims and conditions for the various experiments used to measure the kinetics of the system are shown in Table 5.1.

Table 5.1: The aims and conditions for experiments relating to the MSZ.

Part	Aim(s)	Volume (ml)	Experiment Name	Conc. (Na_2SO_4) (wt%) or species present	Cooling Rate (°C/hour)
A	To investigate: • The stochastic nature of nucleation, • The effect of different cooling rates on ice nucleation and hence the MSZ of ice, • The minimum number of experiments required to obtain similar results to results obtained from 48 experiments.	1.8	$A1_2$, $A2_2$, $A3_2$...$A48_2$	1	2
			$A1_4$, $A2_4$, $A3_4$...$A48_4$		4
			$A1_8$, $A2_8$, $A3_8$...$A48_8$		8
B	To investigate the effect of different ions on the MSZ of ice.	1.8	**Binary:** $B1_{bin}$, $B2_{bin}$, $B3_{bin}$ ...$B24_{bin}$	Na^+, SO_4^{2-}	8
			Ternary: $B1_{ter}$, $B2_{ter}$, $B3_{ter}$ ...$B24_{ter}$	Na^+, Ca^{2+}, SO_4^{2-}	
			Quaternary: $B1_{qua}$, $B2_{qua}$, $B3_{qua}$ ...$B24_{qua}$	Na^+, Ca^{2+}, K^+, SO_4^{2-}	
			Penternary: $B1_{pen}$, $B2_{pen}$, $B3_{pen}$...$B24_{pen}$	Na^+, Ca^{2+}, K^+, Mg^{2+}, SO_4^{2-}	
			Complex: $B1_{com}$, $B2_{com}$, $B3_{com}$...$B24_{com}$	Na^+, Ca^{2+}, K^+, Mg^{2+}, Cl^-, SO_4^{2-}	
			Brine: $B1_{brin}$, $B2_{brin}$, $B3_{brin}$...$B24_{brin}$	Na^+, Ca^{2+}, K^+, Mg^{2+}, Cl^-, SO_4^{2-}, other	
C	To investigate the effect that different solution volumes have on the MSZ of ice.	250	$C1_{250}$, $C2_{250}$, $C3_{250}$...$C12_{250}$	1	8
		1000	$C1_{1000}$, $C2_{1000}$, $C3_{1000}$...$C12_{1000}$		
D	• To determine the MSZ of ice and $Na_2SO_4 \cdot 10H_2O$ near the binary eutectic point of a sodium sulphate system, • To investigate the effect of salt seeding on the crystallization of ice in the ice MSZ.	250	D1	3.44	1.5
			D2	3.47	
			D3	3.55	
			D4	3.64	
			D5	4.32	
			D6	4.46	
			D7	4.64	
			D8	4.72	
			D9	4.79	
			D10	4.24	
			D11	4.76	
			D12	4.79	
			D13	4.84	
			D14	5.12	
			D15	5.22	
			D16	5.95	
			D17	5.97	

5.2.1 Solution Preparation

5.2.1.1 Part A and Part B – Small Volume Experiments

Binary sodium sulphate solutions were prepared from 99wt% Na_2SO_4 (Merck) and de-ionized water of 15mΩ. A 1wt% sodium sulphate solution was used for Part A. All solutions were filtered prior to conducting the experiment. Filtration was conducted using a 300ml Millipore All-Glass filter holder connected to a vacuum pump. The filter paper pore size was 0.45μm.

The **Ternary**, **Quaternary**, **Penternary** and **Complex** (Part B) solutions were prepared from the relevant 99wt% anhydrous (Merck) chemicals, with the exception of calcium sulphate, which was a hydrate ($CaSO_4 \cdot 2H_2O$). The ion concentrations (based on the analysis for **Brine 2**, presented in Chapter 3) for Part B were kept constant, except for the SO_4^{2-} ion concentration. The SO_4^{2-} ion concentration had to change in order to ensure an ion balance for the stream. As a result, the total dissolved solids were different for each experiment (Figure 5.2).

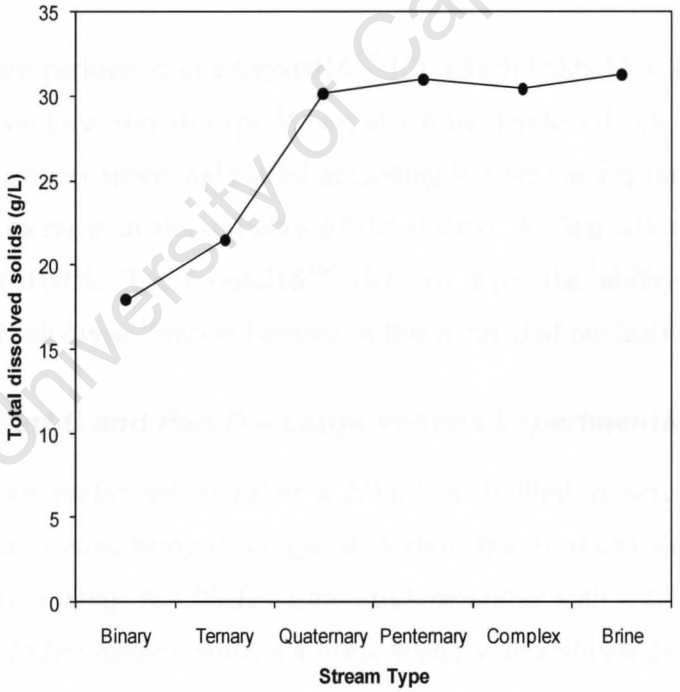

Figure 5.2: Total dissolved solids for Part B.

A total of 48 experiment repetitions were conducted for each cooling rate experiment of Part A, while 24 experiment repetitions were conducted for Part B. A concentration (1wt% Na_2SO_4) less than that of the eutectic concentration (4.2wt% [1], see Figure

5.1) was chosen to ensure that ice crystallization always occurred first since these sets of experiments only focused on the MSZ of ice.

5.2.1.2 Part C and Part D – Large Volume Experiments

Binary sodium sulphate solutions were prepared from 99wt% Na_2SO_4 (Merck) and de-ionized water of 15mΩ. The concentrations for the binary sodium sulphate experiments near the eutectic composition (4.2wt%) are shown in
Table 5.1. A cooling rate of 1.5°C/hour and a solution volume of 250ml were used for these experiments.

Solution volumes (250ml and 1000ml) for the investigation into the effect of solution volume on the MSZ were conducted with 1wt% Na_2SO_4 solutions and a cooling rate of 8°C/hour (Part C).

5.2.2 Experimental Setup

5.2.2.1 Part A and Part B – Small Volume Experiments

Experiments were performed in a Crystal16^{TM} [2], which holds 16 1.8ml HPLC glass vials and can therefore run 16 experiments at a time. Each cell can be magnetically stirred at a fixed stirrer speed and cooled according to a set cooling rate. Nucleation is detected by an increase in the turbidity of the system. A clear solution will have a transmission of 100%. The Crystal16^{TM} did not have the ability to distinguish between ice and salt crystallization because of this method of nucleation detection.

5.2.2.2 Part C and Part D – Large Volume Experiments

Experiments were performed in either a 250ml or 1000ml jacketed glass reactor, depending on the volume being investigated. A Heidolph overhead stirrer was used to provide adequate mixing. A 4 blade rushton turbine stirrer with a diameter of 40mm was used in the 250ml reactor, while a 4 blade stirrer with a 90mm diameter was used in the 1000ml reactor. Cooling was achieved by circulating Kryo40 through the reactor jacket with a Lauda Master thermostatic unit. A 712 Metrohm conductometer was used to measure the conductivity of the solution during Part D. A Testo 175-177 temperature logging device was used to measure the solution temperature in the reactor.

5.2.3 Experimental Procedure

5.2.3.1 Part A and Part B – Small Volume Experiments

To ensure sufficient mixing, the agitation rate of the magnetic stirrers was set to 700rpm for all experiments. Each experiment was initiated by maintaining the solution temperature at approximately 0°C for 1 hour, in order to ensure that the solution temperature had stabilized. The cooling rates of 2°C/hour, 4°C/hour and 8°C/hour were then each applied until the first change in turbidity was detected, thus indicating that spontaneous nucleation had occurred. For all experiments, the vials were cooled to -15°C according to the chosen linear cooling rate. Each experiment was repeated twice by heating the solutions back up to 25°C to ensure that all the ice had melted. They were then cooled back down to 0°C and left at this temperature for 1 hour to stabilize as previously executed.

5.2.3.2 Part C and Part D – Large Volume Experiments

All these experiments were performed batchwise. An experiment was initiated by maintaining the solution temperature at approximately 1.5°C, or a chiller temperature setpoint of 0°C for approximately 30 minutes. The specific cooling rate was then applied until the first sudden temperature increase, indicative of nucleation, occurred. The formation of ice or salt could be easily recognized from visual observation and confirmed by a sudden change in the conductivity reading. During the seeded experiment, salt seeds were added to the solution at the desired temperature and the temperature of the solution was cooled at the same cooling rate (1.5°C/hour).

5.3 Results and discussion

5.3.1 Part A – The MSZ of ice in a 1wt% binary Na_2SO_4 system

The results for Part A are described in this section. Figure 5.3 shows a binary sodium sulphate phase diagram (thermodynamic aspects) as well as a plot of the various ice nucleation temperatures (kinetic aspects) obtained for the three investigated cooling rates (2°C/hour, 4°C/hour and 8°C/hour) imposed on a 1wt% sodium sulphate solution; all shown within the greybound representing 1wt%. The observed nucleation detections (indicated by the first sudden temperature increase) are shown at slightly different concentrations in order to see the spread of data for different cooling rates,

although the solution concentration was 1wt%. A solution is likely to reach equilibrium conditions during slow cooling and nucleation is thus likely to occur at a higher temperature. A number of experimental runs at slower cooling rates would therefore result in a greater probability of nucleation temperatures being observed at higher temperatures. As can be seen, the spread of the data is relatively wide, with an average spread across each data set of approximately 10°C. This confirms the stochastic nature of ice nucleation in this system.

Within the set of 48 experiments carried out for the 1wt% solution concentration, the highest temperature marks the boundary for spontaneous nucleation. This point will be referred to as the metastable zone limit point (MSZLP). The temperature data occurring at lower temperatures than the MSZLP define the conventional MSZW's.

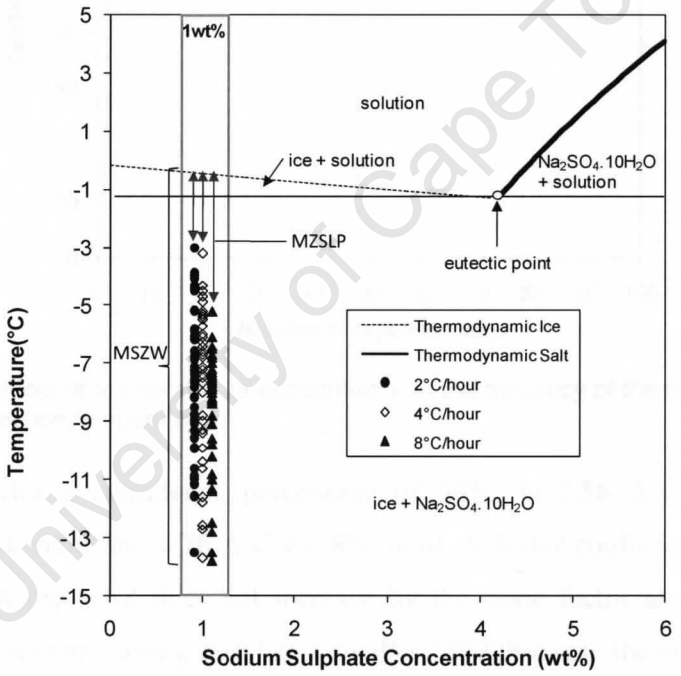

Figure 5.3: Nucleation temperatures for a 1wt%, 1.8ml Na_2SO_4 solution at different cooling rates.

The MSZLP does not define the position of a zero percent probability of ice nucleation (definition of MSZ) but rather a probability of 2% (1 experiment /48 experiments). However, this probability value needs to be compared to the confidence percentage of the experiment set. For example, an experiment set of 48 has a confidence percentage of 98% (100 – 2%), and this merely implies that, by running 48 experiments, the calculated probability confidence is only 98%. There is the chance

that the calculated probability of the sample is *not* a true reflection of the probability of a population from which the sample was taken and this is indicated by the confidence percentage. The confidence percentage therefore increases with more experimental runs. Figure 5.4 shows how the nucleation temperature confidence percentage increases with an increasing number of experiments. The dotted line represents the confidence percentage for 48 experiments (98%).

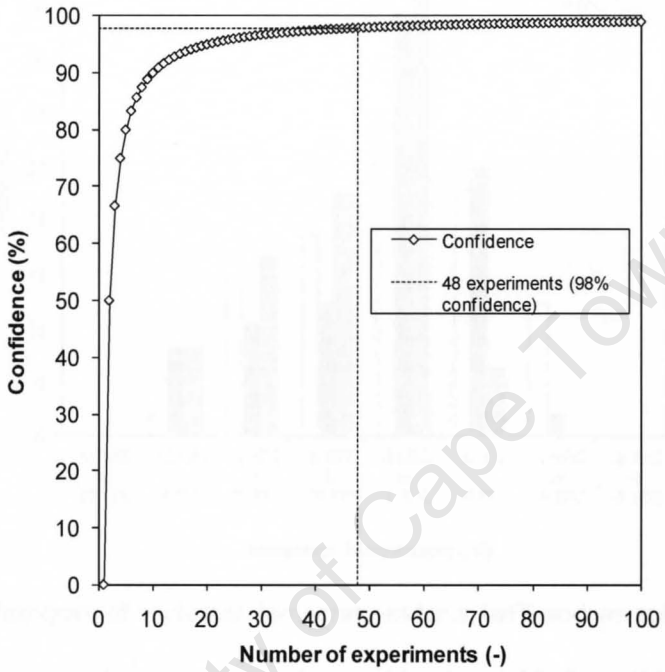

Figure 5.4: The effect of the number of experiments on the accuracy of the highest nucleation temperature.

The MSZW, with a confidence percentage of 98%, is 2.56 Δ°C for 2°C/hour, 2.76 Δ°C for 4°C/hour and 4.76 Δ°C for 8°C/hour. A faster cooling rate results in a wider MSZ, but the MSZ does not increase by the same factor as the increase in cooling rate. A slower cooling rate has a smaller MSZ because the system has more time to reach a new equilibrium. For example, nucleation would likely occur at the solubility temperature (equilibrium) if the solution was cooled infinitely slowly. However, as a rule of thumb, industrial crystallizers are operated in the middle of the MSZ. This ensures that no spontaneous nucleation occurs.

Figure 5.5 shows a histogram (with temperature intervals of 2°C) of the data presented in Figure 5.3 for a 1wt% solution at different cooling rates of 2°C/hour, 4°C/hour and 8°C/hour. The second highest temperature interval (-2.15°C to -4.15°C)

is the one in which spontaneous nucleation first started. In this interval, a larger number of nucleation events (12.5%) are detected for the slowest cooling rate (2°C/hour) compared to the faster cooling rate (2.1% for 4°C/hour) and indicated no detections for the cooling rate of 8°C/hour.

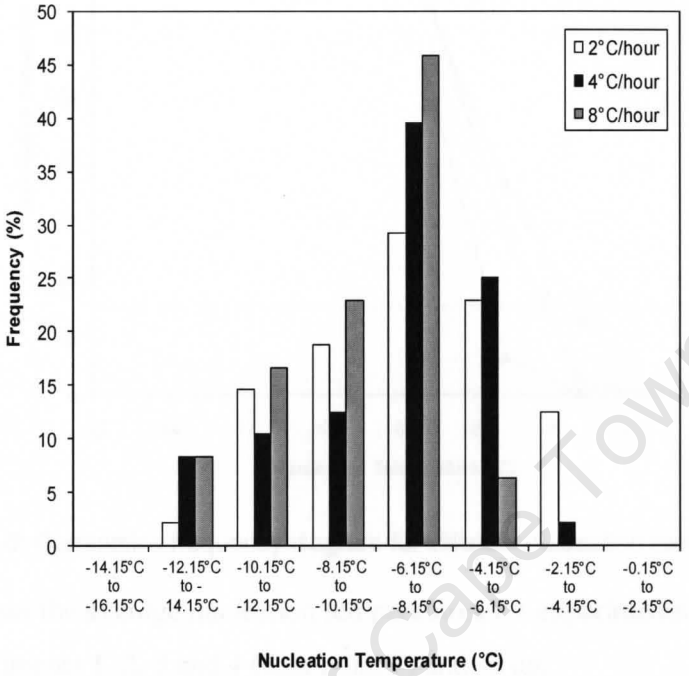

Figure 5.5: Histogram of nucleation temperatures for a 1wt% sodium sulphate solution.

The majority of nucleation events are observed in the -6.15°C to -8.15°C temperature interval with the fastest cooling rate (8°C/hour) having the highest frequency (46%).

Figure 5.6 shows the cumulative distribution of nucleation temperatures at different cooling rates for a 1wt% sodium sulphate solution. The cumulative frequency curves have similar shapes but the 2°C/hour curve occurs at higher temperatures when compared to the other two cooling rates. The initial temperatures at zero probability are different (-1.15°C and -3.15°C), while the final temperatures at ~100% probability are consistently -13.15°C. Figure 5.6 also shows how a single experiment can inaccurately define the MSZW. Consider a single "experiment" represented by the line ABC in Figure 5.6. The MSZW according to this "experiment" is 2.8 Δ°C for 2°C/hour, 4 Δ°C for 4°C/hour and 5.4 Δ°C for 8°C/hour and would change if the "experiment" were repeated, thus indicating the inaccuracies that may arise from too few experiments. It is therefore important to repeat experiments in order to accurately determine the highest temperature and thus the true MSZW.

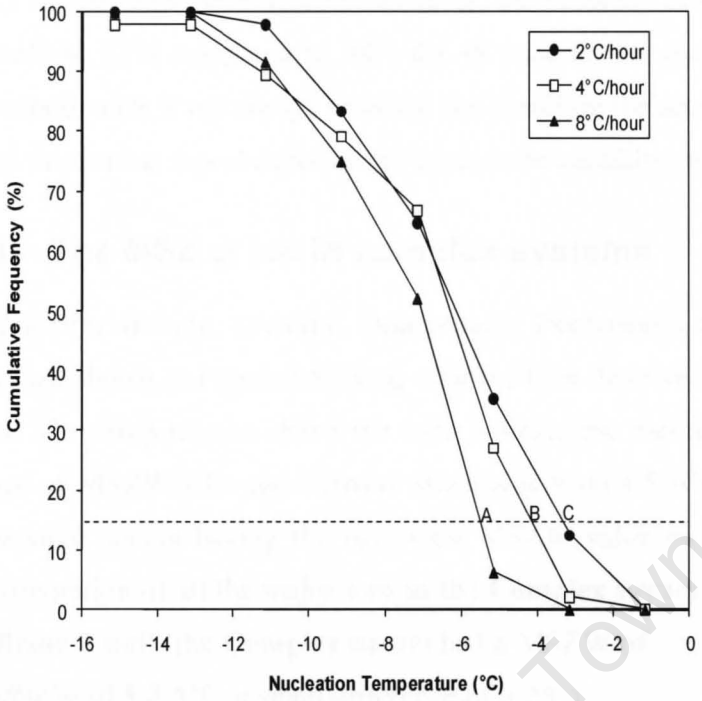

Figure 5.6: Cumulative frequency diagram for different nucleation temperatures.

Figure 5.7 shows the average nucleation temperatures for experiments 1, 2 and 3 (data point 1), experiments 1, 2, 3 and 4 (data point 2) and so on.

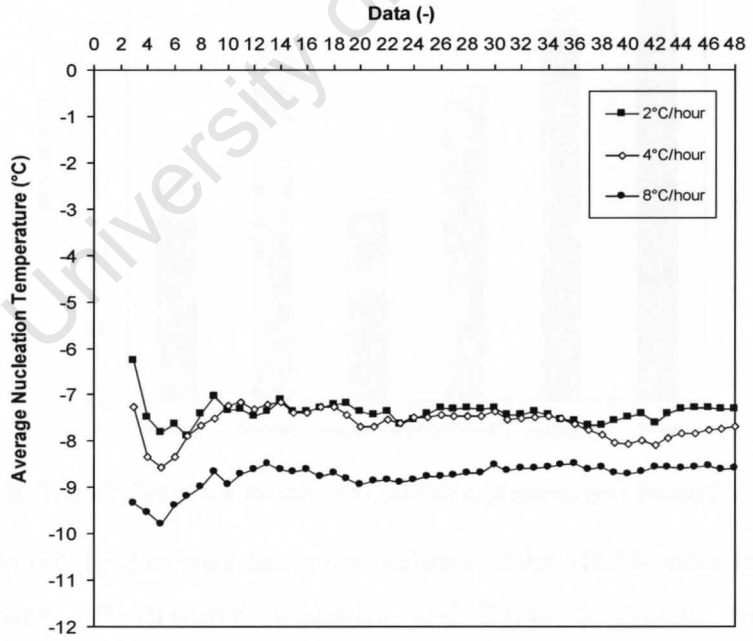

Figure 5.7: Average nucleation temperatures for a 1wt%, 1.8ml sodium sulphate solution.

It shows that the same average nucleation temperature for the 1wt% solution after 48 experiments is achieved after about 12 experiments. This means that, in this instance,

no more than 12 experiments were needed. However, the accuracy of only using 12 experiments would be 92% compared to 98% for 48 experiments (see Figure 5.4). Running many experiments is not always practical and therefore the accuracy together with the required time to run repeat experiments needs to be carefully considered.

5.3.2 Part B – The MSZ of ice in complex systems

The ice MSZW for the **Binary**, **Ternary**, **Quaternary**, **Penternary, Complex** and **Brine 2** samples are shown in Figure 5.8 along with the total dissolved solids (TDS) for each stream. The temperatures above the bars indicate the theoretical freezing points. The range of MSZW's for the different streams is from 4.5 Δ°C to 5.2 Δ°C, with the **Quaternary** stream having the narrowest MSZW value and **Brine 2** the widest. The incorporation of all the major ions in the **Complex** stream approximated the MSZW of **Brine 2** well (the **Complex** stream had a MSZW of 5 Δ°C while **Brine 2** had a MSZW of 5.2 Δ°C; a small difference of 0.2°C).

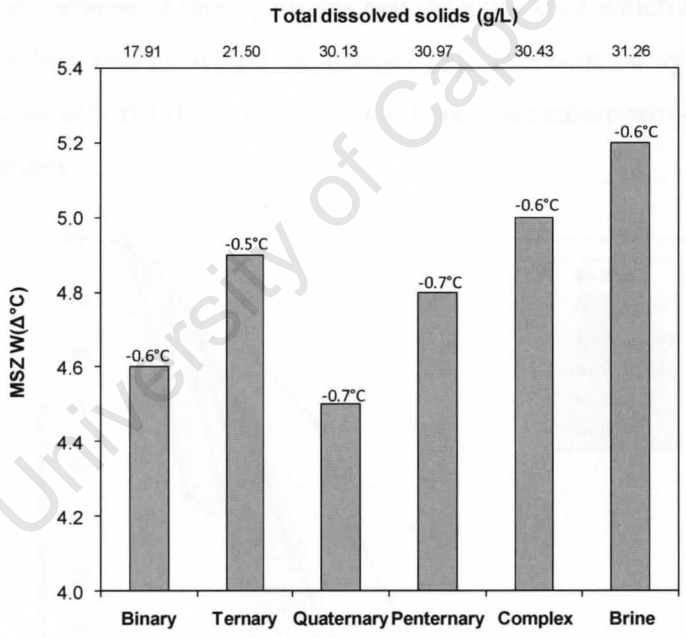

Figure 5.8: The MSZW of ice for different synthetic streams and **Brine 2** (Chapter 3).

The TDS was not the dominant factor that influenced the MSZW since the MSZW for the **Quaternary**, **Penternary**, **Complex** and **Brine 2** streams were different (increasing from 4.5 Δ°C to 5.2 Δ°C), while the TDS remained relatively constant (30.13g/L to 31.26g/L). The presence of different ions must therefore have affected the ice nucleation temperature, even though these ions were not part of the crystallizing material (ice). Wilson and co-workers [3], in their research of ice

nucleation for various aqueous systems, reported that the type of solute had no effect in determining how much a solution could be undercooled by. However, the level of solute concentration did play a role with higher solute concentrations decreasing the level of undercooling (the MSZW). The presence of additional ions (regardless of their type) must therefore act as a catalyst to commence the nucleation process.

Figure 5.9 shows a cumulative frequency plot for the results of Part B. The synthetic streams have been shaded in grey and have similar cumulative distributions, while the cumulative distribution for **Brine 2** shows that the majority of nucleation temperatures occurred at higher temperatures. This is not surprising considering the complex nature of the actual brine sample. The presence of minor components, which did not form part of the synthetic streams, likely resulted in more frequent molecular collisions and therefore increased the probability that ice nuclei would form. A solution practically always has in itself foreign molecules, microscopic particles, bubbles etc. The surfaces of these particles may be a place on which a critical nucleus can form since less energy would be needed [4]. Therefore, a system with more particles would usually require less energy and hence nucleation would likely occur at higher temperatures.

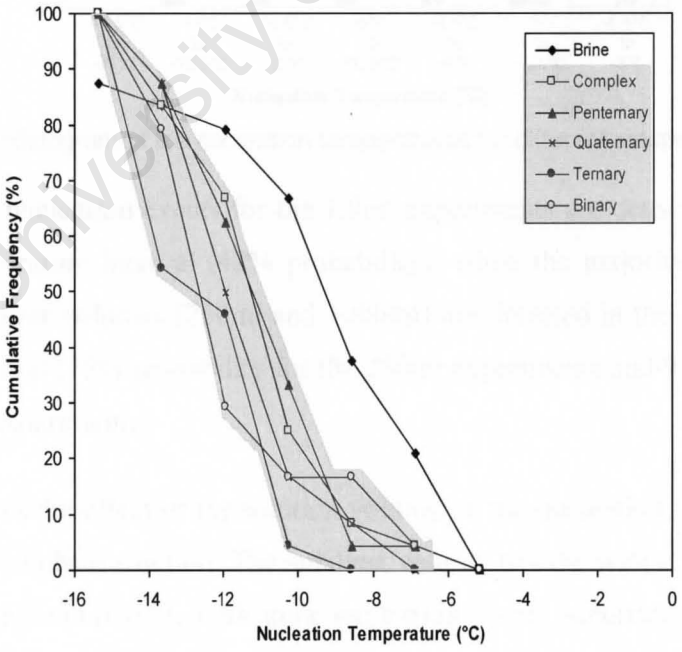

Figure 5.9: Cumulative frequency diagram for different nucleation temperatures obtained from different streams.

5.3.3 Part C – The effect of solution volume on nucleation temperatures

Figure 5.10 shows a histogram of the nucleation temperatures for three different solution volumes (1.8ml, 250ml and 1000ml). The first 12 experiments of the 8°C/hour section for Part A ($A1_8$ to $A12_8$) were used for the 1.8ml volume (Table 5.1). The spread of data is wide for the 1.8ml volume and narrower for the other volumes (250ml and 1000ml).

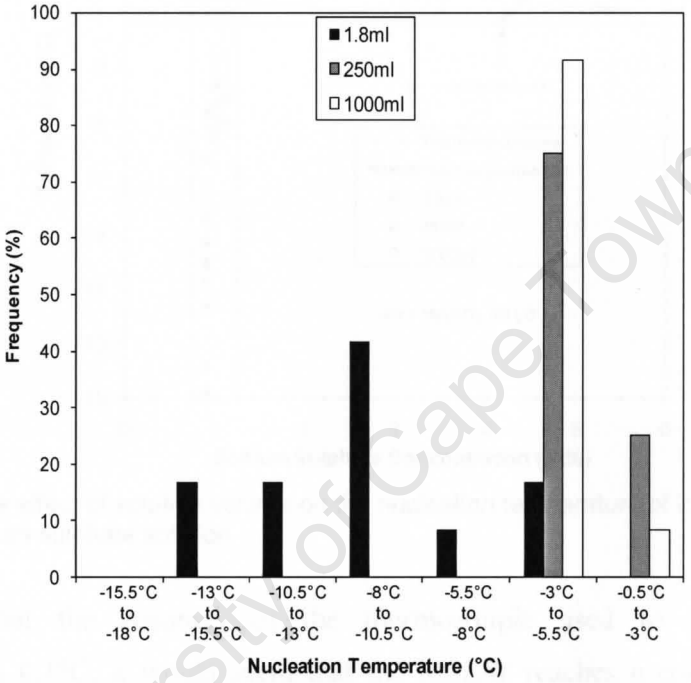

Figure 5.10: Histogram of ice nucleation temperatures for different solution volumes.

The majority of nucleation events for the 1.8ml experiments are detected in the -8°C to -10.5°C temperature interval (42% probability), while the majority of nucleation events for the larger volumes (250ml and 1000ml) are detected in the -3°C to -5.5°C temperature interval (75% probability for the 250ml experiments and 92% probability for the 1000ml experiments).

Figure 5.11 shows the effect of the solution volume on the nucleation temperature for a 1wt% sodium sulphate solution. The smallest volume has the widest range (~10°C) of nucleation temperature data, with some nucleation events occurring at much lower temperatures than the nucleation events for larger solution volumes. This can be related to the effect of volume on nucleation rate. A smaller volume will result in a slower nucleation rate and therefore require more time for nucleation to occur (see

Chapter 2, section 2.2.1.2). The spread of data for the 250ml set of experiments is 2.8°C, while it is slightly lower for the 1000ml set of experiments (2.5°C). The MSZW for the 250ml and 1000ml experiments are similar (2.3 Δ°C and 2.2 Δ°C respectively) while the MSZW for the 1.8ml set of experiments is higher (4.2 Δ°C).

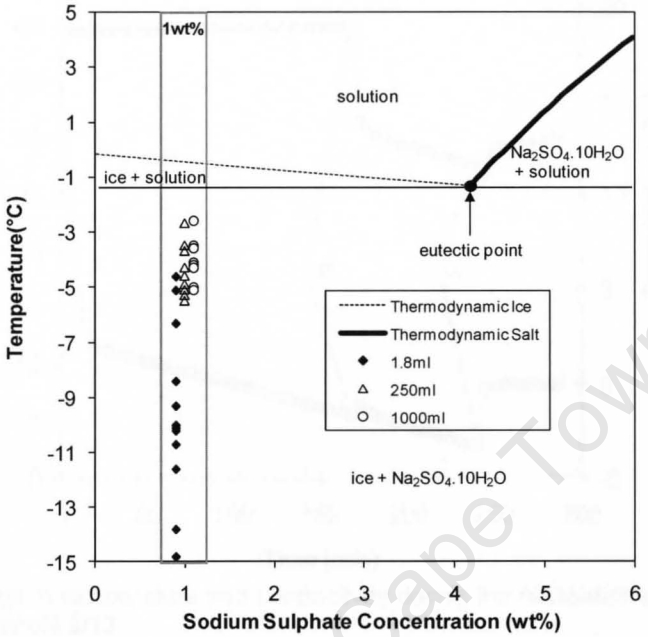

Figure 5.11: The effect of solution volume on the nucleation temperature of ice in a 1wt% sodium sulphate solution.

Considering that the accuracy of the thermocouple used to measure these temperatures is 0.1°C, it would seem that the MSZW reaches a constant value of ~2.3 Δ°C regardless of whether the solution volume is 250ml or higher, but the spread of the nucleation temperature data is slightly different.

5.3.4 Part D – The MSZ of ice and $Na_2SO_4.10H_2O$ near the binary sodium sulphate eutectic point

Figure 5.12 shows the change in temperature and conductivity for a 4.84wt% sodium sulphate system (experiment **D13**). The initial temperature drop is due to the cooling of the solution to 1.5°C (the initial solution starting temperature). The linear cooling rate of 1.5°C/hour was applied once the solution temperature had reached 1.5°C.

Salt crystallization occurred when the solution was cooled further. The crystallization of salt resulted in a slight increase in the solution temperature and the initiation of the

crystallization process was confirmed by a sudden decrease in the conductivity measurement.

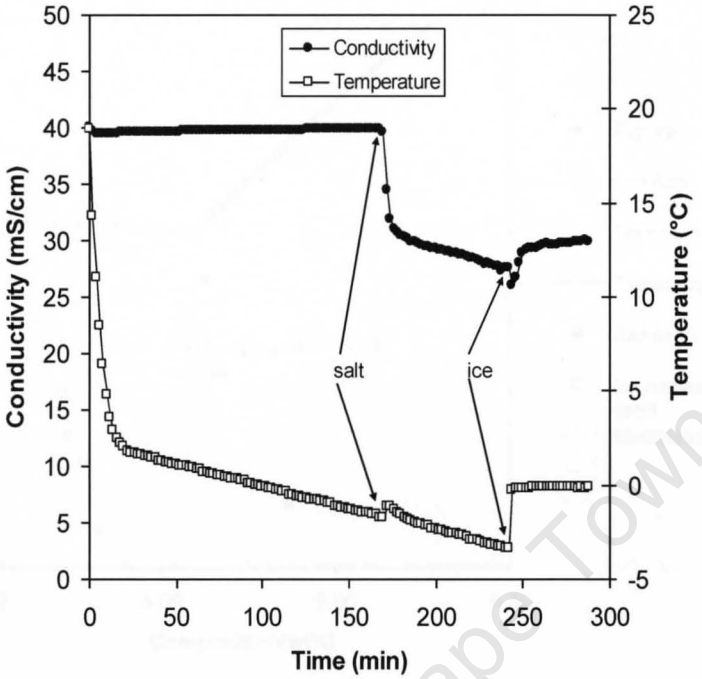

Figure 5.12: Change in temperature and conductivity during the nucleation process for experiment **D13**.

The solution was cooled further until the nucleation temperature of ice was reached. The temperature significantly increased at this point and reached a constant value of approximately 0°C. The conductivity of the solution increased when ice began to crystallize. The conductivity measurements can therefore be used to distinguish between salt and ice formation.

Figure 5.13 shows a region near the binary sodium sulphate eutectic point, along with experimental data defining points of spontaneous ice and salt crystallization. Figure 5.13 also shows the temperature (-2.2°C) at which $Na_2SO_4 \cdot 10H_2O$ seed crystals were added to a 4.24wt% sodium sulphate solution (experiment **D10**). The $Na_2SO_4 \cdot 10H_2O$ seeds were added within the region of non-spontaneous nucleation to see whether ice or salt would crystallize. The addition of the salt seeds only resulted in salt crystallization. The solution was then cooled to the metastable limit (-3.62°C, dotted line in Figure 5.13) to see if ice crystallization occurred at this temperature. Spontaneous ice crystallization did occur at -3.61°C, confirming that the metastable

limit had been reached. Salt seeding will only suppress ice formation within the MSZ. Once the metastable limit has been reached, ice nucleation will occur.

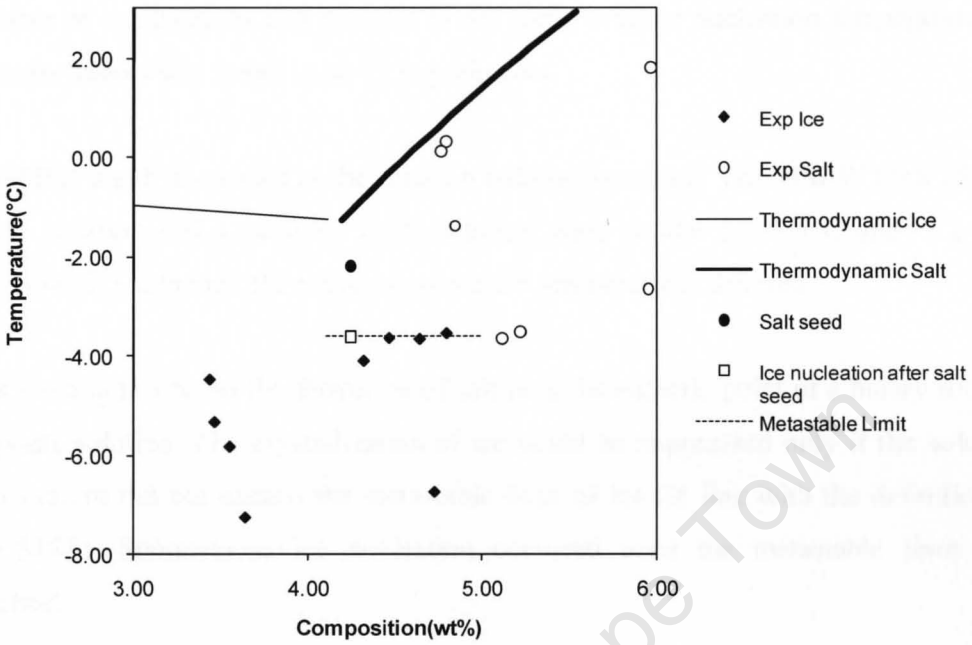

Figure 5.13: Seeding experiment to validate the MSZ of sodium sulphate at a cooling rate of 1.5°C/hour.

The concentration change during the crystallization of $Na_2SO_4 \cdot 10H_2O$ was not measured but Figure 5.13 can be used to explain what happens during the process. The crystallization of $Na_2SO_4 \cdot 10H_2O$ would cause the solution concentration to decrease and thus, on the diagram, move to the left of the initial starting point (closed circle in Figure 5.13). Therefore the crystallization of ice would occur at a different concentration, but still along the metastable limit (dotted line in Figure 5.13).

5.4 Conclusions

A wide distribution of nucleation temperatures was observed for different cooling rates (2°C/hour, 4°C/hour, 8°C/hour), with the fastest cooling rate (8°C/hour) resulting in the lowest nucleation temperatures. The wide range of nucleation temperatures was attributed to the inherently stochastic nature of nucleation. This stochastic nature explained why repeat experiments resulted in different ice nucleation temperatures and why many experiments were necessary for determining the ice MSZ.

The MSZW for a 1wt% sodium sulphate solution (1.8ml volume), with a confidence percentage of 98%, was 2.56 Δ°C for a cooling rate of 2°C/hour, 2.76 Δ°C for a cooling rate of 4°C/hour and 4.76 Δ°C for a cooling rate of 8°C/hour. The minimum number of experiments that resulted in the same average nucleation temperature for 48 experiments was found to be 12 experiments.

The MSZ width decreased as the solution volume increased. The MSZW for a 250ml, 1wt% solution and a 1000ml, 1wt% solution were similar (-2.3 Δ°C and -2.2 Δ°C respectively), although the range of nucleation temperatures differed.

Salt seeding promoted the formation of salt near the eutectic point of a binary sodium sulphate solution. The crystallization of ice could be suppressed only if the solution temperature did not exceed the metastable limit of ice (in line with the definition of the MSZ). Spontaneous ice nucleation occurred once the metastable limit was reached.

The MSZ widths for different synthetic streams and **Brine 2** ranged from 4.5 Δ°C to 5.2 Δ°C, the **Quaternary** stream having the narrowest MSZ width and **Brine 2** the widest. The MSZ width for the **Complex** stream (5.0 Δ°C) was similar to the MSZ width for **Brine 2** (5.2 Δ°C). However, the cumulative distribution curve for the **Complex** stream occurred at lower nucleation temperatures while the cumulative distribution curve for **Brine 2** occurred at higher nucleation temperatures. This was attributed to the complex nature of the brine thus resulting in ice nucleation occurring at higher temperatures.

References

[1] K. Thomsen, Aqueous electrolytes: model parameters and process simulation, PhD Thesis, Technical University of Denmark, Denmark,1997.

[2] Avantium Technologies, www.Crystal16.com.

[3] P.W. Wilson, A.F. Heneghan, A.D.J. Haymet, Ice nucleation in nature: supercooling point (SCP) measurements and the role of heterogeneous nucleation, Cryobiology 46 (2003) 88-98.

[4] D. Kaschiev, Nucleation: Basic theory with applications. 1st edn, Butterworth-Heinemann, Great Britain, 2000.

CHAPTER 6 : PREVENTING SALT CONTAMINATION

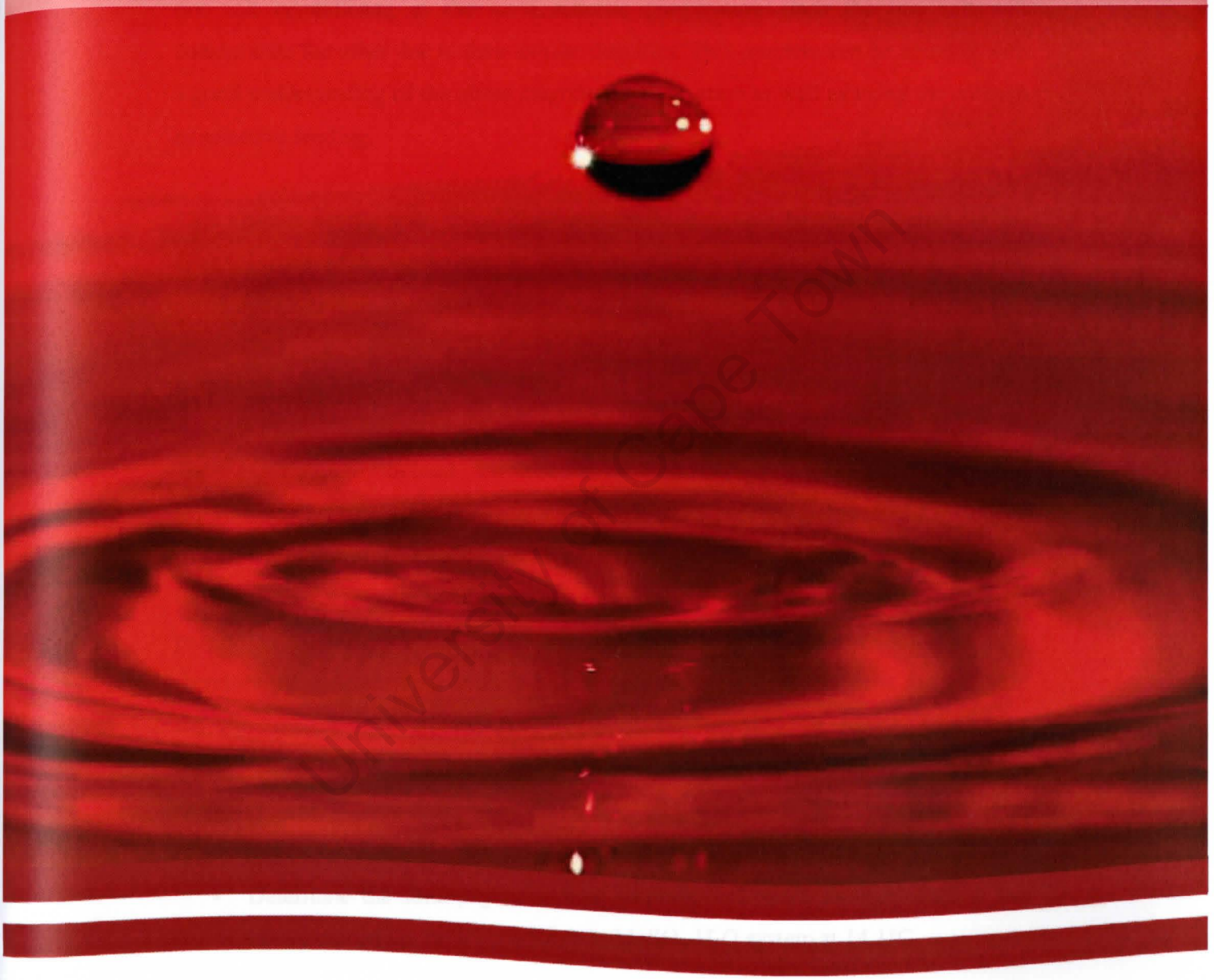

Water is the driver of Nature.

Leonardo da Vinci

Graphic from: http://farm4.static.flickr.com/3070/2782765652_147e199269_o.jpg

6.1 Introduction

The separation of two components formed during Eutectic Freeze Crystallization can be achieved by utilising their density differences. The ice crystals are less dense than the salt(s) and therefore will float to the top of the crystallizer while the salt(s), being more dense, will sink to the bottom. However, a problem arises if there is more than one salt crystallizing at the same eutectic temperature since the one salt will contaminate the other due to their similar densities. This problem can be avoided with a good understanding of the phase diagram for the system as well as using the concept of selective seeding.

This chapter details how phase diagrams and seeding can be used to promote the crystallization of a desired salt in a ternary Na_2SO_4-$MgSO_4$-H_2O system, thereby avoiding salt contamination.

6.2 Methodology

The experiments focused on the crystallization of $Na_2SO_4 \cdot 10H_2O$ and/or $MgSO_4 \cdot 7H_2O$ from a Na_2SO_4-$MgSO_4$-H_2O system supersaturated at 12.0°C. The experimental temperature chosen was 14.1°C because this avoided the nucleation of ice and because reliable solubility data was also available for this temperature. The proportion of ice formed under eutectic conditions is always more than that of salt; therefore the concentration of the solution changes significantly as ice is formed. It is for this reason that all experiments were conducted in a region where ice crystallization would not occur.

The experimental aims were to:

- Determine the solubility of sodium sulphate and magnesium sulphate at the binary eutectic point for the Na_2SO_4-$MgSO_4$-H_2O system at 14.1°C,
- Determine the purity of salt and the loss of salt mass after each subsequent washing stage during the crystallization of a desired salt in a supersaturated Na_2SO_4-$MgSO_4$-H_2O system at 12°C.

A 10.78wt% Na_2SO_4 and 46.8wt% $MgSO_4 \cdot 7H_2O$ solution was prepared from 99w% Na_2SO_4 (Merck), 99wt% $MgSO_4.7H_2O$ (Merck) and de-ionized water of 15mΩ. Table 6.1 shows the type of seed material used in each experiment.

Table 6.1: Type of seed material added during each experiment.

Experiment #	Seed Type
$E_{A,1}$	$Na_2SO_4.10H_2O$
$E_{A,2}$	$Na_2SO_4.10H_2O$
$E_{A,3}$	$Na_2SO_4.10H_2O$
$E_{B,1}$	$MgSO_4.7H_2O$
$E_{B,2}$	$MgSO_4.7H_2O$
$E_{B,3}$	$MgSO_4.7H_2O$
$E_{C,1}$	Sand

6.2.1 Experimental Setup

The solubility experiment was performed in a 1.5L jacketed glass reactor. A Testo 175-177 temperature logging device was used to measure the temperature of the solution in the reactor. An IKA digital stirrer was used to provide adequate mixing with a 6-bladed Rushton turbine. Cooling was achieved by circulating Kryo40 through the jacket of the reactor with a Lauda RE207 thermostatic unit. The setup, excluding the thermostatic unit, was kept in a cold room at a temperature of 14.1°C±0.5°C.

The selective nucleation experiments were performed in a 250ml jacketed glass reactor. The setup was similar to the solubility experiments. Filtration was conducted in the cold room at a temperature of 12.0°C±0.5°C using a 300ml Millipore All-Glass filter holder connected to a vacuum pump. The filter paper pore size was 0.45µm.

6.2.2 Experimental Procedure

For the solubility experiment, the temperature of the solution in the reactor was maintained at 14.1°C for 48 hours to ensure that the system reached equilibrium as indicated by a constant conductivity measurement. The contents of the reactor were then removed and vacuum filtered using a Buchner Funnel. A liquid sample was taken

and analysed by Inductively Coupled Plasma Mass Spectrometry (ICP-MS) to determine the concentration of the Na^+, Mg^{2+} and SO_4^{2-} ions.

A 200ml solid-free sample of the filtrate from the solubility experiments was used for each selective nucleation experiment. The selective nucleation experiment was initiated by maintaining the solution temperature at approximately 16°C for 1 hour to ensure that the solution concentration had stabilized. A supersaturated solution was then created by cooling the solution to 12.0°C. This temperature (12°C) was the metastable limit for the system since cooling below this temperature resulted in spontaneous salt nucleation.

A seed mass percentage of 1% of the dominant solute was used for this study. This meant that a seed mass, regardless of the seed type, of ~0.94g was added to the solution for the experiments in this study. The solution was left for 40 minutes at 12°C once the seed material was added, after which the contents of the reactor were removed and vacuum filtered using the Millipore All-Glass filter holder. The solid, unwashed product in the filtration unit was removed from the vacuum setup and weighed. A small sample was taken of the salt product and dissolved in de-ionised water. This solution was then analysed by ICP-MS to determine the concentration of Na^+, Mg^{2+} and SO_4^{2-} ions. The salt purity, sp, of a specific salt could then be calculated and is defined as follows:

$$sp = \frac{[Cat]}{[Na^+]+[Mg^{2+}]} \qquad \textbf{(6.1)}$$

Where

[Cat] - mass concentration of cation (either Na^+ or Mg^{2+}) (mg/L)
[Na^+] - mass concentration of sodium (mg/L)
[Mg^{2+}] - mass concentration of magnesium (mg/L)

The filtration unit was again attached to the vacuum pump setup where the solid product was washed with ~30g ethanol which had been pre-cooled and maintained at 12°C. The salt product was washed with ethanol rather than a saturated solution of either salt since sodium sulphate is insoluble in ethanol [1] while magnesium sulphate is only slightly soluble in ethanol [2]. This ensured that there was no bias in the analysis as a result of the influence of the washing liquid. The weighing and analysis step was then repeated.

6.3 Results and discussion

6.3.1 The solubility of Na_2SO_4-$MgSO_4$-H_2O at 14.1°C

The solubility of the saturated Na_2SO_4-$MgSO_4$-H_2O solution at 14.1°C was found to be 10.78±0.35wt% Na_2SO_4 and 25.71±0.51wt% $MgSO_4$ (Table 6.2). The concentration of sodium sulphate in the saturated solution at 14.1°C compares more favourably with the values obtained from the extended UNIQUAC model [3] (9.28% difference) than with the values obtained from the revised Helgeson-Kirkham-Flowers model used by OLI Stream Analyser [4] (23.5% difference). The percentage differences, %Diff, were calculated as follows:

$$\%\text{Diff} = \left[\frac{x_{exp} - x_{cal}}{x_{exp}}\right] \cdot 100 \qquad \textbf{(6.2)}$$

Where

x_{exp} - is the experimentally determined solubility (wt%)

x_{cal} - is the calculated solubility from OLI or UNIQUAC model (wt%)

The percentage differences, %Diff, between the experimentally determined and thermodynamic solubilities for magnesium sulphate were 3.2% and 18.87% for OLI and the extended UNIQUAC model respectively.

Table 6.2: Solubility data for a saturated Na_2SO_4-$MgSO_4$-H_2O solution at 14.1°C.

	Experimental			OLI		extended UNIQUAC	
	wt%			wt%	% difference *	wt%	% difference *
Na_2SO_4	10.8	±	0.35	8.25	23.5	9.78	9.28
$MgSO_4$	25.7	±	0.51	26.6	3.2	20.86	18.87

* percentage difference compared to experimental values

6.3.2 Sodium sulphate purity with different seed types

A significant amount of solution is entrained with the salt during the filtration process. This entrainment directly affects the purity of the salt product. Washing the salt increases the purity by removing the entrained solution. Figure 6.1 shows the salt purity and cumulative loss of salt mass after each wash with ethanol for different seed additions. The highest salt purity (96±3.0%) was obtained with $Na_2SO_4 \cdot 10H_2O$

seeding and after two washes with ethanol. The error analysis from three repeat experiments for the initial salt purity in the case of $Na_2SO_4 \cdot 10H_2O$ seeding was 11%. This was probably due to the high concentration of magnesium sulphate (25.7±0.51wt% $MgSO_4$ compared to 10.8±0.35wt% Na_2SO_4) in the solution. Washing the salt product reduced this error significantly (0.64% after one wash).

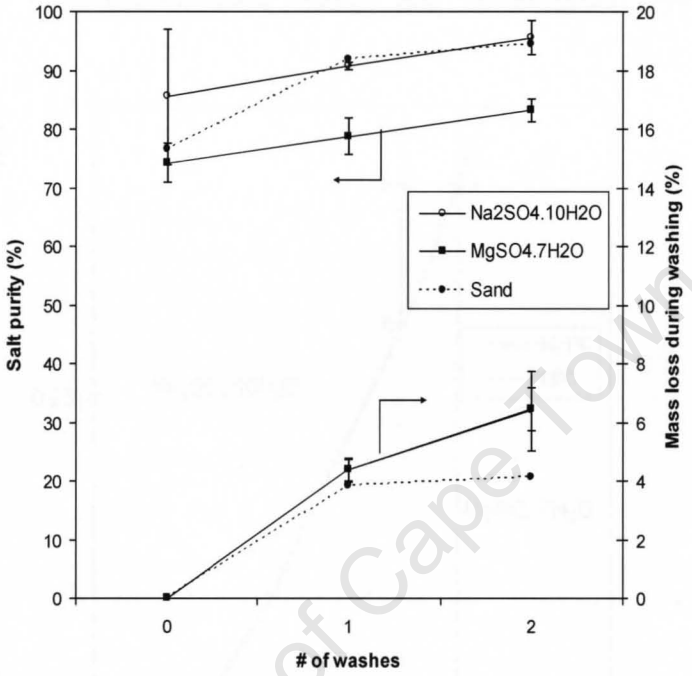

Figure 6.1: Salt purity and loss of salt mass during washing (wrt sodium sulphate).

The sodium sulphate salt purity was on average 11.9% lower when $MgSO_4 \cdot 7H_2O$ seeds were used. It could have been the actual $MgSO_4 \cdot 7H_2O$ seeds affecting the sodium sulphate purity. Since the seeds only contributed ~5.9wt% to the final salt product it is unlikely that it was the actual $MgSO_4 \cdot 7H_2O$ seeds affecting the sodium sulphate purity. A more likely explanation for the low purity could be due to the beginning of $MgSO_4 \cdot 7H_2O$ crystallization.

The initial salt purity with sand seeding (76%) had a similar percentage as the initial salt purity obtained with $MgSO_4 \cdot 7H_2O$ seeding (74%). After one wash the salt purity with sand seeding reached the same percentage as with $Na_2SO_4 \cdot 10H_2O$ seeding.

Figure 6.2 explains this. The initial saturated solution (with respect to both sodium sulphate and magnesium sulphate) (A) becomes supersaturated when it is cooled to 12°C (B). At this point (B) the solution is at conditions where only sodium sulphate

can crystallize therefore any seed material added to the supersaturated solution would result in the crystallization of $Na_2SO_4 \cdot 10H_2O$. The solution concentration becomes depleted in sodium sulphate as more $Na_2O_4 \cdot 10H_2O$ crystallizes out of solution and the solution concentration moves past point (C) where $MgSO_4 \cdot 7H_2O$ begins to crystallize. This explains what happened in these experiments; the experiment duration of 40 minutes resulted in a concentration change and an eventual crystallization of $MgSO_4 \cdot 7H_2O$.

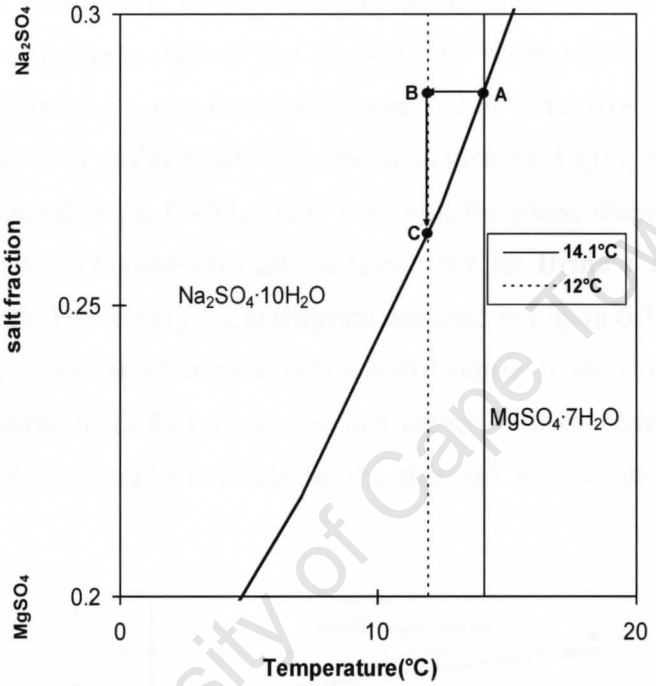

Figure 6.2: Na_2SO_4-$MgSO_4$-H_2O ternary phase diagram with two isotherms at 14.1°C and 12.0°C.

A better understanding of a system can be obtained with the aid of phase diagrams as evident by the information depicted in Figure 6.2.

6.3.3 Loss of salt mass during washing

Washing the salt increases the salt purity but for each wash a certain amount of salt is lost due to the salt product dissolving in the washing medium. A loss in mass can also be attributed to the removal of the entrained brine.

The loss of salt mass for $Na_2O_4 \cdot 10H_2O$ and $MgSO_4 \cdot 7H_2O$ seeding was 4.2% after one wash and increased to 6.2% after two washes (see Figure 6.1). The smallest loss in mass (4.1%) of salt was observed for sand seeding after two washes. The loss in mass after each wash was relatively low and would be even lower if a saturated solution of

the desired salt was used as the washing liquid. This is due the fact that a saturated solution is unable to dissolve any further solute resulting in minimal salt loss.

6.3.4 Application to case study brines

The concept of seeding and the aid of phase diagrams mentioned in this chapter could be used to prevent salt contamination in the industrial brine samples if two salts crystallized out at the same temperature. However, both brine samples, which were investigated in this work, showed that no two salts began to crystallize at the same temperature (Chapter 4). For example, Figure 6.3 is a ternary phase diagram for calcium sulphate and sodium sulphate and is similar to Figure 6.2 but both brine samples are situated in the $CaSO_4 \cdot 2H_2O$ region of the phase diagram with no initial possibility of salt contamination (salt fraction = 0.9 for **Brine 1** and salt fraction = 0.91 for **Brine 2**). The ternary phase diagram depicted in Figure 6.3 is a simplification of the actual brine samples but the results are still similar to the results obtained from the thermodynamic modelling presented in Chapter 4 (both thermodynamic results showed that calcium sulphate would be the first salt to crystallize from the brine samples).

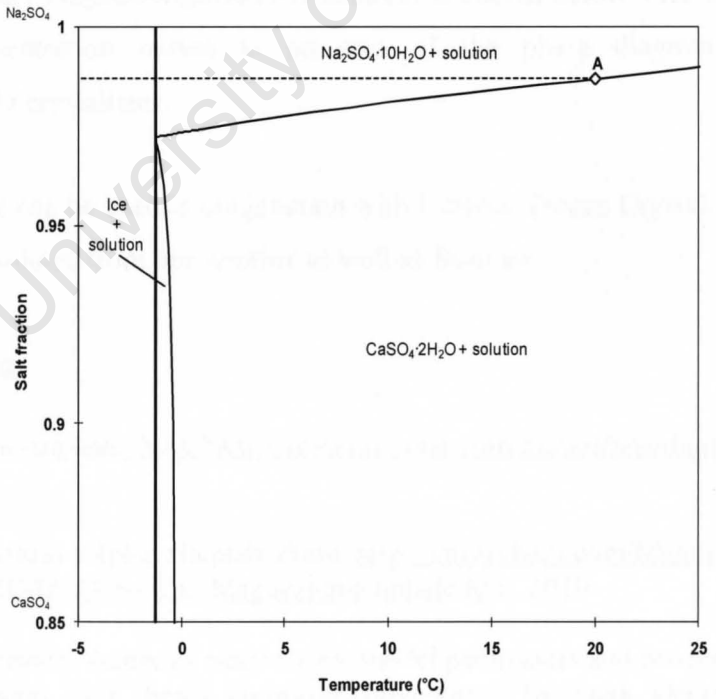

Figure 6.3: Ternary Na_2SO_4-$CaSO_4$-H_2O phase diagram [3].

Hypothetically, if the initial brine composition was situated at point A in Figure 6.3, then the system would be saturated with respect to both $Na_2SO_4 \cdot 10H_2O$ and $CaSO_4 \cdot 2H_2O$ thus providing conditions for salt contamination to occur. However, salt contamination could be avoided by cooling the solution so that only $Na_2SO_4 \cdot 10H_2O$ would crystallize (similar to the experimental work presented in this chapter). Cooling the solution from point A along the dotted line would only result in the crystallization of $Na_2SO_4 \cdot 10H_2O$.

In summary, this work shows how useful phase diagrams are in understanding systems and how they can be used to determine which salts will crystallize. Phase diagrams are also useful in understanding how possible salt contamination could be avoided.

6.4 Conclusion

This chapter has demonstrated how phase diagrams and seeding can be used as a separation technique to prevent salt contamination in a ternary Na_2SO_4-$MgSO_4$-H_2O system. The extended UNIQUAC model has shown why $Na_2SO_4 \cdot 10H_2O$ crystallizes when the ternary Na_2SO_4-$MgSO_4$-H_2O solution is cooled below 14.1°C to 12°C; the solution concentration moves to an area of the phase diagram where only $Na_2SO_4 \cdot 10H_2O$ crystallizes.

This technique can be used in conjunction with Eutectic Freeze Crystallization for the separation of solutes from one another as well as from ice.

References

[1] Sodium sulphate, http://www.mineralszone.com/minerals/sodium-sulfate.html, 2010.

[2] Magnesium sulphate heptahydrate, http://mubychem.com/Magnesiumsulfate-USP-BP-IP-ACS-FCC-Magnesiumsulphate.htm, 2010.

[3] K. Thomsen, Aqueous electrolytes: model parameters and process simulation, PhD Thesis, Technical University of Denmark, Denmark,1997.

[4] OLI Systems Inc., OLI Stream Analyser, Version 3.0, Morris Plains, New Jersey, USA, 2010.

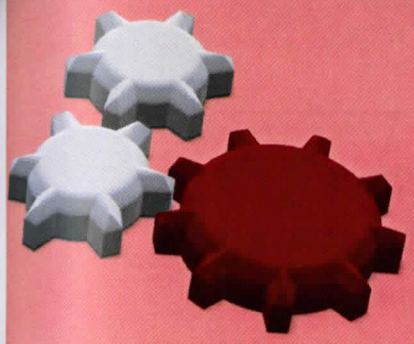

CHAPTER 7 : SEQUENTIAL EFC

We never know the worth of water till the well is dry.

Thomas Fuller, 1732

Graphic from: http://farm4.static.flickr.com/3070/2782765652_147e199269_o.jpg

7.1 Introduction

The eMalahleni Water Reclamation Plant (EWRP) was built by Anglo Coal South Africa and BHP Billiton Energy Coal South Africa (BECSA) in a partnership to address the damage done to the environment and water resources through Acid Mine Drainage in the eMalahleni area of South Africa. The state-of-the-art plant uses the **Hi** recovery **P**recipitating **R**everse **O**smosis (HiPRO) process technology developed by Keyplan. The HiPRO process produces 25 000m^3/d of potable water with recovery rates in excess of 99% [1]. The solid waste produced from the EWRP consists of approximately 100tons/d of gypsum ($CaSO_4 \cdot 2H_2O$) and a liquid waste amounting to approximately 150m^3/d [1], which is currently being disposed of in evaporation ponds.

The solid waste is currently being treated by two processes which were developed by the Council for Scientific and Industrial Research (CSIR) South Africa to offset the high costs associated with gypsum disposal. These two processes, called GypSLiM (**Gyp**sum processed into **S**ulphur, **Li**mestone and **M**agnesite) and GypBump (**Gyp**sum converted into **Bu**ilding and **M**ining **P**roducts), convert the raw gypsum into valuable products which include calcium carbonate, magnesium carbonate, and sulphur, as well as building and mining products. These building products are currently being investigated as an alternative material for the construction of low cost housing [1].

This chapter is the final step of the brine treatment protocol. It looks at the sequential removal of calcium sulphate and sodium sulphate along with ice from brine samples obtained from the EWRP. It also draws on techniques and information presented in the previous chapters of this thesis.

7.2 Methodology

The experimental aims for the sequential removal of salts presented in this chapter are given in Table 7.1.

Table 7.1: The aims of the experimental procedure for the sequential removal of salts during EFC.

Part	Aim(s)	Experiment Name	Concentration		
E	• To demonstrate "proof of concept" of sequential EFC by reducing the volume of brine while at the same time producing potable water and pure salt(s), • To identify the salts that form, • To determine the purity of ice and salt(s) formed, • To carry out a mass balance for the EFC process.	E1, E2, E3...E17	Brine 1 (composition given in Chapter 3)		
F	To determine the purity of ice formed from solutions with different sodium sulphate concentrations (binary system) and to investigate ways to improve the efficiency of ice-salt separation.	F1	1wt% Na_2SO_4		
		F2	5wt% Na_2SO_4		
		F3	5wt% Na_2SO_4		
G	To produce different brine samples of varying concentrations for subsequent tests (Part H).	G1, G2, G3...G26	Brine 2 (Chapter 3)		
H	To determine the mass deposition of calcium at 0°C and 22°C and for different brine concentrations.	H1	Brine 2 (Chapter 3)	22	Temperature (°C)
		H2	Stage 1B (filtrate of H1)		
		H3	Stage 2B (filtrate of H2)		
		H4	Stage 3B (filtrate of H3)		
		H5	Brine 2 (Chapter 3)	0	
		H6	Stage 1B (filtrate of H5)		
		H7	Stage 2B (filtrate of H6)		
		H8	Stage 3B (filtrate of H8)		
		H9	Brine 2 (24 hour period)		
I	To determine the operating conditions for the removal of calcium sulphate and ice under eutectic conditions.	I1	Brine 2 (Chapter 3)		
J	• To determine the operating conditions for the removal of sodium sulphate and ice under eutectic conditions, • To investigate if a synthetic brine can accurately model an actual brine.	J1	Table 7.2		

Brine samples obtained from the RO plant were used in most of the experiments described in this chapter (the other experiments used synthetic streams). The same methodology was used for both brines and synthetic streams, unless otherwise stated.

7.2.1 Solution Preparation

The brine samples were kept at 10°C and filtered before use. The filtrates from experiments for **Brine 1** were kept at ~22°C while the filtrates from experiments for **Brine 2** were kept in a fridge at 3°C. The filtrates for Brine 2 were kept at 3°C to prevent less salt from crystallizing out of solution. The brine samples for Part H were obtained by concentrating **Brine 2.** The filtrates from each stage of the concentrating procedure were used for the experiments. The **Stage G1** brine was obtained by removing 36.7% ice from **Brine 2**. The **Stage G2** brine was obtained by removing 52% ice from the feed to this stage (filtrate from **Stage G1**). Similarly, the **Stage G3** brine was obtained by removing 23.6% ice from the feed to this stage. The synthetic brines (Part J) were prepared from 99% pure chemicals (Merck) (see Table 7.2). The thermodynamics for the synthetic brine in Chapter 4 showed that the synthetic stream was supersaturated with respect to calcium sulphate. The $CaSO_4 \cdot 2H_2O$ mass in Table 7.2 is based on a supersaturated concentration and therefore this amount of calcium sulphate would never fully dissolve. Therefore, the actual amount of calcium sulphate used to make up the synthetic was 1.9305g/L (saturated) and not 2.9214g/L (supersaturated).

Table 7.2: Synthetic brine makeup.

	Mass g/L
Na_2SO_4	38.7626
$MgSO_4$	1.7196
$CaSO_4 \cdot 2H_2O$	2.9214
K_2SO_4	6.7381
$NaHCO_3$	1.0119
NaCl	3.4862
KNO_3	3.4329
$(NH_4)_2SO_4$	1.2132

The binary sodium sulphate solutions used for the ice washing experiments (Part F) were also prepared from 99% (Merck) Na_2SO_4.

7.2.2 Experimental Setup

The industrial brines (Parts E and Part G), synthetic experiments (Part J) and binary sodium sulphate ice washing experiments (Part F) were performed in a 1.5L jacketed

glass reactor. A Testo 175-177 temperature logging device was used to measure the solution temperature of the reactor. An IKA stirrer with variable speed control was used to provide adequate mixing with a 4-bladed rushton turbine impeller. The required level of cooling was achieved with a Lauda RE207 thermostatic unit that continuously circulated the coolant, Kryo40, through the jacket of the reactor. The setup, excluding the thermostatic unit, was kept in a freeze room at different operating conditions depending on the stage of the cascading concentration procedure (Figure 7.1 and Figure 7.2).

Filtration of the final products was conducted in the cold room maintained at the same setpoint temperature as the thermostatic unit. A Buchner funnel connected to a 1L filtration flask was used to filter the ice product. A 300ml Millipore All-Glass filter holder connected to a vacuum pump was used to filter the salt for those experiments that produced salt. The pore size of the filter paper was 0.45μm.

For calcium mass deposition experiments (Part H), 200ml samples of varying concentrations were placed in a 250ml conical flask and sealed with Parafilm M laboratory film. A set of four solutions (H1 to H4) were agitated using a magnetic stirrer at a temperature of 22°C. The other four experiments (H5 to H8) were magnetically stirred whilst being kept at a constant temperature of 0°C in a freeze room. A seed mass of ~1.0g $CaSO_4 \cdot 2H_2O$ was added to each conical flask.

7.2.3 Experimental Procedure

The experiments for Part E and Part G were initiated by adding approximately 1250g (except for experiment G1 which used a 3L crystallizer with a brine feed of 2585g) of the brine that had been previously maintained at 10°C to the crystallizer. The thermostatic unit and setpoint of the freeze room were set to the same temperature and simultaneously adjusted depending on the stage of the cascading concentration procedure. These values were typically 1°C below the expected crystallizing temperature of the ice. For example, in the initial stream of **Brine 1**, ice crystallized at -0.5°C thus the thermostatic unit and freeze room were set at -1.5°C. The data logging of temperature and conductivity measurements were initiated upon addition of the solution to the crystallizer.

The contents of the reactor were then removed and placed in a 3L beaker and kept in the freeze room. The ice and salt were left to stand in the beaker and allowed to separate for ±10minutes following which the ice and its entrained brine were carefully separated from the salt and its entrained brine into separate beakers. The ice was then filtered under vacuum using a Buchner Funnel. The saturated salt solution was filtered with the 300ml Millipore setup. During washing experiments, the ice product was washed with 50ml de-ionised water which was pre-cooled and kept in the freeze room at the same conditions as the experiment.

The ice formed for one of the experiments (F3) during the binary sodium sulphate ice washing experiments was first dispersed in a saturated sodium sulphate solution at the same temperature of the experiment (-0.9°C). This dispersed any salt trapped with the ice. The ice was then removed and washed with de-ionised water as before. The salt present in the saturated sodium sulphate was removed by filtration with the 300ml Millipore setup.

Liquid samples of the feed, ice (after various washes), the filtrate from the ice washing step, and concentrated brine filtrate were withdrawn and analysed using ICP-MS to determine the concentration of the various cations and anions present. For experiments in which salt formed, the salt was dissolved in de-ionised water and the solution analysed using ICP-MS.

Figure 7.1 and Figure 7.2 show the cascading concentration procedures, as described by Baker [2], which were employed during the experiments for Part E and Part G. The blocks show the experiment number as well as the identity of solid contents obtained from each experiment. This approach was adopted because a working volume of the same concentration as that obtained from the cascading concentration procedure could not be achieved with a single 1.5L crystallizer. In addition, it was found that a solid content of more than 30% ice during the co-crystallization with salt made the separation of ice and salt extremely difficult as the entire crystallizer was filled with ice from top to bottom. Thus, to avoid this, the concentrating procedure was spread over a number of experiments.

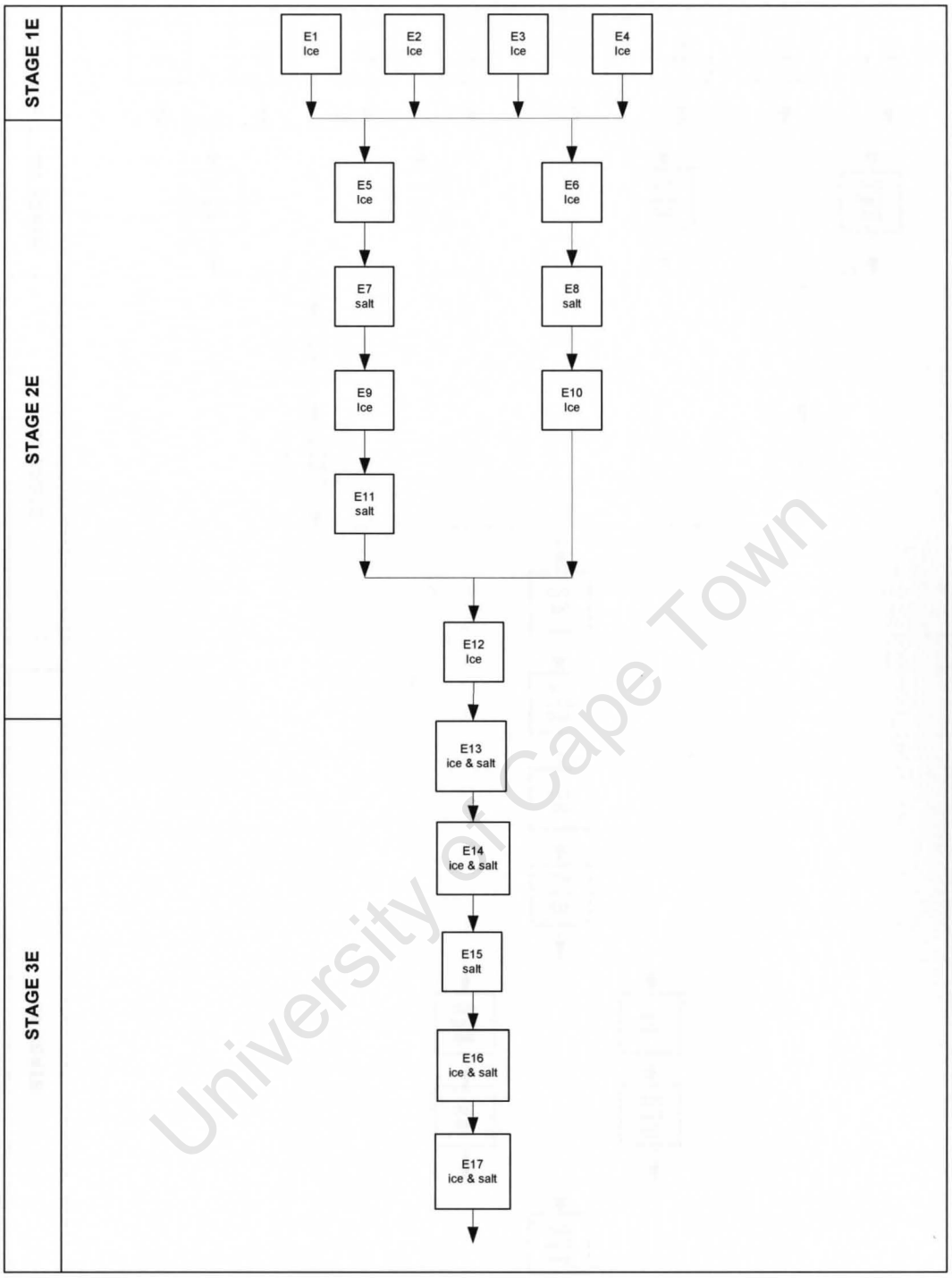

Figure 7.1: Cascading concentration procedure for **Brine 1**.

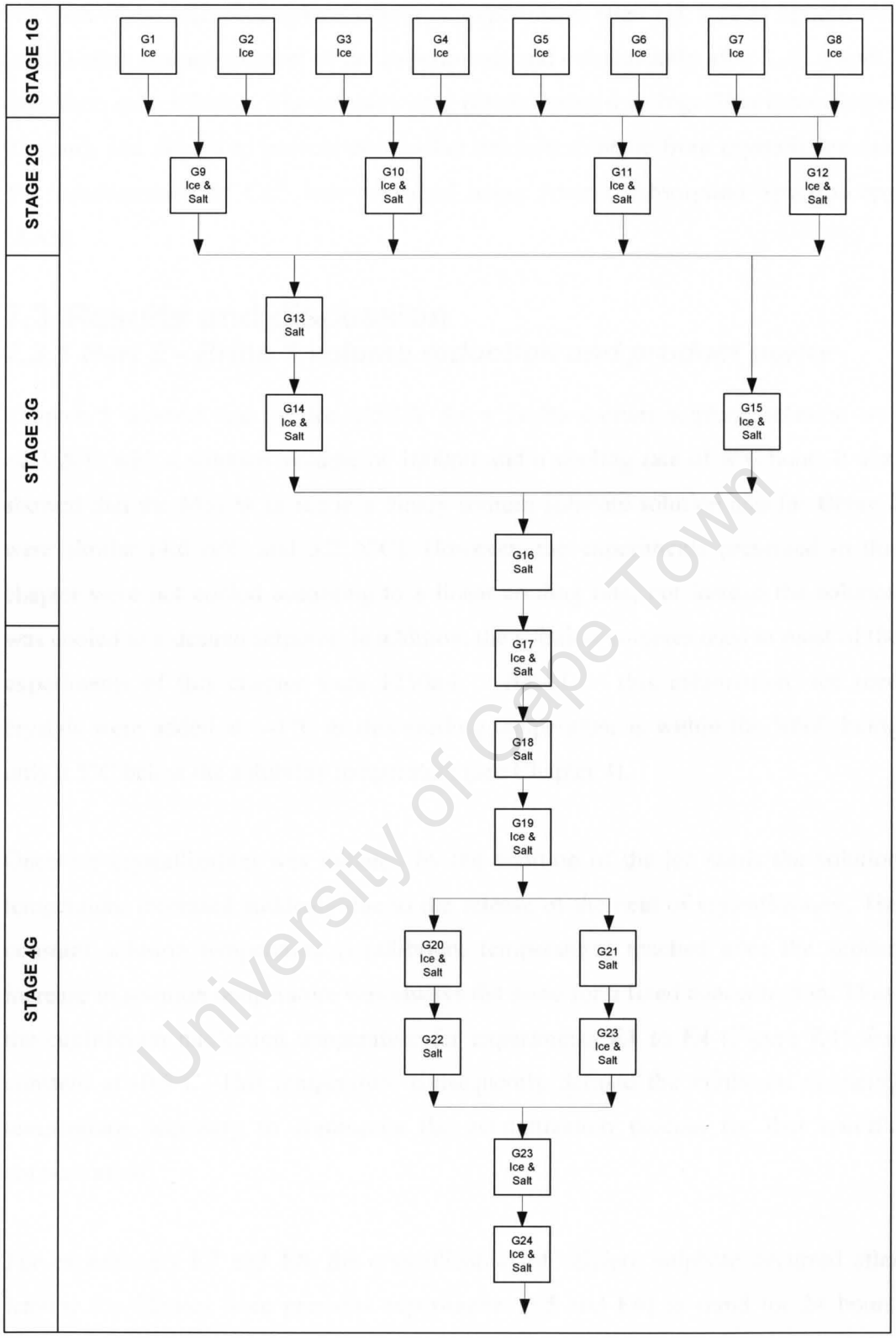

Figure 7.2: Cascading concentration procedure for **Brine 2**.

For each of the calcium sulphate saturation experiments (Part H), a 10ml sample was taken before commencement of the experiments and subsequently after 1, 3, 4 and 7 days from each solution. The samples were filtered using a syringe filter (pore size of 0.20μm), and diluted to prevent any further calcium sulphate from crystallizing out. The concentration of Ca^{2+} was measured using Atomic Absorption Spectroscopy (AAS).

7.3 Results and discussion

7.3.1 Part E - Brine 1 volume reduction and product purity

Chapter 5 showed that the ice MSZW for a 1wt% sodium sulphate solution was ~2.3 Δ°C with a solution volume of 1000ml and a cooling rate of 8°C/hour. It also showed that the MSZW of ice in a binary sodium sulphate solution and for **Brine 2** were similar (4.6 Δ°C and 5.2 Δ°C). However, the experiments presented in this chapter were not cooled according to a linear cooling rate, but instead the solution was cooled to a desired setpoint. In addition, the solution volumes used in most of the experiments of this chapter were 1250ml. Based on this information, ice seed crystals were added at ~-1°C as this seeding temperature is within the MSZ, being only 0.5°C below the solubility temperature (see Chapter 4).

Once ice crystallization was initiated by the addition of the ice seeds the solution temperature increased suddenly due to the release of the heat of crystallization. The constant solution temperature (equilibrium temperature) reached after the sudden increase in solution temperature was always the same for a fixed concentration. Thus, the equilibrium nucleation temperature for experiments **E1** to **E4** (Figure 7.1) was constant at -0.5°C. This temperature consequently defined the minimum operating temperature necessary to commence the crystallization process for that specific concentration.

For experiments **E7** and **E8**, the crystallization of calcium sulphate occurred after leaving the filtrates from previous experiments (**E5** and **E6**) to stand for 24 hours. This was due to the slow crystallization of calcium sulphate and its inverse solubility [3]. This was verified by leaving the filtrate obtained from experiment **E9** in the laboratory at a temperature of 22°C whilst the filtrate from experiment **E10** was kept in the freeze room at 5°C for 24 hours. From this test, it was found that experiment **E9**

resulted in the crystallization of calcium sulphate while experiment **E10** did not. This provided the basis for investigating this phenomenon further by conducting separate experiments to determine the mass deposition of calcium at different temperatures and concentrations. **Brine 2** and its different concentrations were used for this investigation.

The results obtained from the cascading concentration procedure are shown in Figure 7.3. Pure calcium sulphate (98.0%) and pure sodium sulphate (96.4%) were produced along with potable water. The salt products were not washed and thus the purity is expected to increase further with washing. On a mass basis, a 97% reduction in the initial feed was obtained. However, calcium sulphate was not produced under EFC conditions since it did not crystallize along with ice but rather it crystallized within 24 hours. **Brine 2** was used to investigate if EFC conditions could be achieved with the crystallization of calcium sulphate and ice.

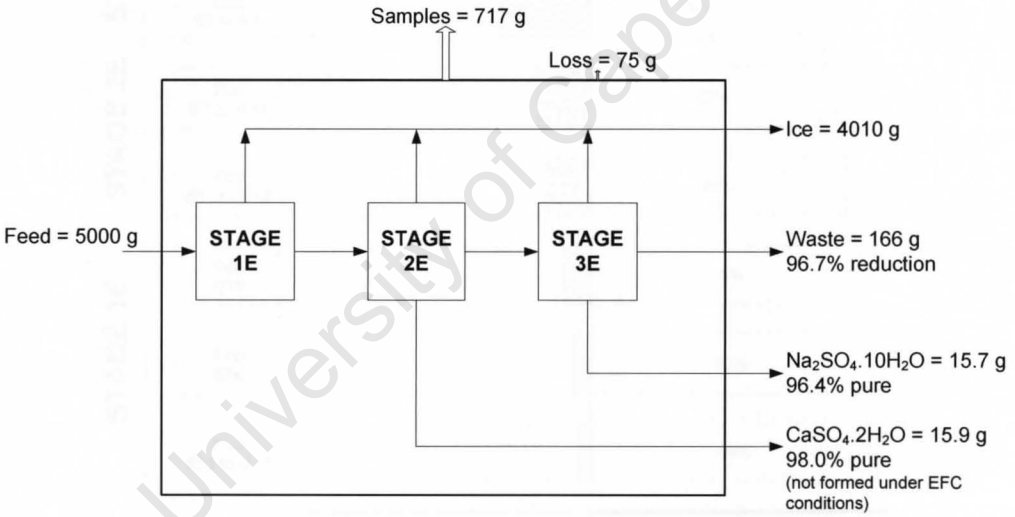

Figure 7.3: Mass balance for **Brine 1**.

The loss calculated during the cascading concentration procedure for **Brine 1** was due primarily to the amount of liquid removed for sampling. Approximately 30ml of solution was removed after each experiment which resulted in a loss of about 14% of the feed towards sampling. Other minor losses due to evaporation and human error only amounted to about 1.5% of the experiment feed not being accounted for.

Figure 7.4 shows the conversion of waste (brine) to viable products (ice and salts) at different stages of the cascading concentration procedure. Experiments **E1** to **E4**

resulted in the highest single conversion (54%) of the brine to ice. The overall conversion of waste to products for **Stage 1E** was 71% ice only since this stage was a pre-concentration stage with no salt crystallization occurring. The conversion increased marginally when salt crystallization occurred. The waste conversion for **Stage 2E** was 85% and 96% for **Stage 3E**. There was thus a lower increase in waste conversion from **Stage 2E** to **Stage 3E** (85% to 96%) compared to the waste conversion from **Stage 1E** to **Stage 2E** (71% to 85%) due to the majority of the ice forming in **Stage 1E**. Therefore the total salt and water recovery from stages 1E to 3E was 96%.

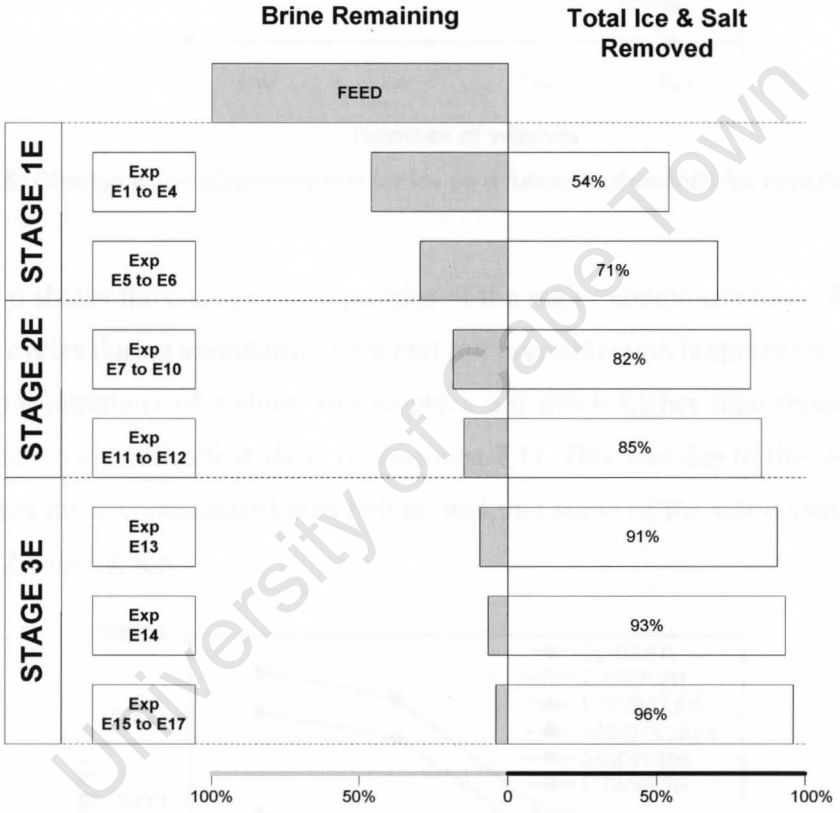

Figure 7.4: Waste conversion for different steps in the cascading concentration procedure.

The concentration changes of the major components are shown in Figure 7.5 during the crystallization of ice only (experiment **E1**). The limits are within acceptable South African water drinking standards after one wash [4]. These results indicate that washing can significantly reduce the entrainment of the brine with the ice crystals.

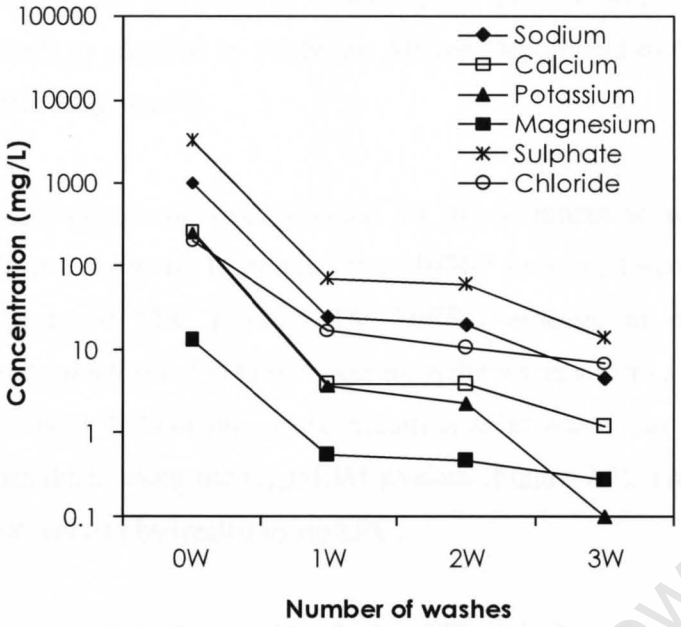

Figure 7.5: Change in ion concentrations for ice as a function of washes for experiment E1.

Figure 7.6 shows the concentration profiles of the major components as a function of washing cycles during simultaneous ice and salt crystallization (experiment **E14**). The initial concentrations of sodium and sulphate are much higher than those obtained during the ice crystallization alone (experiment **E1**). This was due to the fact that the stream was more concentrated than before, and that some of the salt crystals became entrapped with the ice.

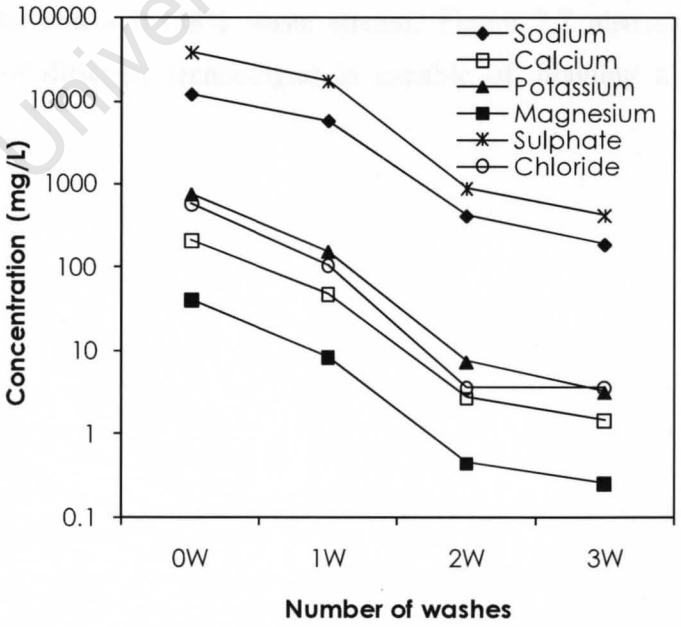

Figure 7.6: Change in ion concentrations for ice as a function of washes for experiment E14.

Washing the ice reduced the impurity concentration levels to within acceptable water drinking standards as required by the South African Department of Water Affairs and Forestry [3] after three washes.

Figure 7.7 shows an overall mass balance for the treatment of waste water using different treatment methods. It includes the HiPRO process, GypSLIM process, as well as the proposed EFC process. The HiPRO process, as mentioned in the introduction, recovers 99% of potable water from the waste stream and produces a 1% waste stream. About 40% of this waste stream is solid waste that can be converted into valuable products using the GypSLIM process (Figure 7.7). The remaining 60% of this waste stream can be treated using EFC.

The EFC process could in theory add a further 120m^3/d of potable water to the plant. A production of 476kg/d $CaSO_4 \cdot 2H_2O$ and 471kg/d $Na_2SO_4 \cdot 10H_2O$ would also be obtained. Whilst the additional amount of water recovered using EFC may appear relatively low considering that the amount of water currently produced using the HiPRO process is 25 000m^3/d, the primary emphasis should be on waste minimization and conversion of all possible waste products to useful ones (in this case calcium sulphate and sodium sulphate) rather than having to dispose of them at an additional cost. The bar on the right of Figure 7.7 shows the overall conversion of the feed stream (waste) to valuable products. The product stream is 99.6% water, 0.286% pure individual salts and a 0.138% waste stream. Figure 7.7 also shows that only a combination of different technologies is capable of attaining a near zero waste discharge.

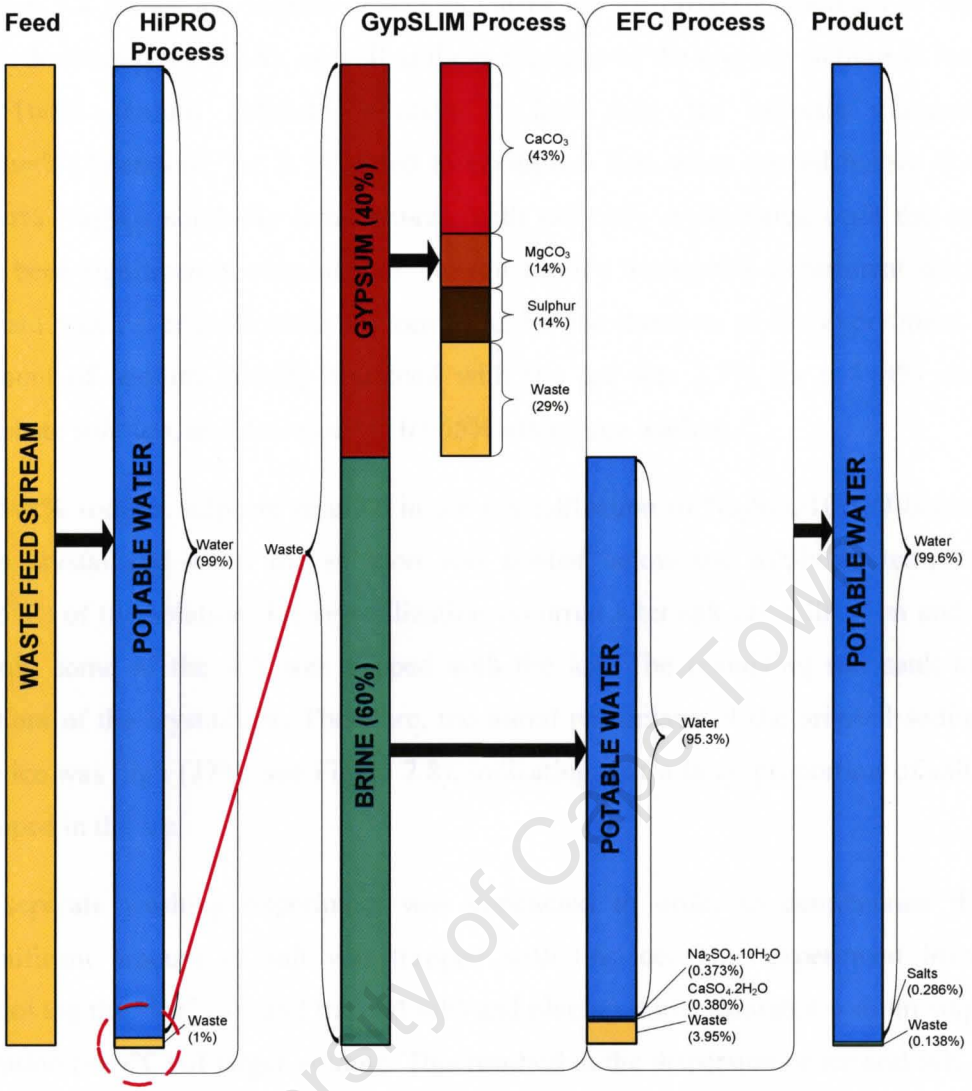

Figure 7.7: Overall mass balance for a combination of treatment methods.

As can be seen, novel technologies such as EFC can offer a sustainable method for the treatment of brines in accordance with the necessity for current water treatment processes to reduce the volume and extent of water pollution. There also needs to be a paradigm shift that focuses on new approaches that include wise investments and technological innovation that not only seeks to obtain treated water but also treats and converts the solid waste products into useful ones [6].

7.3.2 Part F – Ice and salt separation

During EFC conditions, the purity of ice is affected by the efficiency of the ice-salt separation step. A significant amount of salt can be trapped with the ice, thus affecting the purity of the ice and the yield of salt. This section examines this phenomenon.

Figure 7.8 shows the sodium concentration in ice for different numbers of washes with de-ionised water (**A**), as well as the percentage of the original sodium in ice (**B**). A 1wt% sodium sulphate solution is less than the eutectic composition (4.2wt%).Therefore, ice is expected to crystallize first when cooled below -0.44°C (1wt% Na_2SO_4 solubility temperature), with salt only crystallizing once the stream has been significantly concentrated. No salt formed during this experiment since the stream was never sufficiently concentrated for the duration of the experiment. The amount of sodium initially entrained with the ice was 3.7% for a 1wt% sodium sulphate solution, and decreased to 0.065% after three washes.

A 5wt% sodium sulphate resulted in the crystallization of $Na_2SO_4 \cdot 10H_2O$ before ice was crystallized when the solution was cooled below the solubility temperature (1.5°C) of the solution. Ice crystallization occurred after salt crystallization and, as a result, some of the salt was trapped with the ice. The remaining salt sank to the bottom of the crystallizer. Therefore, the initial percentage of the original sodium in the ice was high (27%; see Figure 7.8), indicating that a large proportion of salt was trapped in the ice.

A separate washing experiment was conducted in order to demonstrate that a significant amount of salt was trapped with the ice. This experiment involved removing the "ice" (ice and trapped salt) and placing it in a saturated sodium sulphate solution (-0.9°C) of larger volume. This resulted in the dispersion of ice and salt, with the ice remaining at the top of the solution while the liberated salt sank to the bottom. The "ice" solution was also agitated gently with a spatula during its placement into the saturated salt solution. This also helped with the separation of ice and salt. The results of this experiment are also shown in Figure 7.8 (**5wt%***). The ice was then removed from the saturated salt solution and washed with de-ionised water as before. These results show that the initial sodium concentration in ice was lower (11%), indicating that a significant amount of salt was liberated from the ice using this separation technique. Therefore, the efficiency of the ice-salt separation can be improved by dispersing the "ice" in a larger solution volume as well as by agitating the "ice".

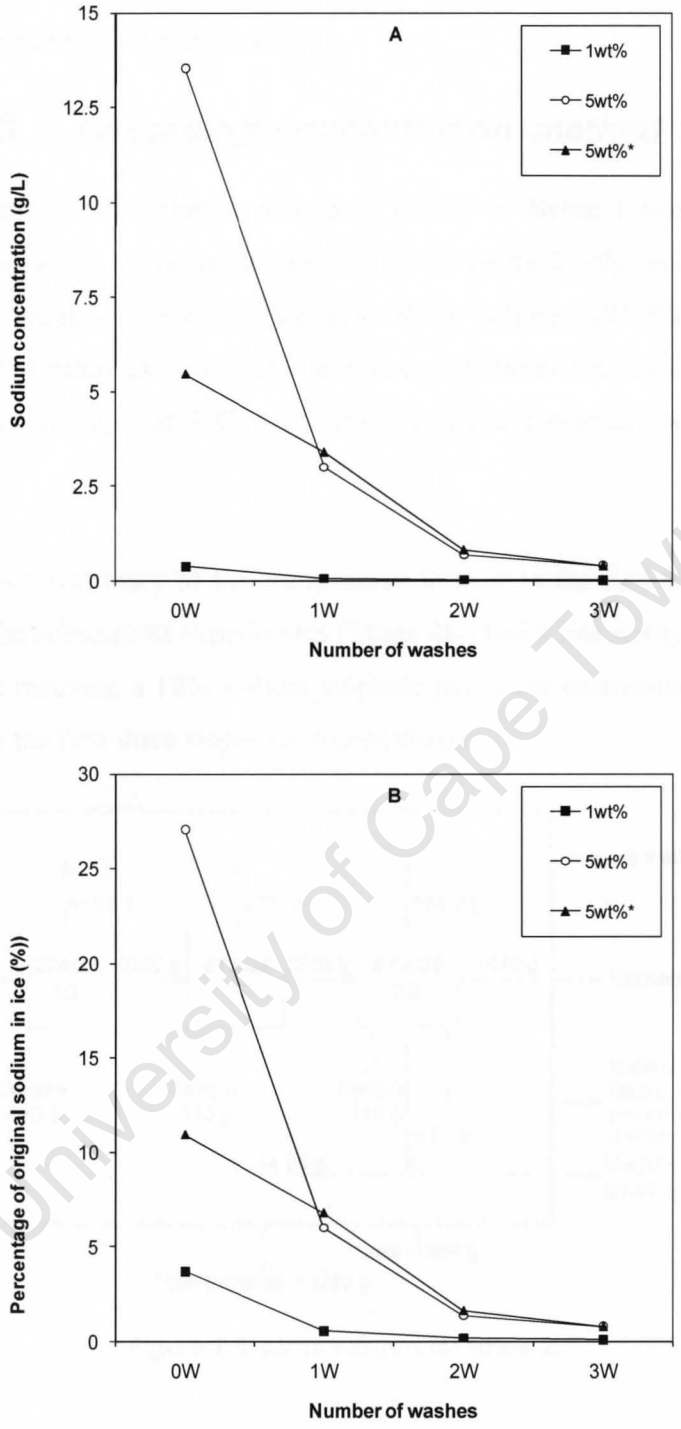

Figure 7.8: Sodium concentration in ice after washing (**A**) and the percentage of original sodium in ice (**B**).

Reddy and co-workers [5] investigated the effect of agitation on the separation of ice and salt which was formed under EFC conditions from a 5wt% sodium sulphate solution. They showed that, with the addition of agitation in the separation vessel, the purity of ice could be improved by as much as 90%. Therefore, it is recommended

that the "ice" be agitated in a larger volume separation vessel to improve the efficiency of the ice-salt separation step.

7.3.3 Part G – Cascading concentration method for Brine 2

A similar cascading concentration procedure to that of **Brine 1** was conducted for **Brine 2**. The cascading concentrating procedure for **Brine 2** only produced ice in the first stage. The procedure produced ice and sodium sulphate (97.5% pure) in **Stage 2G**. The filtrate of **Stage 2G** was highly concentrated and as a result calcium sulphate crystallized out overnight at 3°C. More ice and sodium sulphate was produced in **Stage 3G**.

Figure 7.9 gives a summary of the components formed in the first three stages. The salt formed in the subsequent experiments (**Stage 4G**) had a low purity (<89% sodium sulphate purity; reaching a 12% sodium sulphate purity for experiment **G25**) and for this reason only the first three stages were considered.

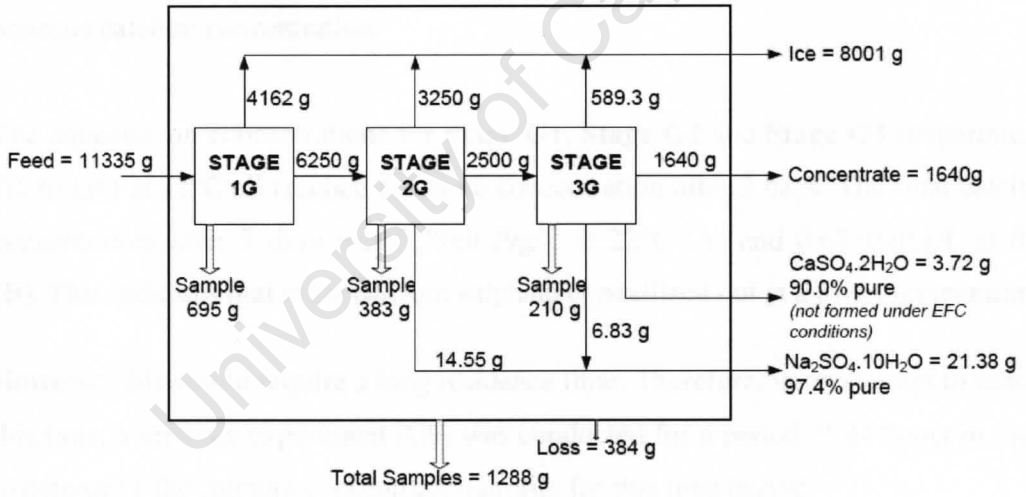

Figure 7.9: Mass balance for **Brine 2.**

7.3.4 Part H – Calcium mass deposition from Brine 2

The potential problem with the calcium sulphate being present at saturation, as predicted by the preceding thermodynamic modelling of Chapter 4 is described in this section.

Seeding can promote the growth or mass deposition of a specific component. For example, if $CaSO_4 \cdot 2H_2O$ seeds are added to a supersaturated calcium solution, the calcium ions crystallize out of solution in order to form more calcium sulphate. This process continues until a new equilibrium is reached. Therefore, a lower aqueous calcium concentration indicates that $CaSO_4 \cdot 2H_2O$ crystallized out of solution. Figure 7.10 shows the amount of calcium remaining in solution for experiments G1 to G9. The initial calcium concentration in **Brine 2** (G1) at 22°C was ~1g/L. The calcium concentration increased to a peak of 2.2g/L after 1 day and subsequently decreased to 0.80g/L after 7 days. The initial aqueous calcium concentration increase in the original **Brine 2** stream was due to dissolution of the seed material, indicating that the original brine sample was initially unsaturated. The subsequent decrease in the aqueous calcium concentration of the original after 1 day to a concentration of 0.75g/L indicated that the solution was no longer supersaturated. The initial aqueous calcium concentration for **Stage G3** was lower than **Stage G2** even though **Stage G3** was slightly (23.6% ice removal from the feed to the stage) more concentrated. This was due to the crystallization of $CaSO_4 \cdot 2H_2O$ overnight at 3°C resulting in a lower aqueous calcium concentration.

The aqueous ion concentrations for **Stage G1**, **Stage G2** and **Stage G3** (experiments G1 to G4) at 22°C all reached the same concentration after 3 days. The final calcium concentration after 7 days was 0.79±0.29g/L at 22°C (A) and 0.67±0.01g/L at 0°C (B). This indicates that more calcium sulphate crystallized out at a lower temperature.

However, this would require a long residence time. Therefore, in an attempt to reduce this time, a separate experiment (G9) was conducted for a period of 24 hours in order to determine the calcium concentration profile for this time period.

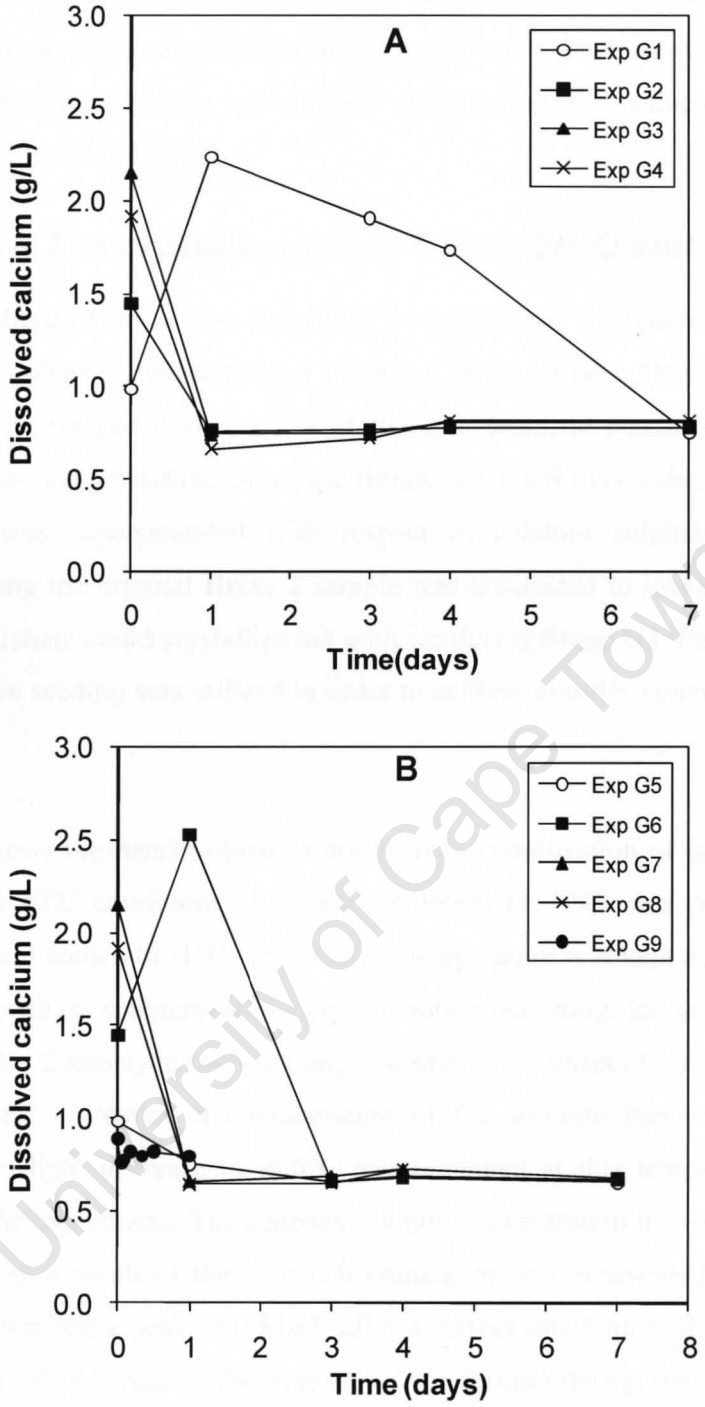

Figure 7.10: Changing aqueous calcium concentrations for different concentrations of **Brine 2** at 22°C (**A**) and 0°C (**B**) (Experiments G1 to G9).

Figure 7.10 also shows the aqueous calcium concentration for the 24 hour period (Experiment G9). The initial calcium concentration for experiment G9 was lower (0.89g/L) than experiment G5 (0.98g/L). This is due to some of the calcium sulphate crystallizing out between the two experiments which were one week apart. The

aqueous calcium concentration decreased to a minimum of 0.76g/L after 1 hour and subsequently increased and stabilized at 0.82g/L from 4 hours onwards. The final value (0.80g/L) after 1 day was slightly different to the values obtained for experiments G1 to G4 (~0.75g/L).

7.3.5 Part I – The crystallization of $CaSO_4.2H_2O$ and ice

The results obtained from the cascading concentrating procedure for **Brine 1** indicated that sodium sulphate formed in **Stage 2E** and **Stage 3E** with little or no calcium sulphate formed during ice crystallization (eutectic conditions). However, calcium sulphate did crystallize out of the filtrate when left overnight, indicating that the solution was supersaturated with respect to calcium sulphate. A separate experiment using the original **Brine 2** sample was conducted to investigate whether the calcium sulphate could crystallize out with ice during **Stage G1**. For this, calcium sulphate and ice seeding was utilized in order to achieve eutectic conditions with this brine sample.

Figure 7.11 shows the results obtained during the crystallization of ice and calcium sulphate under EFC conditions. The initial solution (at 0°C) was seeded with 1g $CaSO_4 \cdot 2H_2O$ and cooled to -1°C. The solution temperature was kept constant for two hours at -1°C with no spontaneous ice crystallization occurring. Ice seeds (~1g) were then added (after 2 hours) to the solution, resulting in the onset of ice crystallization. Due to the heat of fusion, the temperature of the solution increased to -0.5°C, followed by a slight decrease to -0.6°C and remained at this temperature for the remainder of the experiment. The aqueous calcium concentration increased during ice crystallization as a result of the stream becoming more concentrated. The calcium concentration reached a peak of 0.85g/L after a further one hour and decreased to a low of 0.68g/L after 5 hours. The amount of ice formed during the 3 hours of ice crystallization was ~20% of the feed.

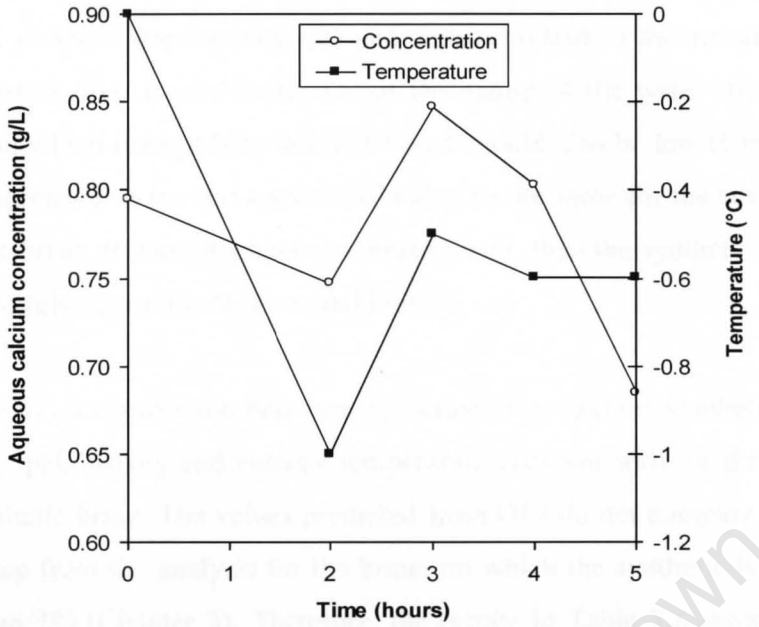

Figure 7.11: Aqueous calcium concentration and temperature change over time.

The results presented in Figure 7.11 indicate that calcium sulphate can crystallize along with ice during the pre-concentration step, provided the stream is seeded with $CaSO_4 \cdot 2H_2O$. The concentration levels of aqueous calcium after three hours of EFC operation (0.68g/L) and the concentration levels during calcium sulphate seeding at 0°C (0.67g/L) are similar. However, the calcium concentration reduction at 0°C with calcium sulphate seeding was obtained after a much longer period (1 week) compared to the three hours of EFC operation.

7.3.6 Part J – The crystallization of $Na_2SO_4.10H_2O$ and ice

The results from the cascading concentrating procedure for **Brine 2** showed that pure sodium sulphate was produced during EFC conditions. However, the sodium concentration profile during this procedure was not measured. In addition, the results were not based on the removal of calcium sulphate prior to this step. Therefore, this section focuses on the sodium concentration change during EFC conditions with reduced calcium and sulphate concentrations.

The experiment was also based on a synthetic brine rather than the actual brine since no remaining brine sample with the required concentration was available. In addition, the brine sample would not have had a reduced calcium concentration.

In order to approximate the brine by means of a synthetic brine, the synthetic brine should have a similar conductivity, pH and density to that of the actual brine, since these parameters give a good indication of the nature of the water stream. The ion imbalance on which the synthetic brine is based should also be low (Chapter 3). The eutectic temperature of ice and a salt should also be the same for the actual brine and the synthetic brine. If these parameters compare well, then the synthetic brine can, in theory, accurately approximate the actual brine.

Table 7.3 shows a comparison between the actual brine and the synthetic brine. The conductivity, pH, density and eutectic temperature compare well for the actual brine and the synthetic brine. The values predicted from OLI do not compare as well. The ion imbalance from the analysis for the brine, on which the synthetic brine is based, was less than 3% (Chapter 3). Therefore, the results in Table 7.3 show that, in this instance, a synthetic brine can approximate an actual brine, provided the key parameters (conductivity, pH, density and eutectic temperature) match and the ion imbalance is low. The fact that the synthetic stream had less calcium sulphate than the real brine also did not affect the approximation of the brine. This was probably due to the low concentration of calcium present in the brine compared to the other major components.

Table 7.3: Comparison between an actual brine and the synthetic brine.

		Brine	Synthetic	OLI
Conductivity	**mS/cm**	40.86	39.23	-
pH	**-**	8.1	8.3	7.35
Density	**g/cm3**	1.041	1.042	1.049
Eutectic temperature ($Na_2SO_4 \cdot 10H_2O$ and ice)	**°C**	-1.5	-1.5	-1.7

Note: all measurements were taken or simulated at 20°C.

Therefore, the synthetic brine was used to investigate the crystallization of sodium sulphate and ice under EFC conditions with a reduced calcium concentration. Figure 7.12 shows the concentration profile for the aqueous Na^+ ion as well as the temperature profile. The solution, initially at 10°C, had a Na^+ concentration of 12.3g/L. The solution was cooled until -1.4°C, at which stage ~1g $Na_2SO_4 \cdot 10H_2O$ seed crystals were added to the solution. This addition of seed material resulted in a decrease in the aqueous sodium ion concentration to a concentration of 11.3g/L after

~30 minutes. The temperature of the solution increased gradually to a maximum of -0.8°C, after which it continued to decrease until it stabilised at -1.5°C. This temperature increase was as a result of the release of the heat of crystallization during the crystallization process of $Na_2SO_4 \cdot 10H_2O$. Ice seed crystals (~1g) were added after one hour. The addition of these ice seeds resulted in an eventual sodium concentration increase after 2 hours. The sodium ion concentration reached a final concentration of 12.1g/L after 4 hours. The temperature of the solution did not increase with the addition of ice seeds because the seeds were probably added at the ice equilibrium temperature (-1.5°C). Therefore, the eutectic temperature for this system was -1.5°C, as this was the temperature at which both ice and $Na_2SO_4 \cdot 10H_2O$ existed.

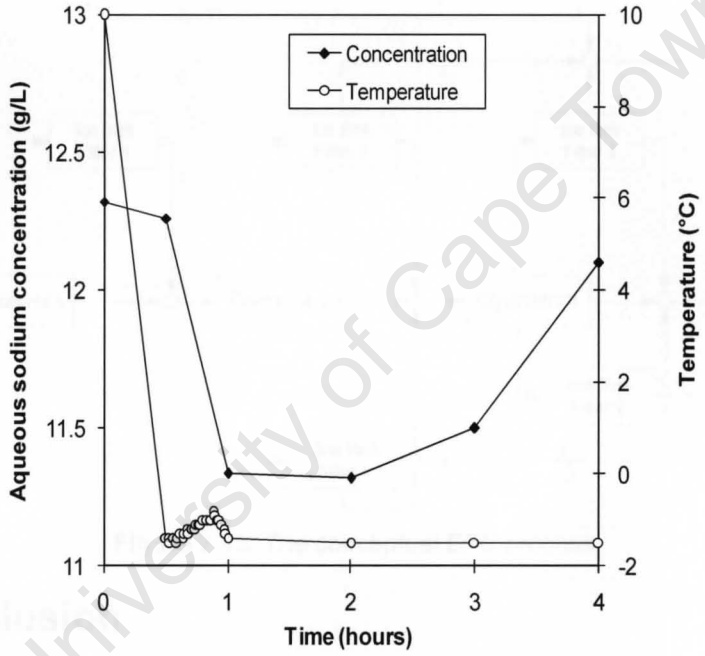

Figure 7.12: Aqueous sodium concentration and temperature change over time.

EFC conditions were successfully achieved with the synthetic brine. The salt formed under EFC conditions was identified as $Na_2SO_4 \cdot 10H_2O$ with a purity of 97.5% after no washing.

7.3.7 Conceptual design for an EFC process

Based on the experimental results, it was found that the sequence of ice and salt removal was: ice, followed by $CaSO_4 \cdot 2H_2O$ and ice and finally $Na_2SO_4 \cdot 10H_2O$ and ice. The proposed EFC process is shown in Figure 7.13. The process consists of three crystallizers as well as ice belt filters and salt belt filters. The filters are used to

separate the ice or salt from the brine. In reality though, these might consist of complex washing columns. The first crystallizer, with an operating temperature of -0.5°C, is essentially a pre-concentration step, while the second crystallizer operates at EFC conditions with the removal of calcium sulphate and ice (operating temperature of -0.6°C). Sodium sulphate and more ice can be recovered in the third crystallizer with an operating temperature of -1.5°C. The operating temperature of the third crystallizer could be lower as this would increase the yield of sodium sulphate. Based on thermodynamics, it is predicted that the majority of the sodium ion (92%) would be recovered by operating at -5°C. Although the results presented in this section were not at an operating temperature of -5°C, it is recommended that the third crystallizer be operated at this temperature in order to maximise the yield.

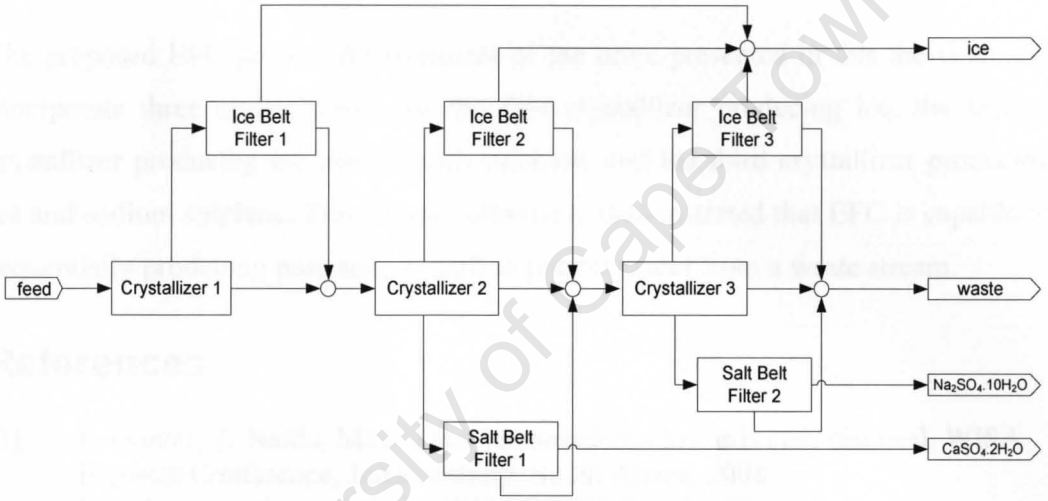

Figure 7.13: The conceptual EFC process.

7.4 Conclusion

The feasibility of using EFC as a brine treatment method was experimentally verified at laboratory scale. The results showed that a 97% waste conversion (by mass) to viable products (pure water and salts) could be achieved. Pure calcium sulphate (98.0% purity) and pure sodium sulphate (96.4% purity) were produced along with potable water.

Ice washing increased the purity of the ice to within acceptable South African water drinking standards. The entrapment of salt crystals within the ice was successfully removed by dispersing the "ice" (ice and salt) in a saturated salt solution. The

agitation of the "ice" was also deemed important as this increased the efficiency of the separation.

The results also showed that calcium sulphate could be removed under EFC conditions by means of seeding with $CaSO_4 \cdot 2H_2O$ and ice. The removal of calcium sulphate under EFC conditions also resulted in a similar calcium ion concentration to that obtained after 1 week (0.68g/L compared to 0.67g/L).

It was possible to use a synthetic brine as an approximation of a real brine for the purposes of measuring the sodium concentration change under EFC conditions ($Na_2SO_4 \cdot 10H_2O$-H_2O).

The proposed EFC process for treatment of the brine presented in this thesis should incorporate three crystallizers with the first crystallizer producing ice, the second crystallizer producing ice and calcium sulphate, and the third crystallizer producing ice and sodium sulphate. This chapter ultimately demonstrated that EFC is capable of sequentially producing pure salts as well as potable water from a waste stream.

References

[1] P. Gunter, T. Naidu, Mine water reclamation – towards zero disposal, WISA Biennial Conference, Johannesburg, South Africa, 2008 http://www.ewisa.co.za/misc/WISAConf/default2008.htm.

[2] R.A. Baker, Trace organic contaminant concentration by freezing – I. Low inorganic aqueous solutions, Water Res. 1 (1967) 61-77.

[3] L.S. Ramsdell, E.P. Partridge, The crystal forms of calcium sulphate. J. Mineralogical Society of America, 14 (1929) 59-74.

[4] Department of Water Affairs and Forestry, South African water quality guidelines, 2nd ed, vol. 1, Department of Water Affairs and Forestry, Pretoria, South Africa, 1996 http://www.dwaf.gov.za/IWQS/wq_guide/domestic.pdf.

[5] S.T Reddy, H.J.M. Kramer, A.E. Lewis, J. Nathool, Investigating factors that affect separation in a eutectic freeze crystallization process, IMWA Conference, Pretoria, South Africa, http://www.imwa.info/docs/imwa_2009/IMWA2009_Reddy.pdf.

[6] E. Corcoran, C. Nellemann, E. Baker, R. Bos, D. Osborn, H. Savelli, Sick Water? The central role of wastewater management in sustainable development. A Rapid Response Assessment, United Nations Environment Programme, UN-HABITAT, 2010 http://www.grida.no/publications/rr/sickwater/ebook.aspx.

CHAPTER 8 : CONCLUSIONS & RECOMMENDATIONS

When you drink the water, remember the spring.

Chinese proverb

Graphic from : http://greatblogabout.com/?p=1332

8.1. Conclusions

One of the most important environmental issues in the mining industry of South Africa is hypersaline brine production. Major methods aimed at reducing these brine volumes consist of either brine disposal in evaporation ponds, or brine treatment using evaporative crystallization. Brine disposal has a negative impact on the environment because of potential ground-water contamination, while evaporative crystallization is costly because of the high amounts of energy required. Both of these methods can reduce the volume of brine, but the final salt product is always contaminated with other salts. This makes separation of the salt waste product extremely unlikely. In addition, these current methods of brine disposal and treatment only offer short-term solutions and have not been shown to be sustainable in the long-term.

A novel technology known as Eutectic Freeze Crystallization (EFC) has the potential of treating brines by operating near the eutectic temperature of a specific salt. Not only is water produced in the form of ice, but pure salts are also produced when EFC conditions are reached. Thus the problem of salt contamination is avoided by the fact that each salt has its own unique eutectic temperature, therefore providing the possibility of crystallizing many pure salts from the brine. Eutectic Freeze Crystallization is an attractive water treatment technology, but to date it has not been utilized for complex systems such as brines. Therefore, a protocol for the treatment of hypersaline brines using EFC is necessary in order to show the feasibility of this technology.

Thus, the objectives of this thesis were to:

1. Establish a brine treatment protocol using Eutectic Freeze Crystallization,
2. Determine the operating region or metastable zone of a brine for Eutectic Freeze Crystallization, and
3. Investigate methods to sequentially remove pure salts from a brine.

The brine treatment protocol consists of three important aspects: brine analysis (Chapter 3), thermodynamics (Chapter 4) and kinetic aspects (Chapters 5-7).

Chapter 3 focused on the brine analysis, the first step of the brine treatment protocol. The complexity and importance of this step is often overlooked. The ion imbalance

for a brine analysis was an important measure of the accuracy of the analysis. The ion imbalance had to be less than 10% to ensure that accurate results were available for the thermodynamic modelling, the second stage of the brine treatment protocol. It was found that the ion imbalances from the analysis of two brine samples, **Brine 1** and **Brine 2**, were 5.8% and 6.3% respectively. The brines were also very dilute with a total dissolved solids of 29.77g/L for **Brine 1** and 31.26g/L for **Brine 2**.

The brine analysis was used to conduct a thermodynamic modelling exercise using OLI Stream Analyser. Chapter 4 presented these results. The model predicted that the system was already saturated with respect to $CaSO_4 \cdot 2H_2O$. It also predicted that water (in the form of ice) would crystallize at -0.8°C followed by $Na_2SO_4 \cdot 10H_2O$ at -1.5°C. A double salt, $K_2SO_4 \cdot CaSO_4 \cdot 1H_2O$, would crystallize at -2.2°C followed by KCl at a lower temperature of -19.6°C for the first brine sample and -16.6°C for the second. It was determined that there was a correlation between the cation and anion concentration of the salt and the crystallization temperature of the corresponding salt. For example, the brine with the lowest Na^+ concentration resulted in the lowest crystallization temperature of $Na_2SO_4 \cdot 10H_2O$ while the brine with the lowest Cl^- concentration resulted in the lowest crystallization temperature of KCl. The thermodynamic results also showed that a high overall ion recovery (85% for **Brine 1** and 71% for **Brine 2**) would be obtained at an operating temperature of -5°C. The thermodynamic modelling provided the first indication of what could be expected during an EFC process. It showed, for example, that the brines were initially saturated with respect to calcium sulphate. This was identified as a possible problem to the EFC process because the calcium sulphate would potentially affect the purity of the dominant sodium sulphate salt.

The third and final stage of the brine treatment protocol involved various kinetic investigations. Chapters 5 to 7 focused on stage 3, the kinetic aspects of the brine treatment protocol.

The fact that thermodynamic predictions of a system were for an infinite amount of time was the reason for the investigation into the kinetics of a EFC system. Chapter 5 focused on determining the metastable zone (MSZ) of ice as this ultimately defined the operating region for ice crystallization. Research to date has focused on

determining the MSZ from one or a few experiments, but the inherently stochastic nature of nucleation indicated that this was not the most accurate method for determining the MSZ. Chapter 5 therefore explored the stochastic nature of ice nucleation and ultimately defined the MSZ more accurately using the stochastic nature of nucleation. A wide distribution of nucleation temperatures of ~10°C was observed for different cooling rates (2°C/hour, 4°C/hour, 8°C/hour) with the fastest cooling rate (8°C/hour) resulting in the lowest nucleation temperatures. The MSZ for a 1wt% sodium sulphate solution (1.8ml volume), with a confidence percentage of 98%, was 2.56 Δ°C for a cooling rate of 2°C/hour, 2.76 Δ°C for a cooling rate of 4°C/hour, and 4.76 Δ°C for a cooling rate of 8°C/hour.

The effect of solution volume on the nucleation process and hence the MSZ was also investigated. The MSZ width decreased as the solution volume increased. The MSZ for a 250ml, 1wt% solution and a 1000ml, 1wt% solution were similar (2.3 Δ°C and 2.2 Δ°C respectively).Chapter 5 also indicated that the presence of ions in a system did not significantly affect the MSZ of ice. For example, the MSZ widths for different synthetic streams and **Brine 2** ranged from 4.5 Δ°C to 5.2 Δ°C.

The use of seeding as a means to selectively crystallize a desired component was also demonstrated in Chapter 5. Salt seeding only promoted the formation of salt near the eutectic point of a binary sodium sulphate provided the operation occurred within the MSZ. The crystallization of ice could be suppressed only if the solution temperature did not exceed the metastable limit of ice. Spontaneous ice nucleation occurred once the metastable limit was reached.

Chapter 6 focused on another kinetic aspect which was thought to be a possible disadvantage to EFC. The EFC operation works under the principle that ice and salt can be separated based on their density differences. This works well for a binary system, but when two salts crystallize at the same temperature in a complex system, the principle operation of EFC is affected. This is due to the fact that the crystallizing salts, having similar densities, sink to the bottom of the crystallizer and hence the separation of these salts becomes unlikely. Chapter 5 identified the selectivity of the EFC process when seeding was adopted for ice and salt. This concept was investigated further in the context of salt-salt contamination. Chapter 6 showed that

seeding could be utilised as means to crystallize a desired component. The use of $Na_2SO_4 \cdot 10H_2O$ seeding in a supersaturated ternary Na_2SO_4-$MgSO_4$-H_2O at 12°C was shown to be a successful method of producing pure $Na_2SO_4 \cdot 10H_2O$ (96% purity). The use of phase diagrams was also shown to be an important step in understanding the system and for obtaining information for the design of an EFC process.

Chapter 7 incorporated the results and techniques of the previous chapters in order to investigate the feasibility of using EFC as a brine treatment method. The results from this chapter showed that a 97% waste conversion to viable products (pure water and salts) could be achieved. Pure calcium sulphate (98.0% purity) and pure sodium sulphate (96.4% purity) were produced along with potable water. In addition, the chapter showed that the initial concern with the saturation of calcium sulphate could be avoided by understanding the kinetics of the system. The experimental work indicated that, although the thermodynamics predicted calcium sulphate was saturated, calcium sulphate was actually only removed after 1 week. The results also showed that calcium sulphate could be removed along with ice under EFC conditions in a period of 3 to 4 hours. Thus, the removal of calcium sulphate under EFC conditions resulted in a similar calcium ion concentration to that obtained after 1 week (0.68g/L compared to 0.67g/L) but in a shorter period of time. In addition, it was determined that the purity of ice crystals formed during the pre-concentration and EFC steps could be increased to fall within acceptable South African water drinking standards by washing the ice crystals with supercooled water.

Chapter 7 also showed it was possible to use a synthetic brine as an approximation of a real brine for the purposes of measuring the sodium concentration change under EFC conditions ($Na_2SO_4 \cdot 10H_2O$-H_2O).

Chapter 7 proposed an EFC process that consisted of three crystallizers, the first crystallizer producing ice, the second crystallizer producing ice and calcium sulphate and the third crystallizer producing ice and sodium sulphate.

Finally, this thesis has ultimately demonstrated that EFC is capable of sequentially producing pure salts as well as potable water from a waste stream. It has also shown that the MSZW should be defined from a number of experiments because of the

stochastic nature of nucleation. The concept of selective nucleation can also be used to prevent salt contamination in an EFC process.

8.2. Recommendations

In view of the results and constraints encountered in this work, the following recommendations are suggested:

- The results presented in this thesis are all based on batch scale, whereas an industrial EFC process would work in a continuous mode. It is therefore recommended that the brine treatment protocol be adapted to a continuous setup. The brine treatment protocol should also be utilised in the operation of a pilot plant to test the feasibility of a sequential EFC process on a larger scale.

- The current work only focused on the crystallization of two salts (calcium sulphate and sodium sulphate) and neglected the crystallization of other salts such as $K_2SO_4 \cdot CaSO_4 \cdot 1H_2O$. It is recommended that further work be conducted in an attempt to crystallize out a third salt.

- The yield of sodium sulphate is currently limited by the operating temperature of -1.5°C while the thermodynamic results predicted that a high recovery (~92%) of Na^+ could be obtained at an operating temperature of -5°C. This should be experimentally verified with a larger volume crystallizer to avoid the need of adopting the time consuming cascading concentration procedure. An optimised crystallizer design would also be beneficial for verifying this recommendation.

- The work presented in this thesis did not evaluate the economics of a sequential EFC process. Previous work has been conducted on the economics of primarily binary EFC systems, but detailed economic analysis of complex systems is currently not available. It is therefore recommended that a detailed economic analysis of the sequential EFC process be conducted.